MATHEMATICAL MODELS OF UNSTEADY OPERATION

OF A PACKED COLUMN

by

Jen-Fu Chao

APPROVAL SHEET

Title of Dissertation:

Mathematical Models of Unsteady Operation of a Packed Column

Name of Candidate:

Jen-Fu Chao
Doctor of Engineering Science, 1983

Dissertation and Abstract Approved:

9/13/83

_____
Dr. Ching-Rong Huang
Professor & Assistant Chairman
Department of Chemical Engineering & Chemistry
Date

_____
Date
9/13/83

_____
Date
9/13/83

_____
Date
9/13/83

_____
Date
9/15/83

VITA

Name: Jen-Fu Chao

Present address:

Degree and date to be conferred: D.Eng.Sc., 1983

Date of birth:

Place of birth:

Secondary education: Changkou High School, Taipei, Taiwan, 1966

Collegiate institutions attended	Dates	Degree	Date of Degree
Chung Yuang University	68/72	B.S.	6/72
Tennessee Technological University	77/79	M.S.	6/79
New Jersey Institute of Technology	79/83	D.Eng.Sc.	10/83

Major: Chemical Engineering

Minor: Mathematics

Publications:

"Calculation of Liquid Viscosity Using a Lattice Model," Master's Thesis at Tennessee Technological University, 1979.

"Continuous Multiaffinity Separation of Proteins: Cyclic Processes," AIChE Symposium Series, No. 219, Vol. 78 (1982).

"Parametric Pumping--A Unique Separation Science," Journal of Parenteral Science & Technology, Jan'Feb (1983).

"Cycling Zone Electrophoresis," submitted to Industrial & Engineering Chemistry Fundamentals.

"Enzyme Purification: A Comparison of Prep-PAGE with Cyclic Processes," accepted by Separation Science & Technology.

<u>Positions Held</u>:

1976-77   Engineer, Taiwan Fertilizer Company Miaoli Plant-
            -Production Department.

1974-76   Junior Engineer, Yue Long Motor Company, Taipei,
            Taiwan.

ABSTRACT

Title of Dissertation:

Mathematical Models of Unsteady Operation

of a Packed Column

Jen-Fu Chao
Doctor of Engineering Science, 1983

Thesis directed by:

Dr. Ching-Rong Huang
Professor & Assistant Chairman
Department of Chemical Engineering & Chemistry

Analytical solutions of differential equations applicable to extraction, ion exchange, or adsorption processes in packed beds are presented. Results are given for three different cases. The first case accounts for adsorption phenomena only. The second one includes surface adsorption on particles and the effects of longitudinal dispersion in the bed. The third one deals with diffusion in particles and longitudinal dispersion in the bed. In the mathematical modelling of these three cases, a linear equilibrium relationship between the solute in the liquid phase and solute in the solid phase is used. The first case is solved using the single boundary condition at the feed end of the column. In the second case, two different sets of boundary conditions are used. One set uses two conditions at the feed end: namely, the feed composition and its variation with respect to length. The other set uses an equation of continuity at the inlet of the column, and solute material balance over the entire

column. In the third case, the feed composition is one boundary condition, while the other assumes a linear concentration profile at the discharge end of the column. Since the boundary conditions involving the mass conservation law and the highest derivative of the differential equations are beyond the criterion which are found in the literature, the applications of boundary conditions for solving differential equations are extended. Comparisons are made with previous models and experimental data in the literature.

ACKNOWLEDGEMENTS

TABLE OF CONTENTS

CHAPTER I .

INTRODUCTION

Separation principles and techniques are widely used in chemical manufacturing operations and pollution controls. Separation is generally defined as an operation which isolates specific components of a mixture without a chemical reaction taking place. Separation is the reverse of mixing. Mixing occurs spontaneously with an increase in the total entropy of the system. Separation does not occur spontaneously since it decreases the total entropy of the system. Therefore different separation techniques are suitable for different systems.

Table 1 summarizes the characteristics of some common separation processes in chemical engineering. The separation processes are analyzed with respect to separation basis, driving force, parameter effects, and the phases involved. By control of the parameters which affect the separation basis, the driving force is induced. Then the separation can be enhanced.

Adsorption has numerous applications in the chemical process industries. In general, adsorption removes one or more species from one fluid phase and transfers them to another fluid phase via an intermediate solid. In many cases the transfer can be made on a selective basis and with good efficiency. The adsorption equilibrium depends strongly on the thermodynamic intensive variables, such as temperature, pressure, pH, ionic strength and affinity. One of the typical quantitative treat-

TABLE 1

Separation Processes

Process	Separation Basis	Driven Forces	Main Parameters Affect S.B.	Phases Involved
Distillation	Volatility	Phase Change	Temperature	G,L
Extraction	Solubility	Molecular Interaction	Concentration	L,L L,S
Filtration	Permeability	Pressure Gradient	Molecular size	F,S (NMT)
Sedimentation	Density	Gravity	Flow Characteristics	L,S (NMT)
Crystallization	Solubility	Phase Change	Temperature	L,S
Electrophosis	Electromobility	Electric Field	Molecular Charge	L,L
Adsorption or Ion Exchange	Selectivity	Molecular Interaction	Any thermo. intensive variable	G,L F,S

F: Fluid; G: Gas; L: Liquid; S: Solid

NMT: No mass transfer between phases

ments of adsorption equilibrium has been reported by Langmuir[1]. In the Langmuir adsorption isotherm, the tendency of binding the fluid molecules on solid adsorbent is said to be equal to the tendency of releasing the fluid molecules from the solid adsorbent when equilibrium is established. The Langmuir equilibrium is written as follows:

$$K \cdot C \cdot (C_{sm} - C_s) = K_r \cdot C_s \tag{1-1}$$

or

$$C_s = \frac{(K/K_r) \cdot C_{sm} \cdot C}{(K/K_r) \cdot C + 1} \tag{1-2}$$

where

  K: binding constant

  K_r: releasing constant

  C: concentration in fluid phase

  C_s: concentration in solid phase

  C_{sm}: maximum concentration in solid phase

Equation (1-2) states that the concentration in the solid phase nonlinearly increases with the concentration in the fluid phase for $(K/K_r) \cdot C$ near unity. The concentration in the solid phase is a constant which is equal to C_{sm} for $(K/K_r) \cdot C$ much larger than unity. The concentration in the solid phase is linear with the concentration in the fluid phase for $(K/K_r) \cdot C$ much smaller than unity. Thus, the assumptions of linear equilibrium relationship is reasonable in a mathematical model when the solute concentration is dilute.

Besides adsorption, ion exchange and liquid-solid extraction separation processes can also be described by the Langmuir

isotherm. Ordinarily these processes are the problem of mass transfer during flow through a packed bed. An essential problem in the design of packed bed operation is the prediction of the concentration-time relationship, or breakthrough curve, of the effluent stream. Theoretical studies of transport phenomena in a packed bed is undertaken since its study can help evaluate transfer factors which can be used in the technological applications.

Apart from the adsorption isotherm itself, a mathematical model of packed bed transport phenomena must account for: 1) surface adsorption; 2) diffusion through the porous network of the particle; and 3) axial dispersion. In fact, these three considerations can contribute to the overall transfer phenomena. However, mathematical modes are usually based on the cases that whether axial dispersion, surface adsorption, or porous diffusion is important. In this work, analytical solutions with different cases have been attempted. Chapter Two deals with a simple model which considers surface adsorption only. Chapter three presents two models which contain surface adsorption and axial dispersion effects. Chapter Four presents a model which includes diffusion through solid particles and axial dispersion. With regard to the adsorption isotherm, the linear equilibrium relationship between the solute in the solid phase with that in fluid phase is adopted in all of the cases. The last chapter contains conclusions.

CHAPTER II

SIMPLE MODEL

Material balance of solid phase:

$$(1-\epsilon)SdZ \frac{\partial C_{AS}}{\partial t} = k_f a(C_A - C_A^*)SdZ \tag{2-1}$$

Material balance of liquid phase:

$$\epsilon SdZ \frac{\partial C_A}{\partial t} = -Q \frac{\partial C_A}{\partial Z} dZ - K_f a(C_A - C_A^*)SdZ \tag{2-2}$$

Equilibrium relationship on solid surface:

$$C_A^* = m\, C_{AS} \tag{2-3}$$

Change variable,

Let $t' = t - Z(\frac{\epsilon S}{Q})$

Use chain rule transfer Eq. (2-1) to

$$(\frac{\partial C_{AS}}{\partial t'})_Z = \frac{k_f a}{1-\epsilon} (C_A - C_A^*) \tag{2-4}$$

and Eq. (2-2) to

$$(\frac{\partial C_A}{\partial t})_{t'} = \frac{-k_f a S}{Q} (C_A - C_A^*) \tag{2-5}$$

With

    B.C.1:   at $t' = 0$, $C_{AS} = 0$ for all $Z > 0$

    B.C.2:   at $Z = 0$, $C_A = C_{A0}$ for all $t' > 0$

Introduce dimensionless form:

$$X = \frac{C_A}{C_{A0}}, \quad Y = \frac{mC_{AS}}{C_{A0}}, \quad \zeta = \frac{k_f a Z S}{Q}, \quad \tau = \frac{mt'k_f a}{1-\epsilon}$$

Eqs. (2-4) and (2-5) become:

$$\frac{\partial X}{\partial \zeta} = -(X - Y) \tag{2-6}$$

$$\frac{\partial Y}{\partial \tau} = (X - Y) \tag{2-7}$$

B.C.1: at $\tau = 0$, $Y = 0$ for $\zeta \geq 0$

B.C.2: at $\zeta = 0$, $X = 1$ for all τ

Take Laplace Transform with respect to τ

$$\frac{d\overline{X}}{d\zeta} = -\overline{X} + \overline{Y} \tag{2-8}$$

$$\overline{Y} = \frac{1}{p+1}\overline{X} \tag{2-9}$$

Combine Eqs. (2-8) and (2-9) and integrate

$$\int_{\overline{X}=\frac{1}{p}}^{\overline{X}} \frac{d\overline{X}}{\overline{X}} = -\frac{p}{p+1}\int_{\zeta=0}^{\zeta} d\zeta$$

By using Shifting Theorem and Convolution rule to inverse Laplace Transform, the solutions are

$$X(\zeta,\tau) = e^{-(\zeta+\tau)}J_O(i\sqrt{4\zeta\tau}) + \int_O^\tau e^{-(\zeta+\sigma)}J_O(i\sqrt{4\zeta\sigma})d\sigma \tag{2-10}$$

$$Y(\zeta,\tau) = \int_O^\tau e^{-(\zeta+\sigma)}J_O(i\sqrt{4\zeta\sigma})d\sigma \tag{2-11}$$

The above two equations are for the step input function.

For the pulse input function like

$$X_{in} = 1[u(\tau) - u(\tau - \alpha)]$$

For $0 < \tau \leq \alpha$, the solutions are the same as Eqs. (2-10) and (2-11).

For $\tau > \alpha$,

$$X(\zeta,\tau) = e^{-(\zeta+\tau)}J_O(i\sqrt{4\zeta\tau}) + \int_O^\tau e^{-(\zeta+\sigma)}J_O(i\sqrt{4\zeta\sigma})d\sigma$$

$$-e^{-(\zeta+\tau-\alpha)}J_O(i\sqrt{4\zeta(\tau-\alpha)}) - \int_O^{(\tau-\alpha)} e^{-(\zeta+\sigma-\alpha)}J_O(i\sqrt{4\zeta(\sigma-\alpha)})d\sigma \tag{2-12}$$

$$Y(\zeta,\tau) = \int_{0}^{\tau} e^{-(\tau+\sigma)} J_0(i\sqrt{4\zeta\sigma})$$

$$-\int_{0}^{(\tau-\alpha)} e^{-(\zeta+\sigma-\alpha)} J_0(i\sqrt{4\zeta(\sigma-\alpha)})d\sigma \qquad (2\text{-}13)$$

The calculated breakthrough curves are shown in Figures 2.1 to 2.8 for various values of the parameters.
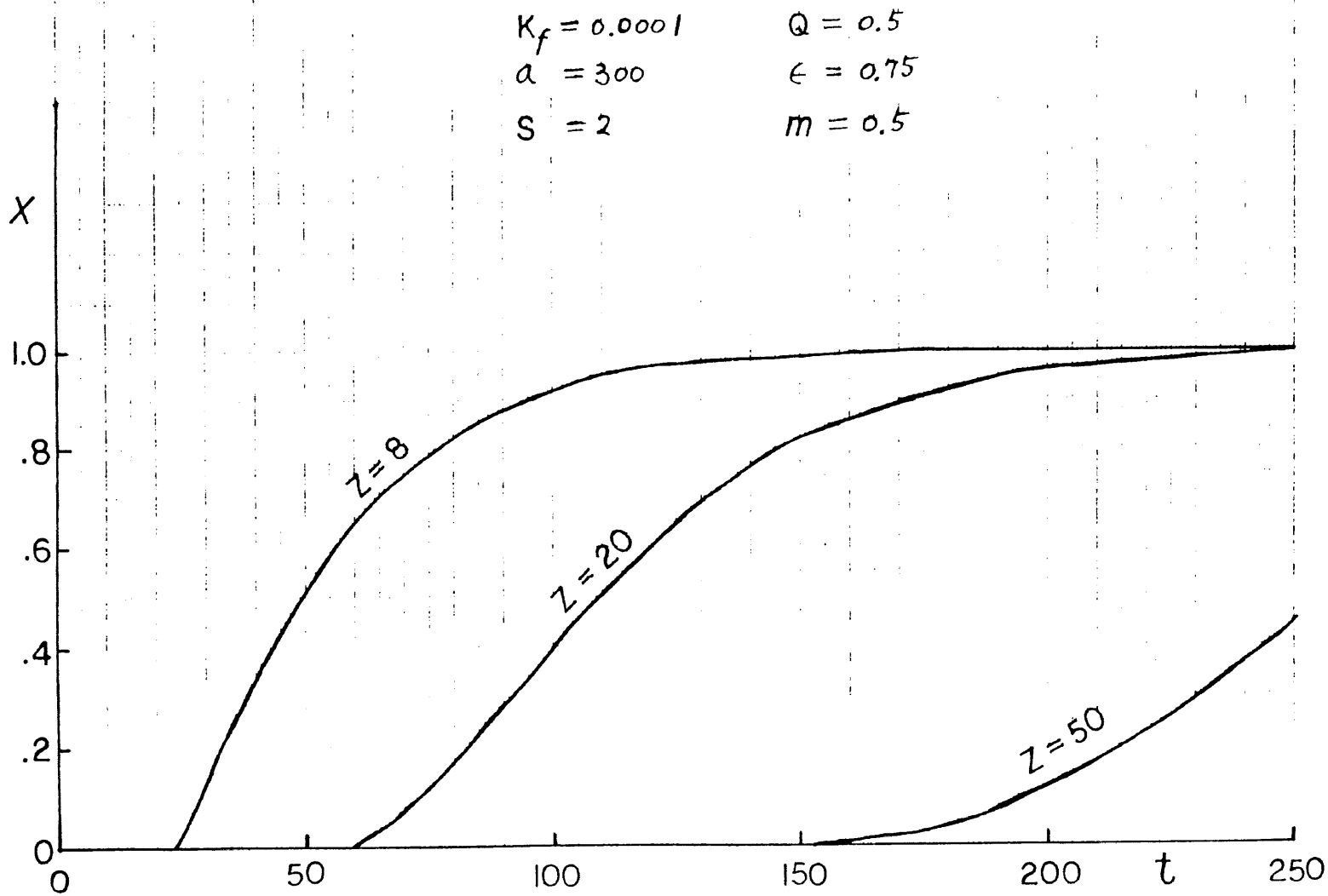
FIGURE 2.1
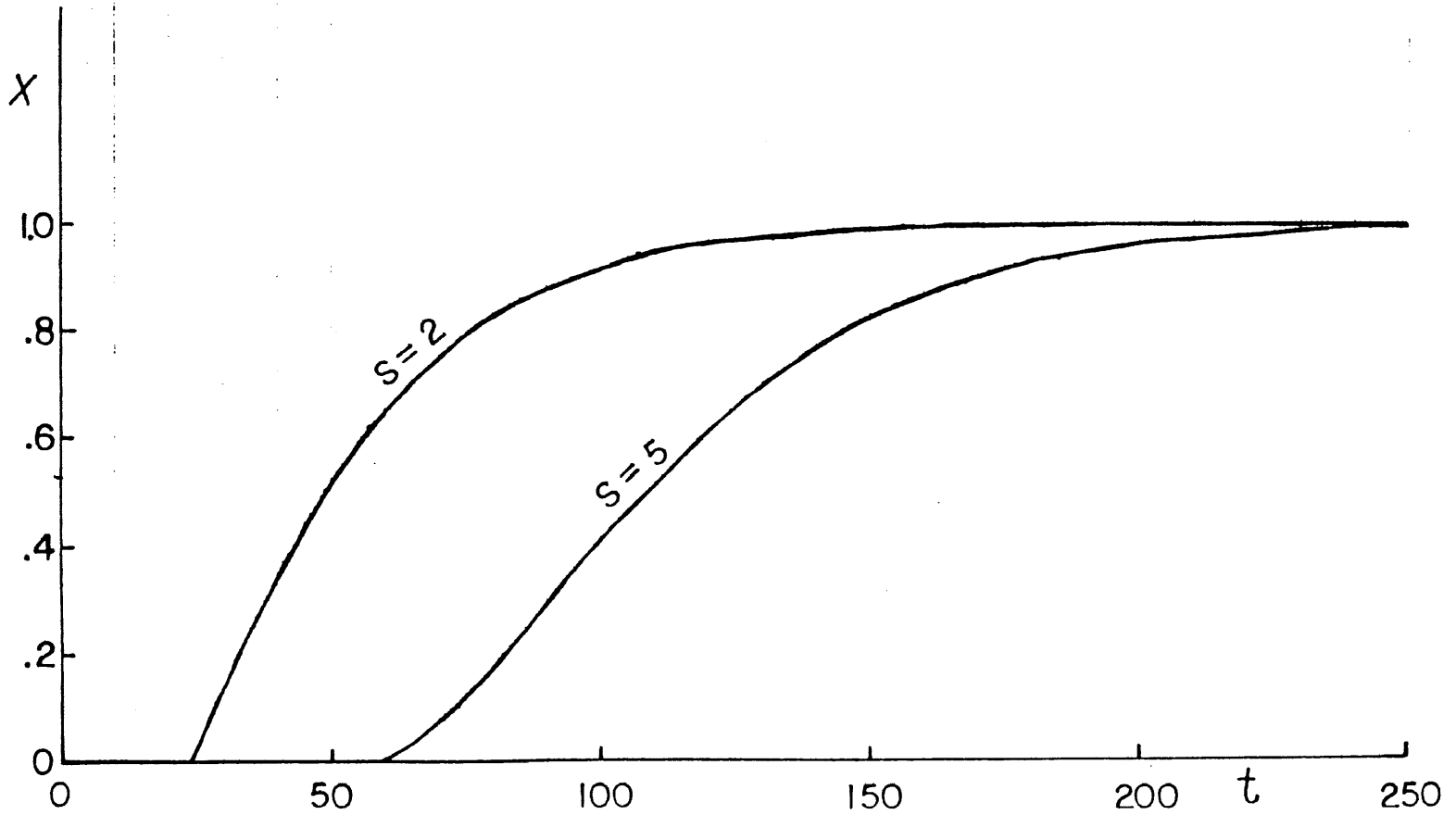
FIGURE 2.2

FIGURE 2.3

FIGURE 2.4

FIGURE 2.5

FIGURE 2.6

$K_f = 0.0001$
$a = 300$
$Z = 8$
$S = 2$
$Q = 0.5$
$\epsilon = 0.75$

m	t_I
0.1	500
0.5	100
1.0	50

$m=1.0$

$m=0.5$

$m=0.1$
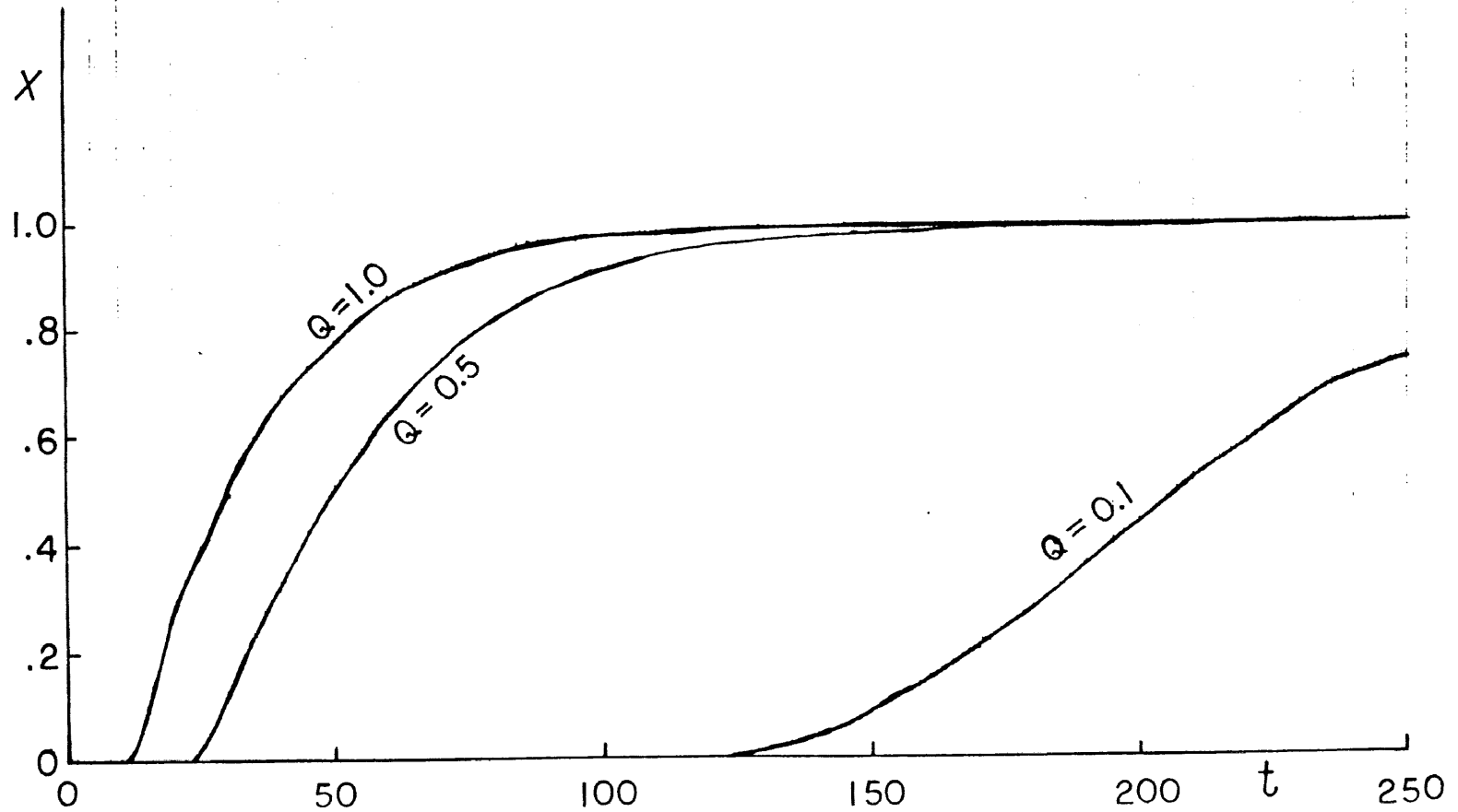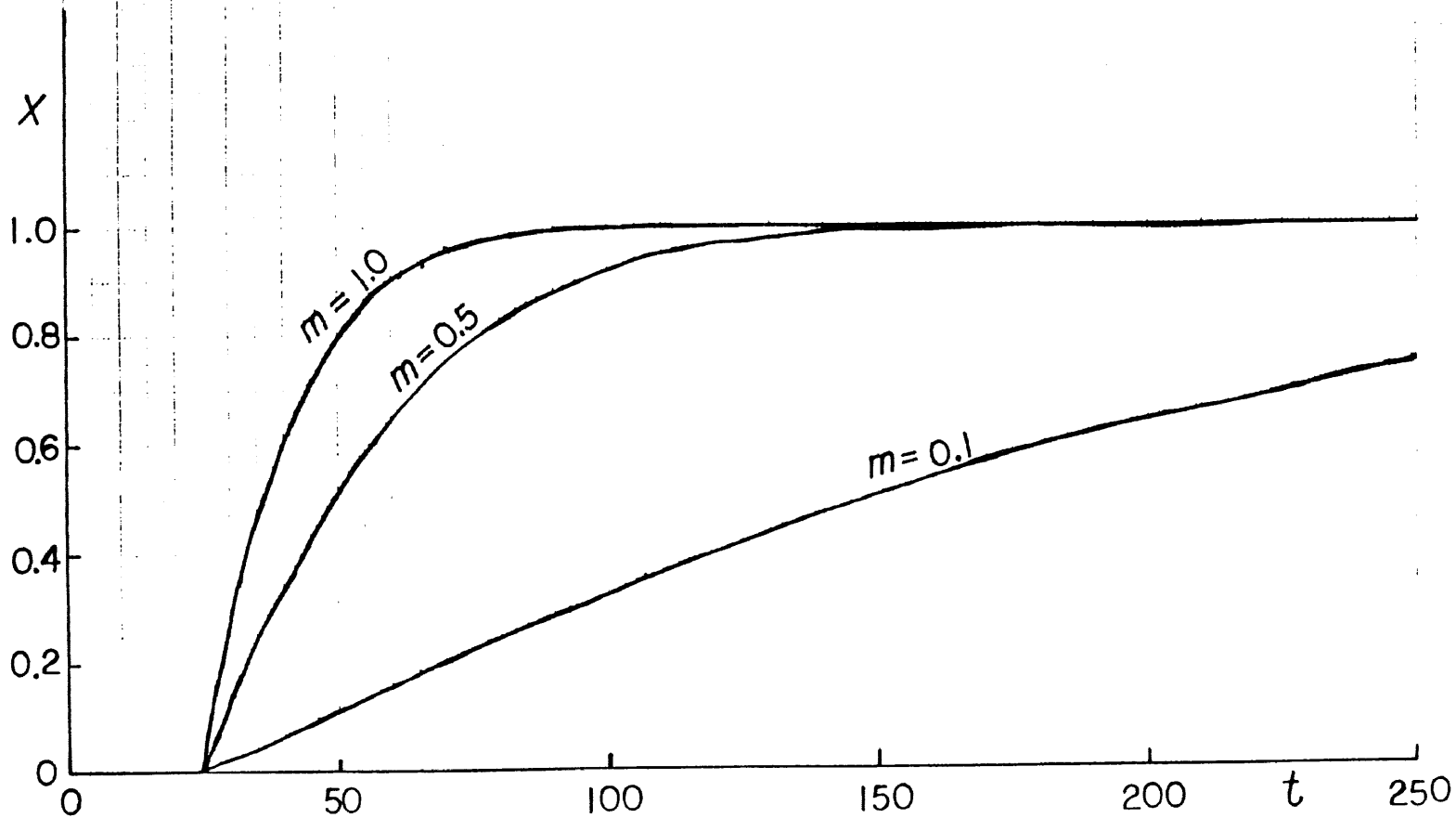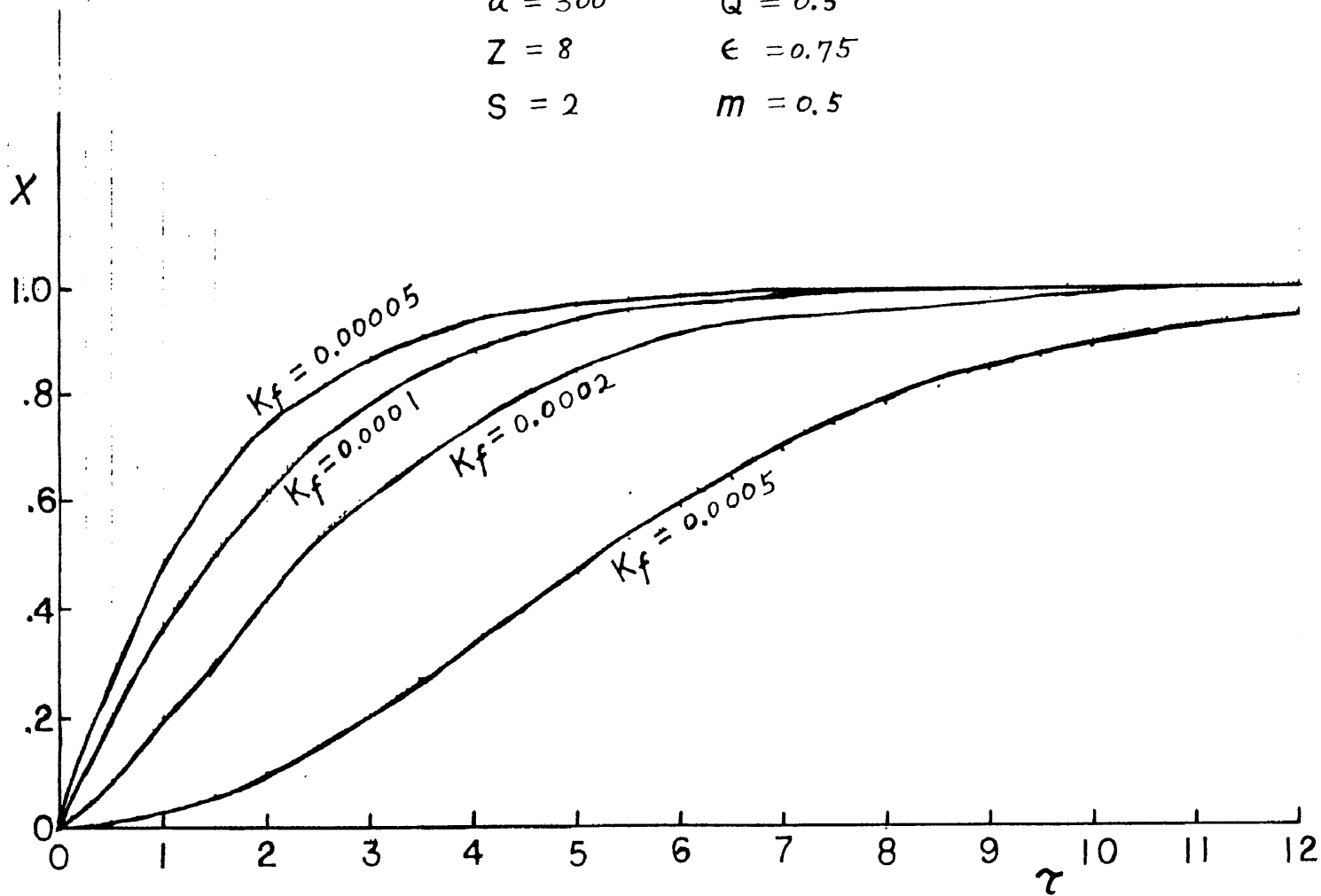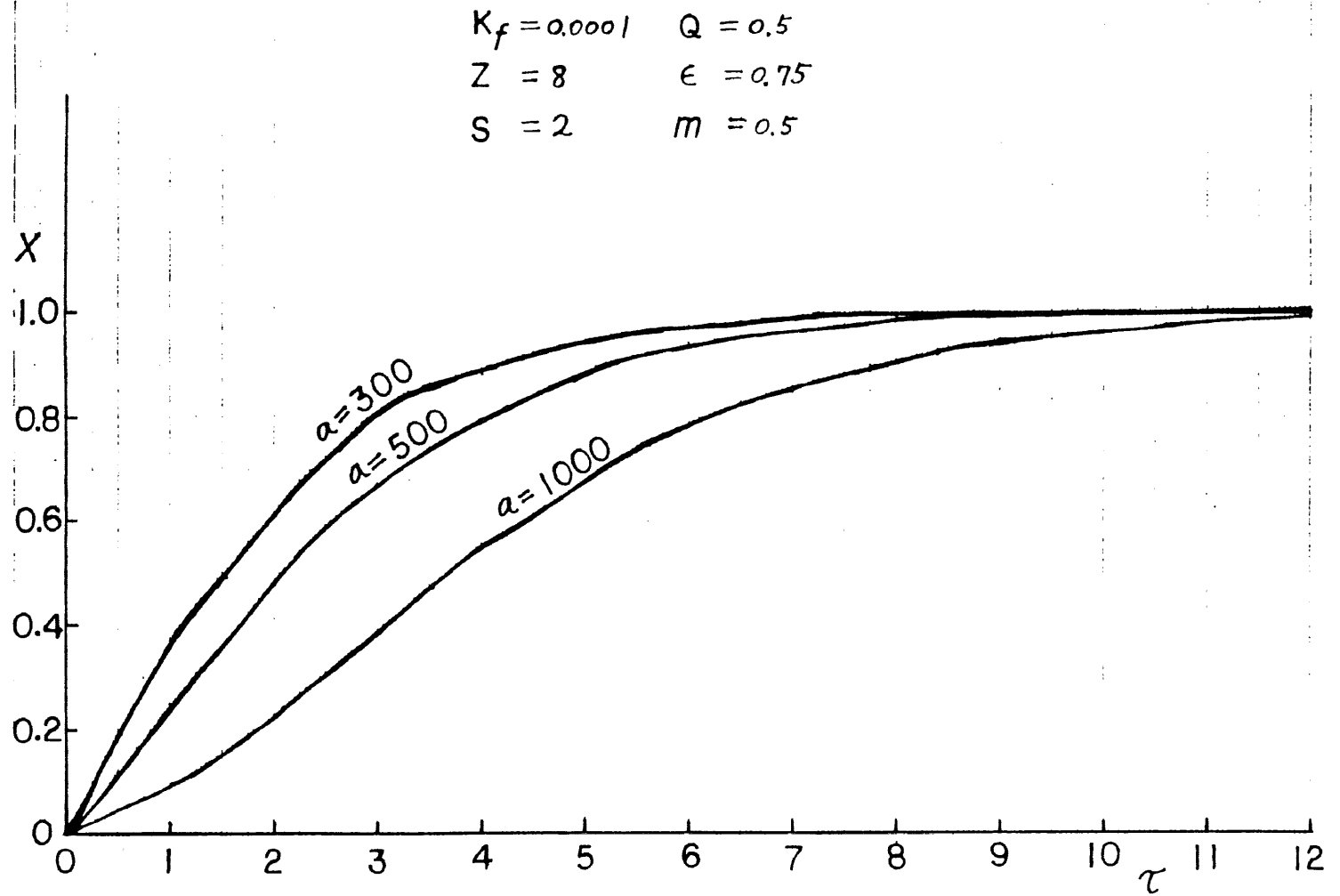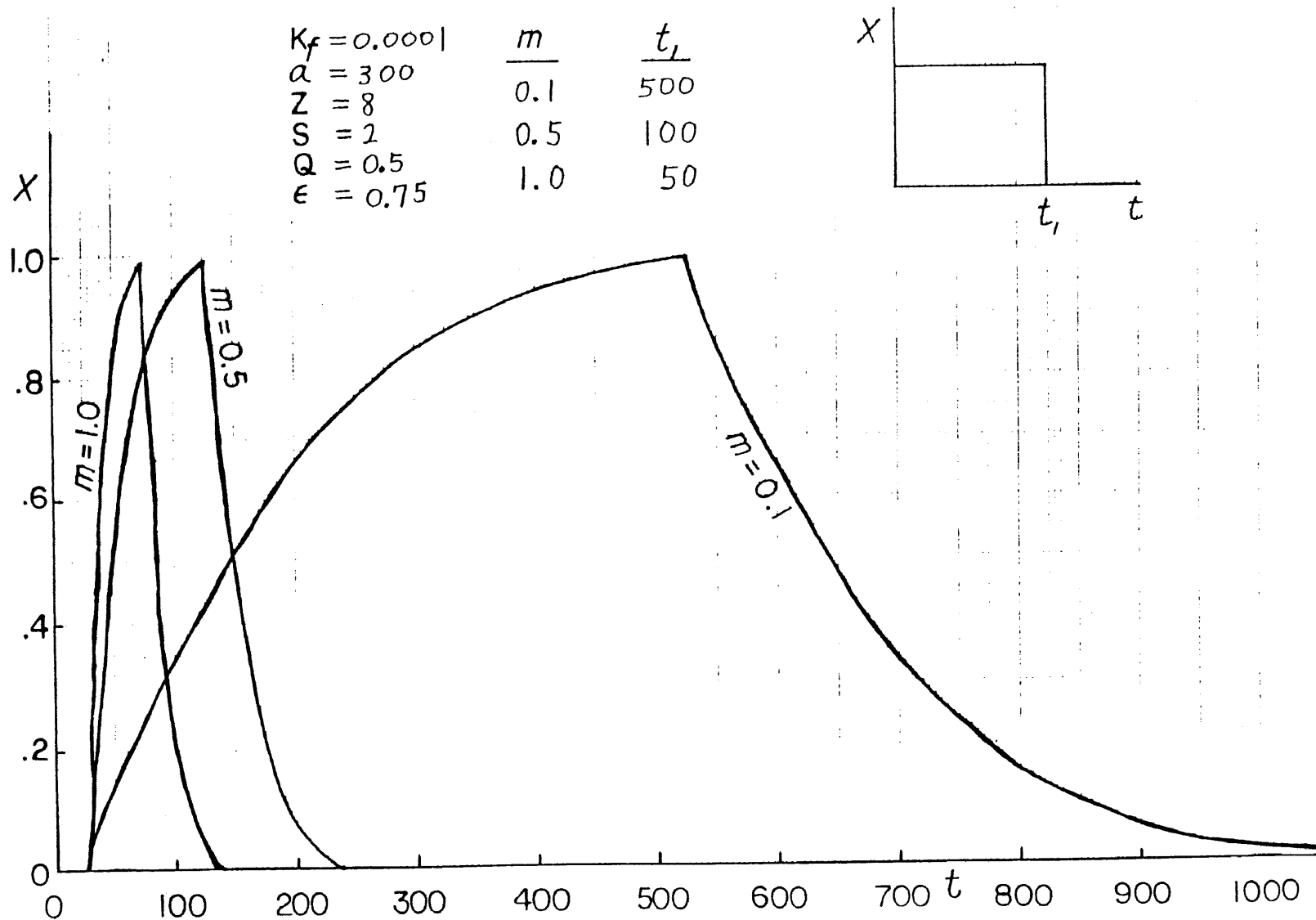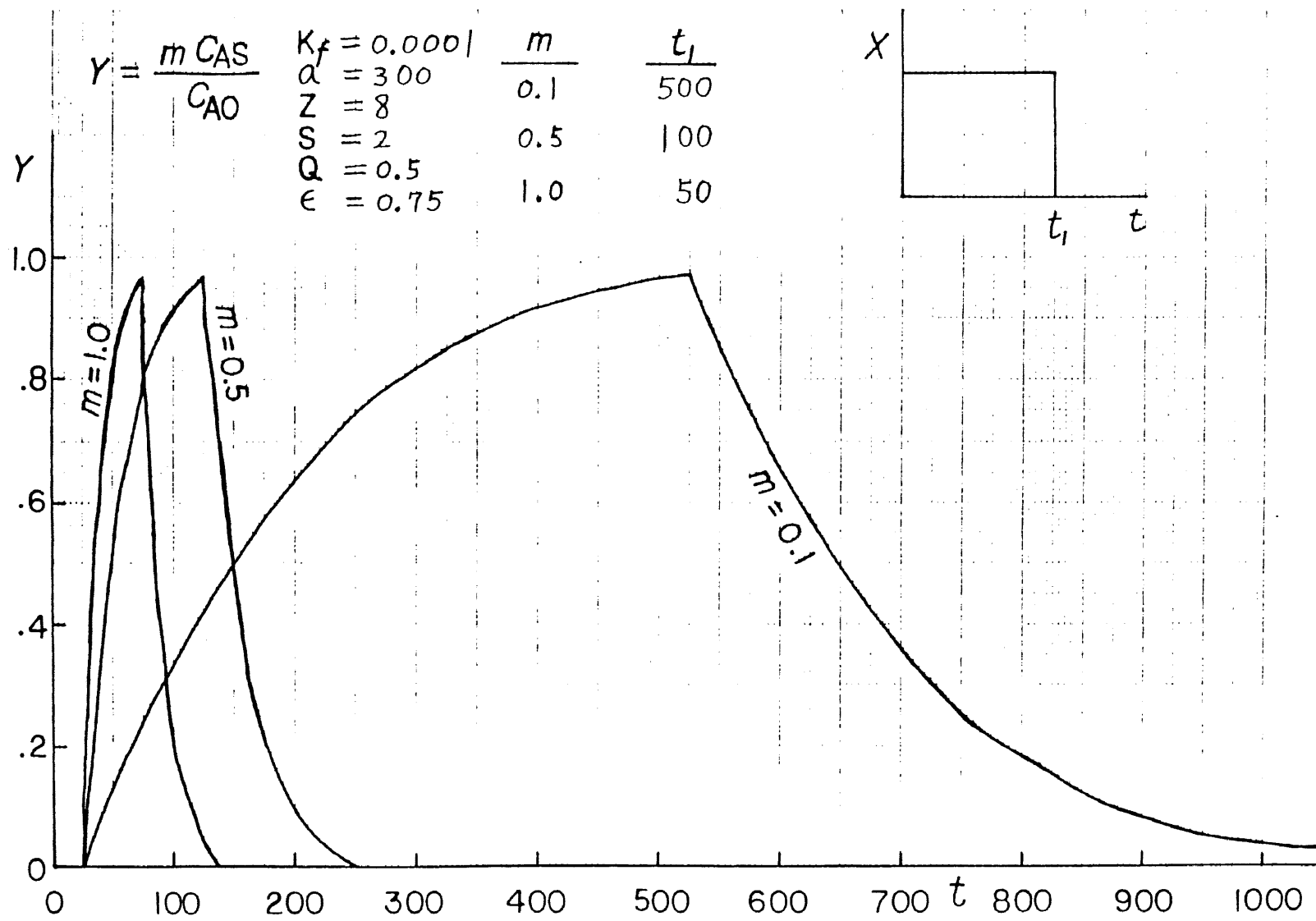
FIGURE 2.7

FIGURE   2.8

CHAPTER III

LONGITUDINAL DISPERSION

Model A

Material balance of solid phase:

$$(1 - \epsilon)SdZ \frac{\partial C_{AS}}{\partial t} = k_f a(C_A - C_A^*)SdZ \qquad (3-1)$$

Material balance of liquid phase:

$$\epsilon SdZ \frac{\partial C_A}{\partial t} = -Q \frac{\partial C_A}{\partial Z} dZ -(1-\epsilon)SdZ \frac{\partial C_{AS}}{\partial t} + E_d \frac{\partial^2 C_A}{\partial Z^2} \epsilon SdZ \qquad (3-2)$$

Equilibrium relationship between solid phase and liquid phase:

$$C_A^* = mC_{AS} \qquad (3-3)$$

With initial conditions:

I.C. 1 $C_A(Z,t=0) = C_{A,t_o}$

I.C. 2 $C_A^*(Z,t=0) = C_{A,t_o}$

I.C. 3 $C_{AS}(Z,t=0) = C_{A,t_o}$

Boundary Conditions (assume step change):

at $Z = 0$, $C_A = C_{AO}$

$$C_A^* = C_{AO}$$

$$\frac{\partial C_A}{\partial Z} = 0$$

$$\frac{\partial C_A^*}{\partial Z} = 0$$

Define

$$C_{AS}' = \frac{C_{AS} - C_{AS,t_o}}{C_{AO} - C_{A,t_o}}$$

$$C_A = \frac{C_A' - C_{A,t_o}}{C_{AO} - C_{A,t_o}}$$

$$C_A'^* = \frac{C_A^* - C_A^*,t_o}{C_{A0} - C_{A,t_o}}$$

Note $\quad C_A^*,t_o = C_{A,t_o}$

Equations (3-1), (3-2) and (3-3) become

$$\frac{\partial C_{AS}'}{\partial t} = \frac{k_f a}{1-\epsilon} (C_A' - C_A'^*) \tag{3-4}$$

$$\frac{\partial C_A'}{\partial t} + \frac{1-\epsilon}{\epsilon} \frac{\partial C_{AS}'}{\partial t} = E_d \frac{\partial^2 C_A'}{\partial Z^2} - \frac{Q}{\epsilon S} \frac{\partial C_A'}{\partial Z} \tag{3-5}$$

$$C_A'^* = m C_{AS}' \tag{3-6}$$

With I.C.'s

$$C_A'(z,t=0)=0, \quad C_A'^*(z,t=0)=0, \quad C_{AS}'(z,t=0)=0$$

B.C.'s

$$C_A'(z=0,t)=1, \quad C_A'^*(z=0,t)=1, \quad C_{AS}'(z=0,t)= \frac{1}{m}$$

Take Laplace Transform of Eqs. (3-4), (3-5) and (3-6)

$$p\overline{C}_{AS} = \frac{k_f a}{1-\epsilon} (\overline{C}_A - \overline{C}_A^*) \tag{3-7}$$

$$p\overline{C}_A + (\frac{1-\epsilon}{\epsilon})p\overline{C}_{AS} = E_d \frac{d^2\overline{C}_A}{dZ^2} - \frac{Q}{\epsilon S} \frac{d\overline{C}_A}{dZ} \tag{3-8}$$

$$\overline{C}_A^* = m\overline{C}_{AS} \tag{3-9}$$

With B.C.'s

$$\overline{C}_A|_{z=0} = \frac{1}{p}, \quad \overline{C}_A^*|_{z=0} = \frac{1}{p}, \quad \overline{C}_{AS}|_{z=0} = \frac{1}{mp}$$

Combine Eqs. (3-7) and (3-9)

$$\frac{p}{m} \overline{C}_A^* = \frac{k_f a}{1-\epsilon} (\overline{C}_A - \overline{C}_A^*) \tag{3-10}$$

Combine Eqs. (3-7) and (3-8)

$$p\overline{C}_A + (\frac{1-\epsilon}{\epsilon}) \frac{k_f a}{1-\epsilon} (\overline{C}_A - \overline{C}_A^*) = E_d \frac{d^2\overline{C}_A}{dZ^2} - \frac{Q}{\epsilon S} \frac{d\overline{C}_A}{dZ} \tag{3-11}$$

Put Eq. (3-10) into (3-11)

$$\frac{d^2 \overline{C}_A}{dZ^2} - A \frac{d\overline{C}_A}{dZ} - F \overline{C}_A = 0 \qquad (3-12)$$

where,

$$A = \frac{Q}{SE_d} \quad , \quad B = \left(\frac{1-\varepsilon}{\varepsilon}\right) \frac{1}{E_d} \quad , \quad F = \frac{p}{E_d} + \frac{Bk_a p}{p+mk_a}, \quad k_a = \frac{k_f a}{1-\varepsilon}$$

By using B.C.'s, the solution of Eq. (3-12) is

$$\overline{C}_A = e^{\frac{A}{2}z}\left[\frac{1}{p} \cosh \frac{\sqrt{A^2+4F}}{2} Z - \frac{1}{p} \frac{A}{\sqrt{A^2+4F}} \sinh \frac{\sqrt{A^2+4F}}{2} Z\right] \qquad (3-13)$$

Note F is a function of p

Inverse Eq. (3-13) by using Residue Theorem

$$L^{-1}[\overline{C}_A] = \quad \text{residues of } e^{pt} \cdot \overline{C}_A(p) \qquad (3-14)$$

Check poles and branch point of $\overline{C}_A(p)$:

$$A^2 + 4F = A^2 + 4p\left(\frac{1}{E_d} + \frac{Bk_a}{p+mk_a}\right)$$

$$= A^2 + 4p\left[\frac{1}{E_d} + \frac{B}{m} - \frac{B}{m^2 k_a} p + \frac{B}{m^3 k_a{}^2} p^2 - \ldots + \right.$$

$$\left. \frac{B(-1)^n}{m^{n+1}k_a{}^n} p^n + \frac{\frac{B(-1)^{n+1}p^{n+1}}{m^{n+1} \cdot k_a{}^{n+1}}}{p + mk_f} \right]$$

Since

$$\cosh \frac{\sqrt{A^2+4F}}{2} Z = 1 + \sum_{n=1}^{\infty} \frac{(A^2+4F)^n}{(2n)!} \left(\frac{Z}{2}\right)^{2n}$$

$$\sin \frac{\sqrt{A^2+4F}}{2}Z \Big/ \frac{\sqrt{A^2+4F}}{2}Z = 1 + \sum_{n=1}^{\infty} \frac{(A^2+4F)^n}{(2n+1)!}\left(\frac{Z}{2}\right)^{2n}$$

So there is no branch point in $\overline{C}_A(p)$.

However, there are simple pole at $p = 0$ and an essential singularity at $p = -mk_a$.

Residue at simple pole $p = 0$ is

$$\lim_{p \to 0} p \cdot [e^{pt} \cdot \overline{C}_d(p)] = 1 \tag{3-15}$$

Now apply Laurent's Theorem to find the residue of the essential singularity at $p = -mk_a$.

$$\text{let } \zeta = p + mk_a \quad \text{or} \quad p = \zeta - mk_a$$

and

$$e^{pt} = 1 + \sum_{\ell=0}^{\infty} \frac{p^\ell t^\ell}{\ell!}$$

Therefore,

$$e^{pt} \frac{1}{p} \cosh \frac{\sqrt{A^2+4F}}{2} Z$$

$$= \sum_{\ell=0}^{\infty} \frac{t^\ell}{\ell!} \sum_{n=0}^{\infty} \sum_{k=0}^{n} \binom{n}{k} A^{2(n-k)} \cdot 4^k (\zeta - mk_f)^{k+\ell-1} \cdot \left(\frac{1}{E_d} + \frac{Bk_a}{\zeta}\right)^k \frac{\left(\frac{Z}{2}\right)^{2n}}{(2n)!} \tag{3-16}$$

and

$$e^{pt} \frac{1}{p} \sinh \frac{\sqrt{A^2+4F}}{2}Z \Big/ \frac{\sqrt{A^2+4F}}{2}Z$$

$$= \sum_{\ell=0}^{\infty} \frac{t^\ell}{\ell!} \sum_{n=0}^{\infty} \sum_{k=0}^{n} \binom{n}{k} A^{2n+1-2k} \cdot 4^k (\zeta - mk_f)^{k+\ell-1} \cdot \left(\frac{1}{E_d} + \frac{Bk_a}{\zeta}\right)^k \frac{\left(\frac{Z}{2}\right)^{2n+1}}{(2n+1)} \tag{3-17}$$

The residue at $p = -mk_a$ for Eq. (3-16) is

$$\sum_{\ell=0}^{\infty} \frac{t^{\ell}}{\ell!} \sum_{n=1}^{\infty} \sum_{k=1}^{n} \binom{n}{k} A^{2(n-k)} \cdot 4^k \{ (-mk_a)^{k+\ell-1} \cdot \frac{kBk_a}{E_d^{k-1}}$$

$$+ \binom{k+\ell-1}{1} (-mk_a)^{k+\ell-2} \cdot \frac{\binom{k}{2}(Bk_a)^2}{E_d^{k-2}} + \binom{k+\ell-1}{2} (-mk_a)^{k+\ell-3} \frac{\binom{k}{3}(Bk_a)^3}{E_d^{k-3}} +$$

$$\cdots \} \frac{(\frac{Z}{2})^{2n}}{(2n)!} \tag{3-18}$$

The residue at $p = -mk_a$ for Eq. (3-17) is

$$\sum_{\ell=0}^{\infty} \frac{t^{\ell}}{\ell!} \sum_{n=1}^{\infty} \sum_{k=1}^{n} \binom{n}{k} A^{2n+1-2k} 4^k \{ (-mk_a)^{k+\ell-1} \frac{kBk_a}{E_d^{k-1}}$$

$$+ \binom{k+\ell-1}{1} (-mk_a)^{k+\ell-2} \frac{\binom{k}{2}(Bk_a)^2}{E_d^{k-2}} + \binom{k+\ell-1}{2} (-mk_a)^{k+\ell-3} \frac{\binom{k}{3}(Bk_a)^3}{E_d^{k-3}} +$$

$$\cdots \} \frac{(\frac{Z}{2})^{2n+1}}{(2n+1)!} \tag{3-19}$$

Substitute Eqs. (3-15), (3-18) and (3-19) into Eq. (3-14), the inverse transform of $\overline{C}_A(p)$ is

$$C'_A(z,t) = 1 + \{ \sum_{\ell=0}^{\infty} \frac{t^{\ell}}{\ell!} \sum_{n=1}^{\infty} \sum_{k=1}^{n} 4^k [(-mk_a)^{k+\ell-1} \frac{kBk_a}{E_d^{k-1}}$$

$$+ \binom{k+\ell-1}{1} (-mk_a)^{k+\ell-2} \frac{\binom{k}{2}(Bk_a)^2}{E_d^{k-2}} + \binom{k+\ell-1}{2} (-mk_a)^{k+\ell-3} \frac{\binom{k}{3}(Bk_a)^3}{E_d^{k-3}}$$

$$+ \cdots] \cdot [\binom{n}{k} \cdot A^{2(n-k)} \frac{(\frac{Z}{2})^{2n}}{(2n)!} - \binom{n}{k} \cdot A^{2n+1-2k} \frac{(\frac{Z}{2})^{2n+1}}{(2n+1)!}] \} e^{\frac{A}{2}z} \tag{3-20}$$

Model B

Material balance of solid phase:

$$(1 - \varepsilon)SdZ \, \frac{\partial C_{AS}}{\partial t} = k_f a(C_A - C_A^*)SdZ \tag{3-21}$$

Material balance of liquid phase:

$$\varepsilon SdZ \, \frac{\partial C_A}{\partial t} = -Q \, \frac{\partial C_A}{\partial Z} \, dZ - (1-\varepsilon)SdZ \, \frac{\partial C_{AS}}{\partial t} + E_d \, \frac{\partial^2 C_A}{\partial Z^2} \, \varepsilon SdZ \tag{3-22}$$

Equilibrium relationship between solid phase and liquid phase:

$$C_A^* = mC_{AS} \tag{3-23}$$

Introducing dimensionless variables:

$$C'_{AS} = \frac{C_{AS} - C_{AS,t_o}}{C_{A0} - C_{A,t_o}} \, , \qquad C'_A = \frac{C_A - C_{A,t_o}}{C_{A0} - C_{A,t_o}} \, ,$$

$$C'^*_A = \frac{C_A^* - C_{A,t_o}}{C_{A0} - C_{A,t_o}} \, , \qquad \text{note } C^*_{A,t_o} = C_{A,t_o}$$

Equations (3-21), (3-22) and (3-23) become

$$\frac{\partial C'_{AS}}{\partial t} = \frac{k_f a}{1-\varepsilon} \, (C'_A - C'^*_A) \tag{3-24}$$

$$\frac{\partial C'_A}{\partial t} + \frac{1-\varepsilon}{\varepsilon} \, \frac{\partial C'_{AS}}{\partial t} = E_d \, \frac{\partial^2 C'_A}{\partial Z^2} - \frac{Q}{\varepsilon S} \, \frac{\partial C'_A}{\partial Z} \tag{3-25}$$

$$C'^*_A = mC'_{AS} \tag{3-26}$$

With I.C.'s

$$C'_A(z,t=0)=0, \quad C'^*_A(z,t=0)=0, \quad C'_{AS}(z,t=0)=0$$

Take Laplace Transform of Eqs. (3-24), (3-25) and (3-26)

$$p\bar{C}_{AS} = \frac{k_f a}{1-\varepsilon} \, (\bar{C}_A - \bar{C}_A^*) \tag{3-27}$$

$$p\bar{C}_A + (\frac{1-\varepsilon}{\varepsilon})p\bar{C}_{AS} = E_d \, \frac{d^2\bar{C}_A}{dZ^2} - \frac{Q}{\varepsilon S} \, \frac{d\bar{C}_A}{dZ} \tag{3-28}$$

$$\bar{C}_A^* = m\bar{C}_{AS} \tag{3-29}$$

Combine Eqs. (3-27) and (3-29)

$$\frac{p}{m} \overline{C}_A{}^* = \frac{k_f a}{1-\epsilon} (\overline{C}_A - \overline{C}_A{}^*)$$ (3-30)

Combine Eqs. (3-27) and (3-28)

$$p\overline{C}_A + (\frac{1-\epsilon}{\epsilon}) \frac{k_f a}{1-\epsilon} (\overline{C}_A - \overline{C}_A{}^*) = E_d \frac{d^2\overline{C}_A}{dz^2} - \frac{Q}{\epsilon S} \frac{d\overline{C}_A}{dz}$$ (3-31)

Put Eq. (3-30) into (3-31)

$$\frac{d^2\overline{C}_A}{dz^2} - A \frac{d\overline{C}_A}{dz} - F \overline{C}_A = 0$$ (3-32)

where,

$$A = \frac{Q}{\epsilon S E_d} \quad , \quad B = (\frac{1-\epsilon}{\epsilon}) \frac{1}{E_d} \quad , \quad F = \frac{p}{E_d} + \frac{B k_a p}{p+m k_a}, \quad k_a = \frac{k_f a}{1-\epsilon}$$

The general solution of Eq. (3-32) is

$$\overline{C}_A = e^{\frac{A}{2}z} [C_1 \cosh \frac{\sqrt{A^2+4F}}{2} z + C_2 \sinh \frac{\sqrt{A^2+4F}}{2}z]$$ (3-33)

Note F is a function of p

Boundary condition 1: shell mass balance at the inlet of the column.

$$QC_{A0} - QC_A\big|_{Z=\Delta Z} + S\epsilon E_d \frac{\partial C_A}{\partial Z}\big|_{Z=\Delta Z} = \Delta Z \cdot S \cdot \epsilon \frac{\partial C_A}{\partial t}$$ (3-34)

Divided by Q and letting $\Delta Z \to 0$

$$C_{A0} - C_A\big|_{Z=0} + \frac{S\epsilon E_d}{Q} \frac{\partial C_A}{\partial Z}\big|_{Z=0} = 0$$ (3-35)

After introducing dimensionless variable

$$C'_A = \frac{C_A - C_{A,t_o}}{C_{A0} - C_{A,t_o}}$$

and taking Laplace Transform, Eq. (3-35) becomes

$$\frac{1}{A} \left.\frac{d\overline{C}_A}{dZ}\right|_{Z=0} - \left.\overline{C}_A\right|_{Z=0} + \frac{1}{p} = 0 \qquad (3-36)$$

Boundary Condition 2: Total material balance of column

$$Q\int_{t=0}^{t=t} (C_{A0}-\left.C_A\right|_{Z=L})dt = S\cdot\epsilon\int_{Z=0}^{Z=L}(C_A-C_{A,t_o})dZ + \int_{Z=0}^{Z=L}(C_{AS}-C_{AS,t_o})(1-\epsilon)SdZ$$

After introducing dimensionless variables $C'_A{}^*$ and C'_{AS} and taking Laplace Transform, above equation becomes

$$A(\frac{1}{p} - \left.\overline{C}_A\right|_{X=L}) = F\int_{Z=0}^{Z=L} \overline{C}_A dZ \qquad (3-37)$$

By using B.C. 1 and B.C. 2, find out C_1 and C_2, substitute C_1 and C_2 into Eq. (3-33), then

$$\overline{C}_A = e^{\frac{A}{2}Z}\{\frac{-A\cosh\frac{\sqrt{A^2+4F}}{2} - \sqrt{A^2+4F}\sinh\frac{\sqrt{A^2+4F}}{2}L}{p[\sqrt{A^2+4F}\cosh\frac{\sqrt{A^2+4F}}{2}L + (A+\frac{2F}{A})\sinh\frac{\sqrt{A^2+4F}}{2}]}\sinh\frac{\sqrt{A^2+4F}}{2}Z$$

$$+ \frac{\sqrt{A^2+4F}\cosh\frac{\sqrt{A^2+4F}}{2} + A\sinh\frac{\sqrt{A^2+4F}}{2}L}{p[\sqrt{A^2+4F}\cosh\frac{\sqrt{A^2+4F}}{2}L + (A+\frac{2F}{A})\sinh\frac{\sqrt{A^2+4F}}{2}]}\cosh\frac{\sqrt{A^2+4F}}{2}Z\}$$

$$(3-38)$$

or

$$\overline{C}_A = e^{\frac{A}{2}Z}\frac{A\sinh\frac{(L-Z)\sqrt{A^2+4F}}{2} + \sqrt{A^2+4F}\cosh\frac{(L-Z)\sqrt{A^2+4F}}{2}}{P[\sqrt{A^2+4F}\cosh\frac{\sqrt{A^2+4F}}{2}L + (A+\frac{2F}{A})\sinh\frac{\sqrt{A^2+4F}}{2}L]}$$

$$= \frac{e^{\frac{A}{2}Z}}{p}\frac{j(p)}{\ell(p)} \qquad (3-39)$$

Next: check poles and singularities.

Equation (3-39) can be expressed as

$$\overline{C}_A = \frac{e^{\frac{A}{2}Z} \sum\limits_{n=0}^{\infty} [\frac{(\frac{L-Z}{2})^{2n}}{n!} + A\frac{(\frac{L-Z}{2})^{2n+1}}{(2n+1)!}](A^2+4F)^n}{p\sum\limits_{n=0}^{\infty}[\frac{(\frac{L}{2})^{2n}}{2n!} + (A + \frac{2F}{A})\frac{(\frac{L}{2})^{2n+1}}{(2n+1)!}](A^2+4F)^n} \qquad (3\text{-}40)$$

So there is no singularity in $\overline{C}_A(p)$. However, there are simple poles at $p=0$ and at

$$\sqrt{A^2+4F} \cosh \frac{\sqrt{A^2+4F}}{2}L + (A + \frac{2F}{A})\sinh \frac{\sqrt{A^2+4F}}{2}L = 0.$$

By using the Residue theorem,

$$L^{-1}[\overline{C}_A] = \Sigma \text{ residues of } e^{pt} \cdot \overline{C}_A(p) \text{ at poles.}$$

The residue at simple pole $p=0$ is

$$\lim_{p \to 0} p \cdot [e^{pt} \cdot \overline{C}_A(p)] = 1 \qquad (3\text{-}41)$$

The simple poles are eigenvalues which make $\ell(p)=0$ or

$$\frac{-\sqrt{A^2+4F}}{(A + \frac{2F}{A})} = \tanh \frac{\sqrt{A^2+4F}}{2}L \qquad (3\text{-}42)$$

Let

$$\sqrt{A^2+4F} = i\beta_n \qquad (3\text{-}43)$$

then

$$F = \frac{-\beta_n^2 - A^2}{4} \quad \text{or} \quad \frac{P_n}{E_d} + \frac{Bk_aP_n}{P_n+mk_a} = -\frac{\beta_n^2+A^2}{4} \qquad (3\text{-}44)$$

and

$$\tanh \frac{\sqrt{A^2+4F}}{2}L = \tanh i\beta_n \frac{L}{2} = i \tan \beta_n \frac{L}{2} \qquad (3\text{-}45)$$

Substitute Eqs. (3-43), (3-44) and (3-45) into Eq. (3-42),

Eq. (3-42) becomes

$$\tan \beta_n \frac{L}{2} = \frac{-2A\beta_n}{A^2 - \beta_n^2} \qquad (3-46)$$

So β_n can be solved graphically or numerically. Substituting β_n

values into Eq. (3-44), then p_n can be obtained.

The residues at poles at p_n are

$$\lim_{p \to p_n} (p - p_n) \cdot [e^{pt} \cdot \overline{C}_A(p)]$$

$$= \lim_{p \to p_n} (p - p_n) e^{pt} \cdot e^{\frac{A}{2}z} \frac{j(p)}{p\ell(p)}$$

$$= \{ \lim_{p \to p_n} \frac{(p - p_n)}{\ell(p)} \} \{ \lim_{p \to p_n} e^{\frac{A}{2}z} \frac{j(p)}{p} e^{pt} \}$$

$$= \{ \lim_{p \to p_n} \frac{\frac{d}{dp}(p - p_n)}{\frac{d}{dp} \ell(p)} \} e^{\frac{A}{2}z} \frac{j(p_n)}{p_n} e^{p_n t}$$

$$= e^{\frac{A}{2}z} \frac{j(p_n)}{p_n \ell'(p_n)} e^{p_n t} \qquad (3-47)$$

Now to calculate $\ell'(p)$

$$\ell'(p) = \frac{d}{dp}[\sqrt{A^2+4F} \cosh \frac{\sqrt{A^2+4F}}{2}L + (A + \frac{2F}{A})\sinh \frac{\sqrt{A^2+4F}}{2}L]$$

$$= H(p)[(\frac{2A+LA^2+2LF}{2A})\cosh\frac{\sqrt{A^2+4F}}{2}L + \sqrt{A^2+4F}(\frac{L}{2} + \frac{1}{A})\sinh\frac{\sqrt{A^2+4F}}{2}L]$$

$$(3-48)$$

where

$$H(p) = 2[\frac{1}{E_d} + Bk_aG(p)]/\sqrt{A^2+4F}$$

$$G(p) = \frac{1}{p + mk_a} - \frac{p}{(p + mk_a)^2}$$

The inverse of $\overline{C}_A$ is

$$C'_A(Z,t) = 1 + e^{\frac{A}{2}Z} \sum_{n=1}^{\infty} \frac{j(p_n)}{p_n \ell'(p_n)} e^{p_n t} \qquad (3-49)$$

Since

$$\sqrt{A^2+4F} = i\beta_n \quad , \qquad F = \frac{-\beta_n^2 - A^2}{4} \quad ,$$

$$\sinh(ix) = i \sin x \quad ,$$

$$\cosh(ix) = \cos x$$

Equation (3-49) can be reduced to

$$C'_A(Z,t) = 1-e^{\frac{A}{2}Z} \sum_{n=1}^{\infty} \frac{\beta_n[A\sin\frac{(L-Z)\beta_n}{2} + \beta_n\cos\frac{(L-Z)\beta_n}{2}]}{p_n 2[\frac{1}{E_d} + Bk_aG(p_n)]Q(p_n)} e^{p_n t}$$

$$(3-50)$$

where

$$Q(p_n)=(1 + \frac{LA}{4} - \frac{L\beta_n^2}{4A})\cos\frac{L\beta_n}{2} - \beta_n(\frac{L}{2} + \frac{1}{A})\sin\frac{L\beta_n}{2}$$

The calculated result of Model B is shown in Figures 3.1 and 3.2.

$$Q = 0.5 \qquad m = 0.5$$
$$\epsilon = 0.75 \qquad k_f = 0.0001$$
$$S = 2. \qquad a = 300.$$
$$Z = 10.$$

$\dfrac{C_A}{C_{AO}}$

$E_D = 1.0$

$E_D = 0.2$

$E_D = 0$ (Bird et. al.)

time
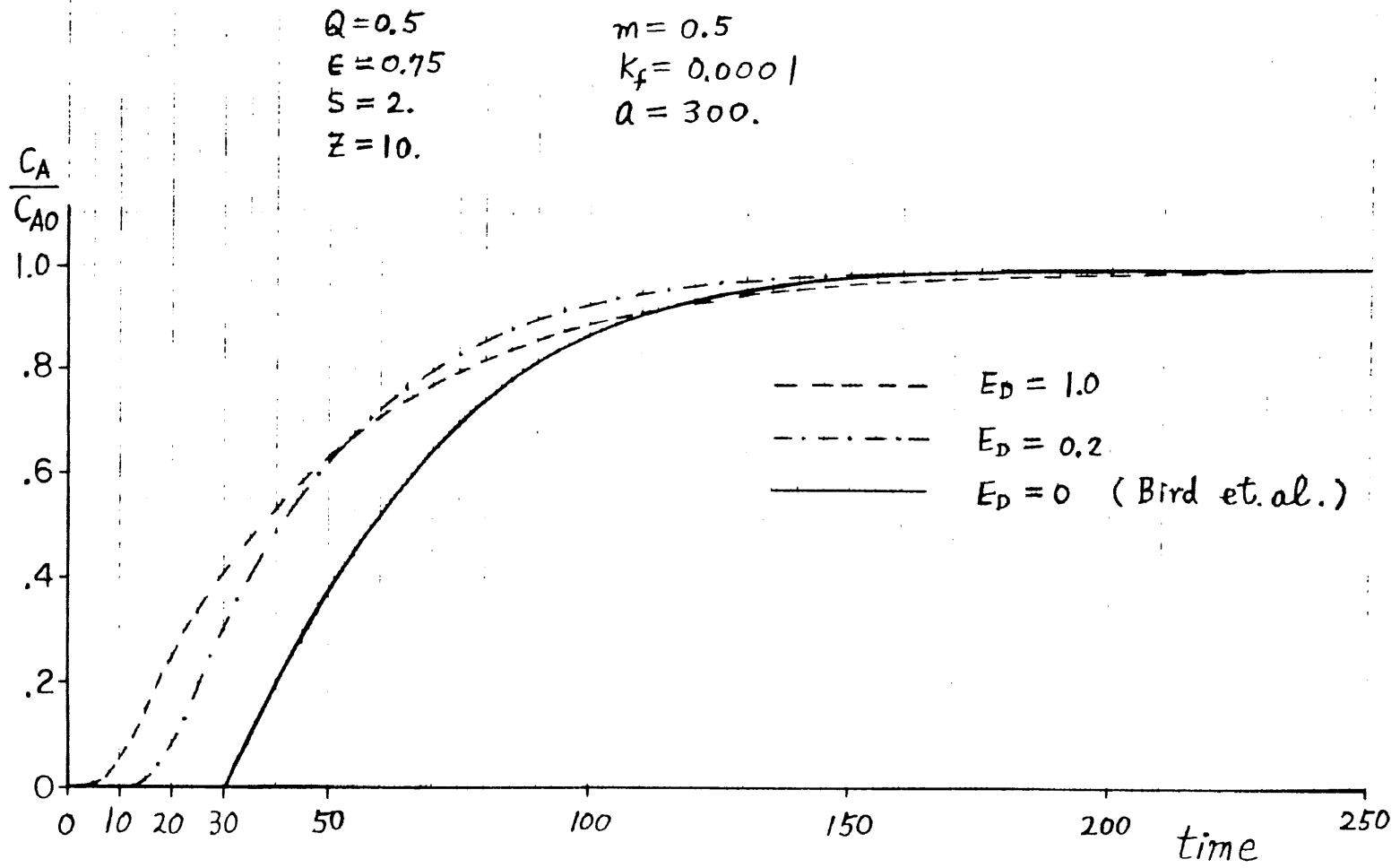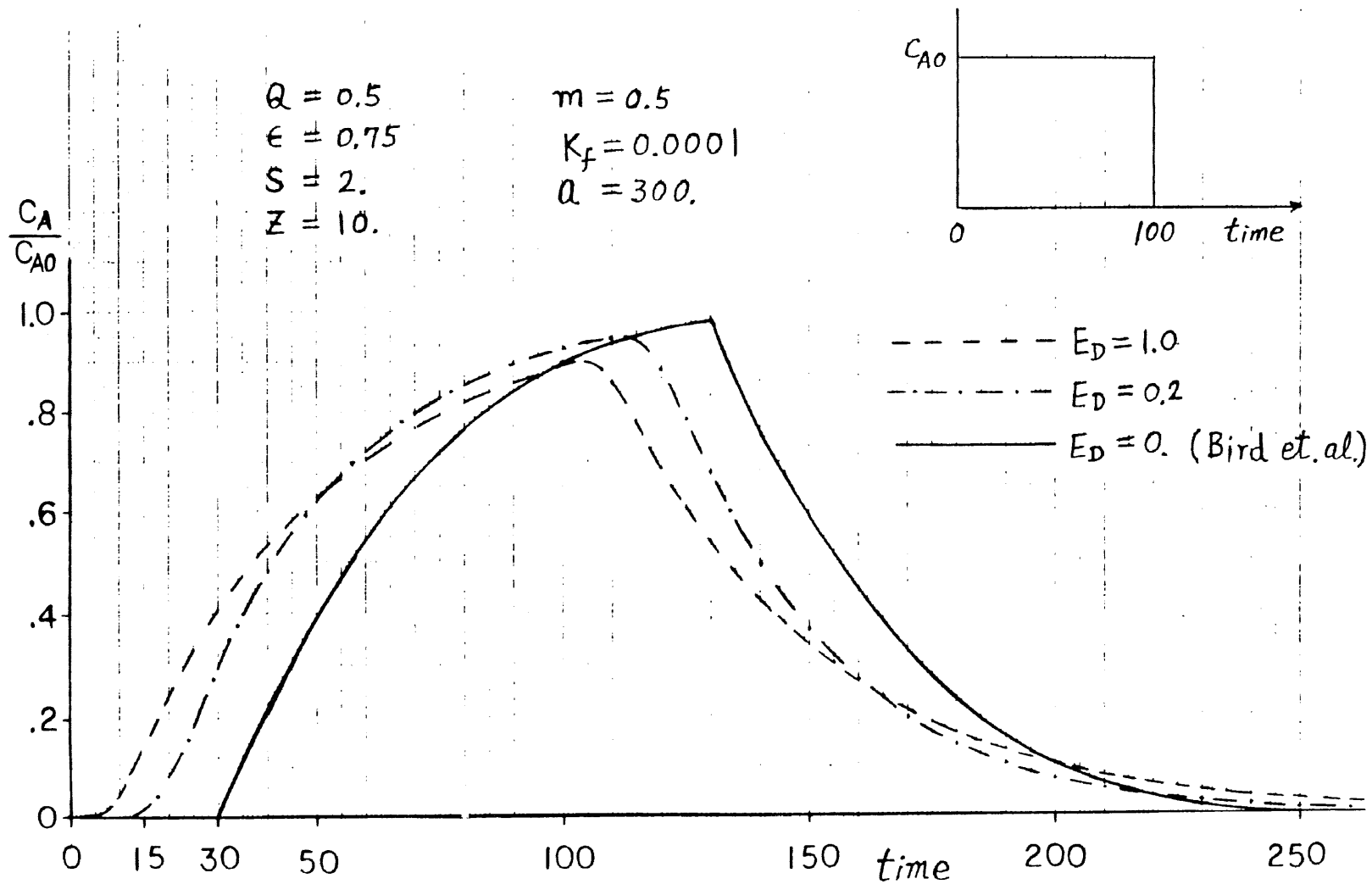
FIGURE 3.1

FIGURE 3.2

CHAPTER IV

WITH DIFFUSION IN PARTICLES AND LONGITUDINAL DISPERSION IN BED

Material balance on fluid phase:

$$\varepsilon S \Delta Z \frac{\partial C_A}{\partial t} = v S C_A \Big|_{Z=Z} - v S C_A \Big|_{Z=Z+\Delta Z}$$

$$- \frac{S \Delta Z (1-\varepsilon)}{\frac{4}{3} \pi r_0^3} \cdot 4 \pi r_0^2 k_f (C_A - C_A^*)$$

$$- \varepsilon S E_D \frac{\partial C_A}{\partial Z} \Big|_{Z=Z} + \varepsilon S E_D \frac{\partial C_A}{\partial Z} \Big|_{Z=Z+\Delta Z}$$

divided by $\Delta Z \cdot \varepsilon \cdot S$; $\Delta Z \to 0$

$$\frac{\partial C_A}{\partial t} = - \frac{v}{\varepsilon} \frac{\partial C_A}{\partial Z} - \frac{1-\varepsilon}{\varepsilon} \frac{3}{r_o} k_f (C_A - C_A^*)$$

$$+ E_D \frac{\partial^2 C_A}{\partial Z^2} \qquad (4-1)$$

Material balance on resin phase:

$$4 \pi r^2 N_{Ar} \Big|_r - 4 \pi (r+\Delta r)^2 N_{Ar} \Big|_{r+\Delta r} = 4 \pi r^2 \Delta r \frac{\partial C_{AS}}{\partial t}$$

divided by $4 \pi \Delta r$; $\Delta r \to 0$

$$- \frac{\partial (r^2 N_{Ar})}{\partial r} = r^2 \frac{\partial C_{AS}}{\partial t}$$

Since

$$\dot{N}_{Ar} = -D_S \frac{\partial C_{AS}}{\partial r}$$

$$\frac{\partial C_{AS}}{\partial t} = D_S \left(\frac{\partial^2 C_{AS}}{\partial r^2} + \frac{2}{r} \frac{\partial C_{AS}}{\partial r} \right) \qquad (4-2)$$

Equilibrium relationship between solid and liquid phases:

At $C_{AS}(r=r_0)$, we may assume a linear relationship

$$mC_{AS}(r=r_0, Z, t) = C_A^*(Z, t) \tag{4-3}$$

Note: m is a function of T, pH, etc.

I.C. and B.C.:

$$C_A(Z, t=0) = C_{A, t_0} \tag{4-4}$$

$$C_A^*(Z, t=0) = C_{A, t_0} \tag{4-5}$$

$$C_{AS}(r, Z, t=0) = C_{AS, t_0} \tag{4-6}$$

Note: $C_{AS, t_0} = C_{A, t_0}$

$$\frac{v}{\varepsilon} C_A(Z=0, t) - E_D \frac{\partial C_A}{\partial Z}\Big|_{Z=0} = \frac{v}{\varepsilon} C_{A0} \tag{4-7}$$

$\dfrac{\partial C_A}{\partial Z}(Z=L, t) = 0$ for small t

$C_A(Z=L, t) = C_{A0}$ for large t $\left.\phantom{\rule{0pt}{3em}}\right\}$ $\dfrac{\partial^2 C_A}{\partial Z^2}\Big|_{Z=L} = 0$

$\dfrac{\partial C_A}{\partial Z}\Big|_{Z=L}$ = finite for intermediate t $\tag{4-8}$

$$\frac{\partial C_{AS}}{\partial r}(r=0, Z, t) = 0 \tag{4-9}$$

$$D_S \frac{\partial C_{AS}}{\partial r}(r=r_0, Z, t) = k_f(C_A - C_A^*) \tag{4-10}$$

Introduce $-C'_{AS} = C_{AS} - C_{AS, t_0}$ into Eq. (4-2)

$$\frac{\partial C'_{AS}}{\partial t} = D_S\left(\frac{\partial^2 C'_{AS}}{\partial r^2} + \frac{2}{r} \frac{\partial C'_{AS}}{\partial r}\right) \tag{4-11}$$

Laplace Transform of above equation and use I.C. Eq. (4-6)

$$r^2 \frac{d^2\overline{C}_{AS}}{dr^2} + 2r \frac{d\overline{C}_{AS}}{dr} - \frac{p}{D_S} r^2 \overline{C}_{AS} = 0 \qquad (4\text{-}12)$$

From Mickley, Sherwood and Reed, page 174

$$\overline{C}_{AS} = r^{-1/2}[C_1 I_{1/2}(\sqrt{\frac{|p|}{D_S}} r) + C_2 I_{-1/2}(\sqrt{\frac{|p|}{D_S}} r) \qquad (4\text{-}13)$$

Note:

$$I_{1/2}(\sqrt{\frac{|p|}{D_S}} r) = \frac{(|p|/D_S)^{1/4}}{2^{1/2} \cdot \frac{1}{2}!} r^{1/2} \text{ for small } r$$

$$I_{-1/2}(\sqrt{\frac{|p|}{D_S}} r) = \frac{2^{1/2}}{(-\frac{1}{2})!} (\frac{|p|}{D_S})^{-1/4} \cdot r^{-1/2} \text{ for small } r$$

From Eq. (4-9)

$$C_{AS}(r=0, Z, t) = \text{finite}$$

or $\overline{C}_{AS} = -(C_{AS} - C_{AS,t_0})/p = \text{finite at } r = 0$

so $C_2 = 0$

$$\therefore \overline{C}_{AS} = C_1 r^{-1/2} I_{1/2}(\sqrt{\frac{|p|}{D_S}} r) \qquad (4\text{-}14)$$

Note: $C_1 = f(Z)$, since $\overline{C}_{AS} = f(r,Z)$

$$\frac{\partial \overline{C}_{AS}}{\partial r} = C_1 \sqrt{\frac{|p|}{D_S}} r^{-1/2} I_{3/2}(\sqrt{\frac{|p|}{D_S}} r)$$

$$\therefore \frac{\partial \overline{C}_A}{\partial r}\Big|_{r=r_0} = C_1 \sqrt{\frac{|p|}{D_S}} r_0^{-1/2} I_{3/2}(\sqrt{\frac{|p|}{D_S}} r_0) \qquad (4\text{-}15)$$

Introduce $C'_A = -(C_A - C_{A,t_0})$

$$C'_A{}^* = -(C_A{}^* - C^*{}_{A,t_0})$$

into Eq. (4-1), then

$$\frac{\partial C'_A}{\partial t} + \frac{(1-\varepsilon)}{\varepsilon} \frac{3}{r_0} k_f(C'_A - C'^*_A) = E_D \frac{\partial^2 C'_A}{\partial z^2} - \frac{v}{\varepsilon} \frac{\partial C'_A}{\partial z} \tag{4-16}$$

Laplace transform of Eq. (4-16) and use I.C. Eqs. (4-4) and (4-5)

$$p\overline{C}_A + \frac{(1-\varepsilon)}{\varepsilon} \frac{3}{r_0} k_f(\overline{C}_A - \overline{C}^*_A) = E_D \frac{d^2\overline{C}_A}{dz^2} - \frac{v}{\varepsilon} \frac{d\overline{C}_A}{dz} \tag{4-17}$$

From Eq. (4-10)

$$D_S \frac{\partial C'_{AS}}{\partial r}(r_0, z, t) = k_f(C'_A - C'^*_A)$$

Laplace Transform the above equation

$$D_S \frac{\partial \overline{C}_S}{\partial r}\bigg|_{r=r_0} = k_f(\overline{C}_A - \overline{C}^*_A) \tag{4-18}$$

Note: each term of Eq. (4-18) is a function of z only.

From Eq. (4-3), at t = 0

$$mC_{AS,t_0} = C^*_{A,t_0}$$

so

$$-m(C_{AS} - C_{AS,t_0}) = -(C^*_A - C^*_{A,t_0})$$

or

$$mC'_{AS} = C'^*_A \text{ at } r = r_0$$

Laplace transform the above equation

$$m\overline{C}_{AS} = \overline{C}^*_A \text{ at } r = r_0 \tag{4-19}$$

All basic equations (4-14), (4-15), (4-17), (4-18), and (4-19) are in the Laplace domain.

Put Eq. (4-14) into Eq. (4-19); at $r = r_0$, rid of $\overline{C}_{AS}$:

$$\overline{C}_A{}^* = C_1 m r_0^{-1/2} \, I_{1/2}\left(\sqrt{\frac{|p|}{D_S}}\, r_0\right) \tag{4-20}$$

Put Eq. (4-15) and (4-20) into Eq. (4-18)

$$C_1 = \frac{k_f \overline{C}_A}{\sqrt{D_S|p|}\cdot r_0^{-1/2}\cdot I_{3/2}\left(\sqrt{\frac{|p|}{D_S}}\, r_0\right)+ k_f m r_0^{-1/2} I_{1/2}\left(\sqrt{\frac{|p|}{D_S}}\, r_0\right)} \tag{4-21}$$

Put Eq. (4-21) into Eq. (4-20) to rid of C_1:

$$\overline{C}_A{}^* = \frac{k_f m I_{1/2}\left(\sqrt{\frac{|p|}{D_S}}\, r_0\right)\overline{C}_A}{\sqrt{D_S|p|}\, I_{3/2}\left(\sqrt{\frac{|p|}{D_S}}\, r_0\right) + k_f m I_{1/2}\left(\sqrt{\frac{|p|}{D_S}}\, r_0\right)} \tag{4-22}$$

Put Eq. (4-22) into Eq. (4-17) to obtain an ordinary differential equation of $\overline{C}_A$

$$\frac{d^2\overline{C}_A}{dZ^2} - A\,\frac{d\overline{C}_A}{dZ} - (Bp + D(p))\overline{C}_A = 0 \tag{4-23}$$

where,

$$A = \frac{v}{E_D}$$

$$B = \frac{1}{E_D}$$

$$D(p)= \frac{1-\varepsilon}{\varepsilon}\, \frac{3K_f}{E_D r_0}\left[1- \frac{k_f m I_{1/2}\left(\sqrt{\frac{|p|}{D_S}}\, r_0\right)}{\sqrt{D_S|p|}\, I_{3/2}\left(\sqrt{\frac{|p|}{D_S}} r_0\right)+k_f m I_{1/2}\left(\sqrt{\frac{|p|}{D_S}}\, r_0\right)}\right.$$

$$\therefore \overline{C}_A = e^{\frac{A}{2}Z}\left\{C_3 \sinh \frac{\sqrt{A^2+4(Bp+D(p))}}{2}Z + C_4 \cosh \frac{\sqrt{A^2+4(Bp+D(p))}}{2}Z\right\} \tag{4-24}$$

Now need find constants C_3 and C_4

From B.C. of Eq. (4-7): at $z=0$, $C_A = C_{A0}$ (simplified case)

so $\left. C'_A \right|_{z=0} = -\left. (C_A - C_{A,t_0}) \right|_{z=0} = -(C_{A0} - C_{A,t_0})$

After Laplace Transform

$$\left. \overline{C}_A \right|_{z=0} = -\frac{C_{A0} - C_{A,t_0}}{p}$$

Substitute above equation into (4-24), one obtains

$$C_4 = -\frac{C_{A0} - C_{A,t_0}}{p} \tag{4-25}$$

From B.C. of Eq. (4-8): at $Z=L$,

$$\frac{\partial^2 C_A}{\partial z^2} = 0 \qquad \text{or} \qquad \frac{d^2 \overline{C}_A}{dz^2} = 0$$

Therefore,

$$\frac{A^2}{2} e^{\frac{A}{2}L}\left[C_3 \sinh \frac{\sqrt{H(p)}}{2}L + C_4 \cosh \frac{\sqrt{H(p)}}{2}L\right] + Ae^{\frac{A}{2}}\left[C_3 \frac{\sqrt{H(p)}}{2}\cosh \frac{\sqrt{H(p)}}{2}L\right.$$

$$\left. + C_4 \frac{\sqrt{H(p)}}{2}\sinh \frac{\sqrt{H(p)}}{2}L\right] + [Bp+D(p)]e^{\frac{A}{2}L}\left[C_3 \sinh \frac{\sqrt{H(p)}}{2}L +\right.$$

$$\left. C_4\cosh \frac{\sqrt{H(p)}}{2}L\right] = 0$$

where

$$H(p) = A^2 + 4[Bp + D(p)]$$

So,

$$C_3 = -\frac{\frac{A^2}{2}\cosh \frac{\sqrt{H(p)}}{2}L + \frac{A\sqrt{H(p)}}{2}\sinh \frac{\sqrt{H(p)}}{2}L + [Bp+D(p)]\cosh \frac{\sqrt{H(p)}}{2}L}{\frac{A^2}{2}\sinh \frac{\sqrt{H(p)}}{2}L + \frac{A\sqrt{H(p)}}{2}\cosh \frac{\sqrt{H(p)}}{2}L + [Bp+D(p)]\sinh \frac{\sqrt{H(p)}}{2}L}C_4$$

$$\tag{4-26}$$

Note:

$$\sinh u = u + \frac{u^3}{3!} + \frac{u^5}{5!} + \frac{u^7}{7!} + \cdots$$

$$\cosh u = 1 + \frac{u^2}{2!} + \frac{u^4}{4!} + \frac{u^6}{6!} + \cdots$$

$$I_{1/2}(u) = \sum_{k=0}^{\infty} \frac{(u/2)^{2k+1/2}}{k!(k+1/2)!}$$

$$I_{3/2}(u) = \sum_{k=0}^{\infty} \frac{(u/2)^{2k+3/2}}{k!(k+3/2)!}$$

Use the method of residues for the inverse Laplace trans-
formation (page 296-303, Sherwood, Mickley and Reed).
Let

$$\overline{f}(p) = \frac{j(p)}{\ell(p)} ,$$

where $j(p)$, $\ell(p)$ are polynomial of p and the degree of $\ell(p)$
is at least one greater than that of $j(p)$.

Then

$$f(t) = \sum_{n=1}^{\infty} \zeta_n(t)$$

where

$\zeta_n(t)$ is the residue of $\overline{f}(p)$ at pole p_n

and

$$\zeta_n(t) = \frac{j(p_n)}{\ell'(p_n)} e^{p_n t} \qquad \text{for simple pole}$$

where

$$\ell'(p_n) = \frac{d\ell(p)}{dp}\bigg|_{p=p_n}$$

The next step is to take the inverse Laplace transformation:

$$I_{1/2}(\alpha\sqrt{|p|}) = a_1|p|^{1/4} + a_2|p|^{1+1/4} + a_3|p|^{2+1/4} + \ldots =$$

$$\frac{1}{2^{\frac{1}{2}}!}\frac{r_0^{1/2}}{D_S^{1/4}}|p|^{1/4} + \ldots$$

with $\alpha = \dfrac{r_0}{\sqrt{D_S}}$

$$I_{\frac{3}{2}}(\alpha\sqrt{|p|}) = b_1|p|^{\frac{3}{4}} + b_2|p|^{1+\frac{3}{4}} + b_3|p|^{2+\frac{3}{4}} + \ldots =$$

$$\frac{r_0^{\frac{3}{2}}|p|^{\frac{3}{4}}}{2^{3/2}(\frac{3}{2})!D_S^{3/4}} + \ldots$$

$$\sqrt{p}\; I_{\frac{3}{2}}(\alpha\sqrt{|p|}) = b_1|p|^{1+\frac{1}{4}} + b_2|p|^{2+\frac{1}{4}} + b_3|p|^{3+\frac{1}{4}} + \ldots =$$

$$\frac{r_0^{\frac{3}{2}}|p|^{1\frac{1}{4}}}{2^{3/2}(\frac{3}{2})!D_S^{3/4}} + \ldots$$

$$\therefore\; \frac{I_{\frac{1}{2}}(\alpha\sqrt{|p|})}{\sqrt{|p|}\; I_{\frac{3}{2}}(\alpha\sqrt{|p|}) + I_{\frac{1}{2}}(\alpha\sqrt{|p|})}\;\; \text{is a polynomial of } p$$

and $D(p) = $ a polynomial of p

so that

$$\frac{\sqrt{H(p)}}{2}L \;\;\text{is a polynomial of } p$$

Since $\cosh u = 1 + \dfrac{u^2}{2!} + \dfrac{u^4}{4!} + \dfrac{u^6}{6!} + \ldots$

and

$$\sinh u = u(1 + \frac{u^2}{3!} + \frac{u^4}{5!} + \frac{u^6}{7!} + \ldots)$$

so

$\cosh \frac{\sqrt{H(p)}}{2}L$ is a polynomial of p

$[\frac{\sqrt{H(p)}}{2}L]^{-1} \sinh \frac{\sqrt{H(p)}}{2}L$ is a polynomial of p

Look at Eq. (4-26), in order to have Eq. (4-24) in terms of

$\overline{C}_A = \frac{j(p)}{\ell(p)}$, we have to devide the first term of Eq. (4-24)

by

$$\frac{\sqrt{H(p)}}{2}L \cosh \frac{\sqrt{H(p)}}{2}L$$

in the numerator and denominator. After introducing Eq.
(4-25) and Eq. (4-26) into Eq. (4-24), Eq. (4-24) becomes,

$$\overline{C}_A = e^{\frac{A}{2}Z}[- \frac{j_1(p)}{\ell_1(p)} + \frac{j_2(p)}{\ell_2(p)}] \tag{4-27}$$

with

$$j_1(p) = (C_{A0} - C_{A,t_0})\cosh \frac{\sqrt{H(p)}}{2}Z$$

$$\ell_1(p) = p$$

$$j_2(p) = (C_{A0}-C_{A,t_0})[\frac{A^2}{2}+A\frac{\sqrt{H(p)}}{2}\tanh\frac{\sqrt{H(p)}}{2}L+[Bp+D(p)]]\frac{\sinh\frac{\sqrt{H(p)}}{2}Z}{\frac{\sqrt{H(p)}}{2}L}$$

$$\ell_2(p) = p[\frac{A^2}{2} \frac{\tanh\frac{\sqrt{H(p)}}{2}L}{\frac{\sqrt{H(p)}}{2}L} + \frac{A}{L} +[Bp+D(p)]\frac{\tanh\frac{\sqrt{H(p)}}{2}L}{\frac{\sqrt{H(p)}}{2}L}]$$

The pole of $\frac{j_1(p)}{\ell_1(p)}$ is at $p = 0$

$\therefore$ The residue $\zeta(t) = \dfrac{j_1(p=0)}{\ell'_1(p=0)} e^{0 \cdot t} = j_1(p=0)$

$$= (C_{A0} - C_{A,t_0}) \cosh \frac{\sqrt{H(p=0)}}{2} Z$$

$$= (C_{A0} - C_{A,t_0}) \cosh \frac{A}{2} Z \qquad (4-28)$$

Poles of $\dfrac{j_2(p)}{\ell_2(p)}$ are the roots make $\ell_2(p)=0$:

$p_1 = 0$, also

$$\frac{A^2}{2} \frac{\tanh \frac{\sqrt{H(p_n)}}{2} L}{\frac{\sqrt{H(p_n)}}{2} L} + \frac{A}{L} + [Bp_n + D(p_n)] \frac{\tanh \frac{\sqrt{H(p_n)}}{2} L}{\frac{\sqrt{H(p_n)}}{2} L} = 0$$

$$(4-29)$$

where

$$n = 2, \ 3, \ 4, \ \ldots$$

Let

$$\frac{\sqrt{A^2 + 4[Bp_n + D(p_n)]}}{2} L = i \, b_n \qquad (4-30)$$

then

$$\tanh \frac{\sqrt{A^2 + 4[Bp_n + D(p_n)]}}{2} L = \tanh ib_n = i \tan b_n$$

$$(4-31)$$

and

$$\sqrt{A^2 + 4[Bp_n + D(p_n)]} = ib_n \frac{2}{L}$$

$$[Bp_n + D(p_n)] = -\frac{b_n^2}{L^2} - \frac{A^2}{4} \qquad (4-32)$$

Equation (4-29) becomes

$$\frac{A^2}{2} \frac{i\tan b_n}{ib_n} + \frac{A}{L} - \left(\frac{b_n^2}{L^2} + \frac{A^2}{4}\right) \frac{i\tan b_n}{ib_n} = 0$$

or

$$\tan b_n = \frac{\frac{A}{L} b_n}{\frac{b_n^2}{L^2} - \frac{A^2}{4}} = \frac{4Ab_nL}{4b_n^2 - L^2A^2} \tag{4-33}$$

Equation (4-33) is used to solve for b_n, $n = 2, 3, 4, \ldots$, b_n can be solved graphically or by computer.

Note: From Eq. (4-32), knowing values of b_n; p_n (n=2, 3, 4, ...) can be obtained numerically. Since $C_A(Z,t)$ decreases with t, p_n (n=2, 3, 4, ...) should be negative quantities.

Once p_n is known, the next step is to find out

$$\ell'_2(p_n) = \frac{d\ell_2(p)}{dp}\bigg|_{p=p_n} , \text{ where } n = 2, 3, 4, \ldots$$

$$\frac{d}{dx}[xI_m(\alpha x)] = \alpha x I_{m-1}(\alpha x) + (1-m)I_m(\alpha x)$$

$$\frac{d}{dx}[I_m(\alpha x)] = \alpha I_{m-1}(\alpha x) - \frac{m}{x} I_m(\alpha x)$$

$$I_{m-1}(\alpha x) = \frac{2m}{\alpha x} I_m(\alpha x) + I_{m+1}(\alpha x)$$

$$\frac{d}{dp}[\sqrt{|p|}\, I_{\frac{3}{2}}(\frac{r_0}{\sqrt{D_S}}\sqrt{|p|})] = \frac{d[\sqrt{|p|}\, I_{\frac{3}{2}}(\frac{r_0}{\sqrt{D_S}}\sqrt{|p|})]}{d\sqrt{|p|}} \cdot \frac{d\sqrt{|p|}}{dp}$$

$$= \frac{r_0}{2\sqrt{D_S}} I_{\frac{1}{2}}(\frac{r_0}{\sqrt{D_S}}\sqrt{|p|}) - \frac{1}{4\sqrt{|p|}} I_{\frac{3}{2}}(\frac{r_0}{\sqrt{D_S}}\sqrt{p})$$

$$\frac{d}{dp}[I_{\frac{1}{2}}(\frac{r_0}{\sqrt{D_S}}\sqrt{|p|})] = \frac{d[I_{\frac{1}{2}}(\frac{r_0}{\sqrt{D_S}}\sqrt{|p|})]}{d\sqrt{|p|}} \cdot \frac{d\sqrt{|p|}}{dp}$$

$$= [\frac{r_0}{\sqrt{D_S}} I_{-\frac{1}{2}}(\frac{r_0}{\sqrt{D_S}}\sqrt{|p|}) - \frac{1}{2\sqrt{|p|}} I_{\frac{1}{2}}(\frac{r_0}{\sqrt{D_S}}\sqrt{|p|})]\frac{1}{2} \cdot \frac{1}{\sqrt{|p|}}$$

$$= \frac{r_0}{2\sqrt{|p|}D_S} I_{\frac{3}{2}}(\sqrt{\frac{|p|}{D_S}} r_0) + \frac{1}{4|p|} I_{\frac{1}{2}}(\sqrt{\frac{|p|}{D_S}} r_0)$$

From the definition of D(p)

$$D(p) = \frac{1-\epsilon}{\epsilon} \cdot \frac{3K_f}{E_D r_0}[1 - \frac{K_f m I_{\frac{1}{2}}(\sqrt{\frac{|p|}{D_S}} r_0)}{\sqrt{D_S|p|}I_{\frac{3}{2}}(\sqrt{\frac{|p|}{D_S}} r_0) + K_f m I_{\frac{1}{2}}(\sqrt{\frac{|p|}{D_S}}r_0)}$$

$$\frac{dD(p)}{dp} = \frac{3(1-\epsilon)K_f}{\epsilon E_D r_0}[\frac{K_f m r_0}{2}(I_{\frac{1}{2}}(\sqrt{\frac{|p|}{D_S}}r_0))^2 - \frac{K_f m r_0}{2}(I_{\frac{3}{2}}(\sqrt{\frac{|p|}{D_S}}r_0))^2$$

$$- \frac{K_f m}{2}\sqrt{\frac{D_S}{|p|}}I_{\frac{1}{2}}(\sqrt{\frac{|p|}{D_S}}r_0)I_{\frac{3}{2}}(\sqrt{\frac{|p|}{D_S}}r_0)]/[\sqrt{D_S|p|}I_{\frac{3}{2}}(\sqrt{\frac{|p|}{D_S}}r_0)$$

$$+ K_f m I_{\frac{1}{2}}(\sqrt{\frac{|p|}{D_S}}r_0)]^2$$

$$= F(p) \tag{4-34}$$

$$\frac{d(\frac{\sqrt{H(p)}}{2}L}{dp} = \frac{d}{dp}\{\sqrt{A^2 + 4[Bp + D(p)]} \cdot \frac{L}{2}\}$$

$$= \frac{L}{2} \cdot \frac{1}{2} \cdot \frac{4B + 4\frac{dD(p)}{dp}}{\sqrt{A^2 + 4Bp + D(p)}}$$

$$= \frac{B + F(P)}{\sqrt{A^2 + 4[Bp + D(p)]}} \cdot L = Q(p) \tag{4-35}$$

$$\frac{d(\tanh \frac{\sqrt{H(p)}}{2}L)}{dp} = \frac{d(\tanh \frac{\sqrt{H(p)}}{2}L)}{d(\frac{\sqrt{H(p)}}{2}L)} \cdot \frac{d(\frac{\sqrt{H(p)}}{2}L)}{dp}$$

$$= (\text{sech} \frac{\sqrt{A^2+4[Bp+D(p)]}}{2}L)^2 \cdot \frac{[B + F(p)]L}{\sqrt{A^2+4(Bp+D(p))}}$$

$$= G(p) \tag{4-36}$$

Now we can evaluate $\ell'_2(p)$:

$$\ell'_2(p) = \frac{d}{dp}\{p[\frac{A^2}{2}\frac{\tanh \frac{\sqrt{H(P)}}{2}L}{\frac{\sqrt{H(p)}}{2}L} + \frac{A}{L} +[Bp+D(p)]\frac{\tanh \frac{\sqrt{H(p)}}{2}L}{\frac{\sqrt{H(p)}}{2}L}]\}$$

$$= \frac{A^2}{2}\frac{\tanh \frac{\sqrt{H(p)}}{2}L}{\frac{\sqrt{H(p)}}{2}L} + \frac{A}{L} + [Bp+D(p)]\frac{\tanh \frac{\sqrt{H(p)}}{2}L}{\frac{\sqrt{H(p)}}{2}L}$$

$$+ p\{\frac{A^2}{2}[\frac{G(p)}{\frac{\sqrt{H(p)}}{2}L} - \frac{(\tanh \frac{\sqrt{H(p)}}{2}L)\cdot Q(p)}{(\frac{\sqrt{H(p)}}{2}L)^2}]+[B+F(p)]\frac{\tanh \frac{\sqrt{H(p)}}{2}L}{\frac{\sqrt{H(p)}}{2}L}$$

$$+ \frac{Bp+D(p)}{\frac{\sqrt{H(p)}}{2}L}G(p) - \frac{[Bp+D(p)]\tanh \frac{\sqrt{H(p)}}{2}L}{(\frac{\sqrt{H(p)}}{2}L)^2}Q(p)\} \tag{4-37}$$

Therefore the inverse Laplace transform of $\overline{C}_A$ is

$$C'_A(Z,t) = e^{\frac{A}{2}Z}[-L^{-1}(\frac{j_1(p)}{\ell_1(p)}) + L^{-1}(\frac{j_2(p)}{\ell_2(p)})]$$

$$= e^{\frac{A}{2}Z}\{-(C_A-C_{A,t_0})\cosh\frac{A}{2}Z + \frac{j_2(p_1=0)}{\ell'_2(p_1=0)} + \sum_{n=2}^{\infty}\frac{j_2(p_n)}{\ell'_2(p_n)}e^{p_n t}\}$$

$$\tag{4-38}$$

Since

$$\frac{j_2(p_1=0)}{\ell'_2(p_1=0)} = (C_{A0} - C_{A,t_0})\sinh\frac{A}{2}Z$$

Equation (4-38) can be written as

$$C'_A(Z,t) = -(C_{A0} - C_{A,t_0}) + e^{\frac{A}{2}Z} \sum_{n=2}^{\infty} \frac{j_2(p_n)}{\ell'_2(p_n)} e^{p_n t} \qquad (4-39)$$

Also;

$$\sqrt{A^2 + 4[Bp_n + D(p_n)]} = i\, b_n\frac{2}{L} \quad,$$

$$A^2 + 4[Bp_n + D(p_n)] = -b_n^2\frac{4}{L^2} \quad,$$

$$Bp_n + D(p_n) = \frac{-b_n^2}{L^2} - \frac{A^2}{4} \quad,$$

$$\tanh\frac{\sqrt{A^2 + 4[Bp_n + D(p_n)]}}{2}L = \tanh ib_n = i\tan b_n\,,$$

$$\text{sech}\frac{\sqrt{A^2 + 4[Bp_n + D(p_n)]}}{2}L = \text{sech}\, ib_n = i\sec b_n$$

Therefore the final solution is

$$C'_A = -(C_{A0}-C_{A,t_0}) + (C_{A0}-C_{A,t_0})e^{\frac{A}{2}Z}\sum_{n=2}^{\infty}\frac{u(b_n)}{v(b_n)}e^{p_n t}$$

or

$$\frac{C_A - C_{A,t_0}}{C_{A0} - C_{A,t_0}} = 1 - e^{\frac{A}{2}Z}\sum_{n=2}^{\infty}\frac{u(b_n)}{v(b_n)}e^{p_n t} \qquad (4-40)$$

where

$$u(b_n) = [\frac{A^2}{4} - \frac{b_n^2}{L^2} - \frac{Ab_n}{L}\tan b_n]\frac{\sin b_n\frac{Z}{L}}{b_n}$$

$$v(b_n) = p_n[B+F(p_n)][\frac{\frac{A^2L^2}{2} + 2b_n^2}{4b_n^3}\tan b_n - \frac{\frac{A^2L^2}{2} - 2b_n^2}{4b_n^2}(\sec b_n)^2]$$

The calculation results are shown in Figs. 4.1 and 4.2.

$$v = 0.25 \qquad m = 0.5$$
$$\mathcal{E} = 0.75 \qquad K_f = 0.0001$$
$$S = 2. \qquad D_S = 0.05$$
$$Z = 10. \qquad r_0 = 0.1$$

- - - - - $E_D = 0.2$
- · - · - $E_D = 0.5$
——— $E_D = 1.0$

FIGURE   4.1

$v = 0.25$ $m = 0.5$
$\epsilon = 0.75$ $k_f = 0.0001$
$S = 2.$ $D_S = 0.05$
$Z = 10.$ $E_D = 0.2$

$\dfrac{C_A}{C_{AO}}$

$r_o = 0.01$
$r_o = 0.1$
$r_o = 0.5$

time
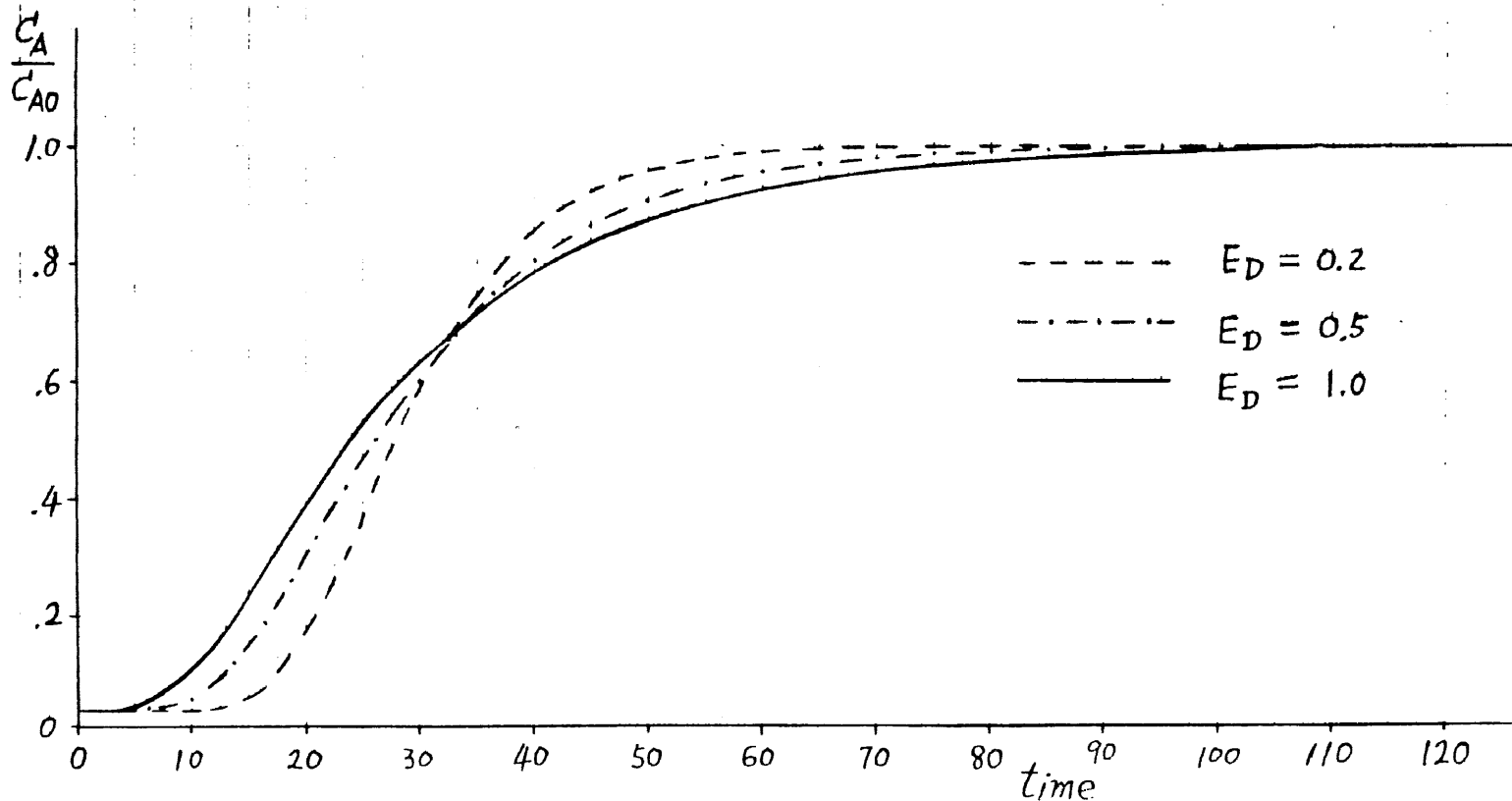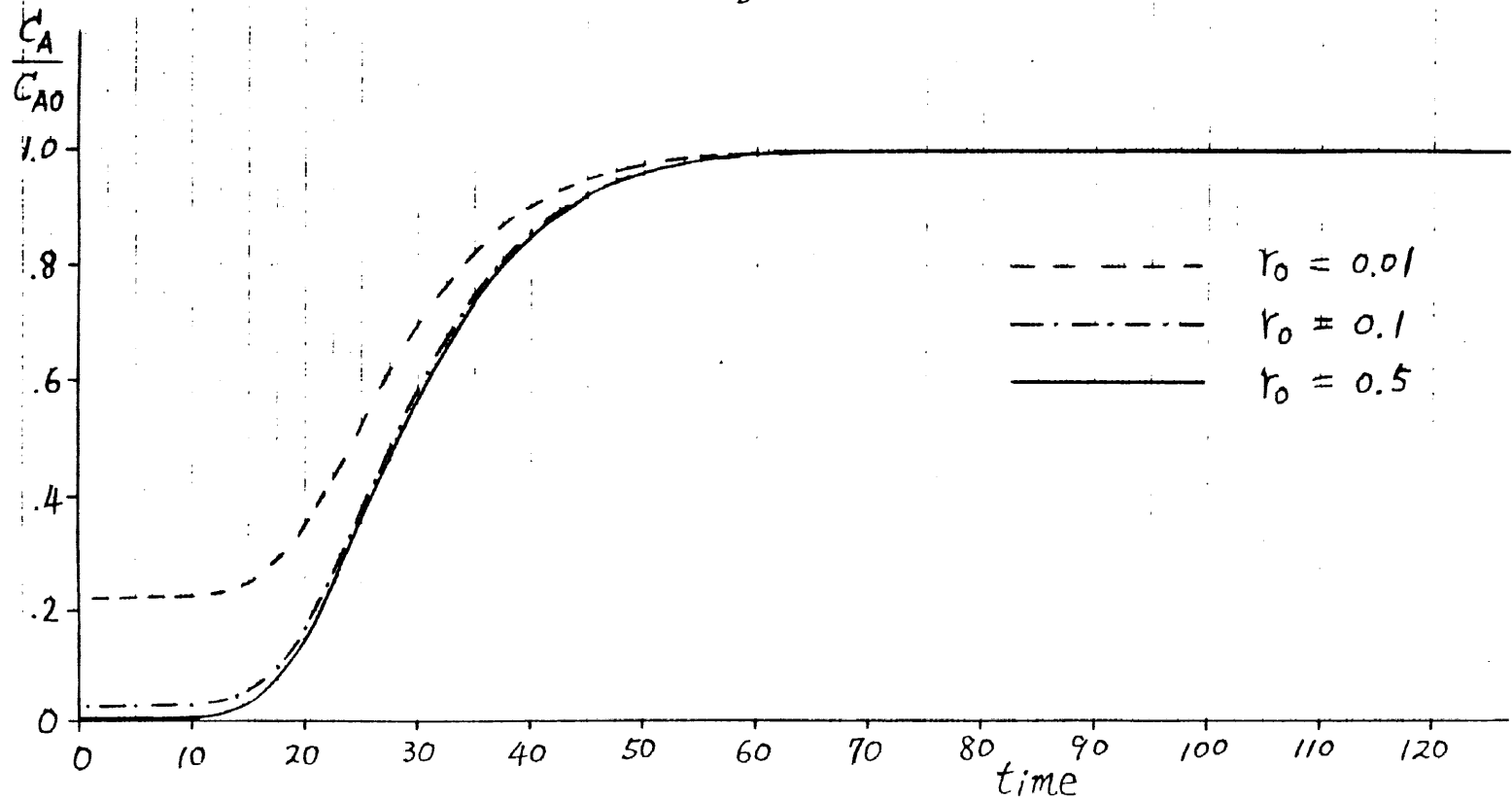
FIGURE   4.2

CHAPTER V

DISCUSSION AND CONCLUSIONS

The analytical solutions of the differential equations, which describe the dynamic behavior of packed bed operations, have been derived. Three different cases are examined. The first one takes account of surface adsorption on particles only. The second one includes surface adsorption on particles and the effect of longitudinal dispersion in the bed. The third one illustrates diffusion through the network of the particles and longitudinal dispersion in the bed. Since models for the above cases already exist in the literature[2,3,4], a comparison of the present work with previous work is listed in Table 5-1.

Bird et al.[2] obtained the solution to the first case by adopting the solution of the analogous heat transfer problem. The heat-transfer case was originally solved by Anzelius[5] by an analytical technique different from this work. Bird et al. provided a solution for the liquid phase in an integral form. This work provides the final solutions both for liquid and solid phases also in an integral form. The numerical values of their solution and this work are consistent.

Lapidus and Amundson[3] derived a model which considered the effect of linear surface adsorption and longitudinal dispersion in the bed (case II). They assumed that at $Z=\infty$, the concentration in the liquid phase is zero. Therefore the mathematical manipulation can be simplified by dropping the term with the positive

TABLE 5-1. Characteristics of Various Models

	This Work	Published Models	Ref.
With diffusion in particles and longitudinal dispersion in packed bed	(1) $Z=0$, $C=C_{in}$ (2) $Z=L$, $\dfrac{\partial^2 C}{\partial Z^2}=0$ (3) solution in summation form	(1) $Z=0$, $C=C_{in}$ (2) $Z=\infty$, $C=0$ (3) solution in integral form	Rasmuson (1981)
With longitudinal dispersion in packed bed	(1) $Z=0$, $C=C_{in}$ (2) $Z=0$, $\dfrac{\partial C}{\partial Z}=0$ (3) solution in summation form	(1) $Z=0$, $C=C_{in}$ (2) $Z=\infty$, $C=0$ (3) solution in integral form	Lapidus & Amundson (1952)

(1) $Z=0$, $C_{in}-C\big|_{Z=0}+\dfrac{S\,\varepsilon E_D}{Q}\,\dfrac{\partial C}{\partial Z}\bigg|_{Z=0}=0$

(2) $Q\displaystyle\int_{t=0}^{t}(C_{in}-C\big|_{Z=L})dt$
$=S\cdot\varepsilon\displaystyle\int_{Z=0}^{Z=L}(C-C_{in})dZ+\int_{Z=0}^{Z=L}(C_S-C_{SO})(1-\varepsilon)SdZ$

(3) solution in summation form

| Simple model | (1) $x=e^{-(\zeta+\tau)}J_0(i\sqrt{4\zeta\tau})$ $+\displaystyle\int_0^{\zeta}e^{-(\zeta+\tau)}J_0(i\sqrt{4\zeta\tau})d\sigma$
 (2) $Y=\displaystyle\int_0^{\tau}e^{-(\zeta+\sigma)}J_0(i\sqrt{4\zeta\sigma})d\sigma$ | (1) $x=1-\displaystyle\int_0^{\zeta}e^{-(\zeta+\tau)}J_0(i\sqrt{4\zeta\tau})d\zeta$ | Bird et al. |

exponential power. However, this boundary condition is not in the region of real systems. In this work, there are two attempts in the second case which have been tried. The first attempt uses boundary conditions at $Z=0$, $C=C_{in}$ and at $Z=0$, $\partial C/\partial Z=0$. It is interesting to note that such a system is not well posed mathematically, since the solution will not be a continuous function at break point. The second attempt uses the equation of continuity at $Z=0$ and a solute mass balance for the total column. It is clear that both boundary conditions in this work are rigorous. Also, the calculations have shown rational breakthrough curves as various parameters are altered.

By using the same boundary conditions of Lapidus and Amundson, Rasmuson and Neretnieks [4] gave the solution in an integral form of a model for diffusion in particles and longitudinal dispersion in packed beds (case III). Instead of boundary condition at $Z=\infty$, $C=0$; this work uses a boundary condition which is at $Z=L$, $\partial^2 C/\partial Z^2=0$. It is a second derivative term and possesses the highest order of the differential equation. Although it is an approximation, it does possess physical meaning. The numerical results fail at a short interval when the particle sizes are small. The reason for this is probably due to the fact that in small particles the diffusion coefficient is also small, and therefore diffusion through the porous networks of the particles is not significant.

In solving problems of differential equations, the boundary conditions which are usually applied and commonly mentioned are

of three types. The first type is called the Dirichlet condition which is the value, U, at the boundaries. The second type is called the Neumann condition which is dU/dx at the boundaries. The third type is hU+dU/dx at the boundaries. Here h is either a constant or a function of independent variables. Since the boundary condition which is the mass conservation law, and the boundary condition which possesses the highest derivative order of the differential equation are beyond the criterion mentioned in mathematical textbooks, the applications of boundary conditions for solving differential equations is extended.

In the previous derivation of mathematical models, a linear equilibrium relationship of solute in liquid phase and solid phase was assumed. This assumption is reasonable when the solute concentration in a system is dilute. However, in most of the operations the solute concentration is not dilute and the linear equilibrium relationship of solute between the two phases can not be held. A question is posed as how to apply previous mathematical models to the nonlinear equilibrium relationship case. A demonstration of this application is given by comparisions with experimental data from Katch et al. [6].

Katch et al. [6] gave the equilibrium curve and adsorption data points of trypsin-sepharose 4B-agrinine peptides system as in Figures 5.1 and 5.2 respectively. The three curves in Figure 5.2 were calculated from mathematical models in this work. Curve 1 is calculated by using the simple model (in Chapter II) with the average equilibrium constant at $C=0.5\ C_o$. Curve 2 is
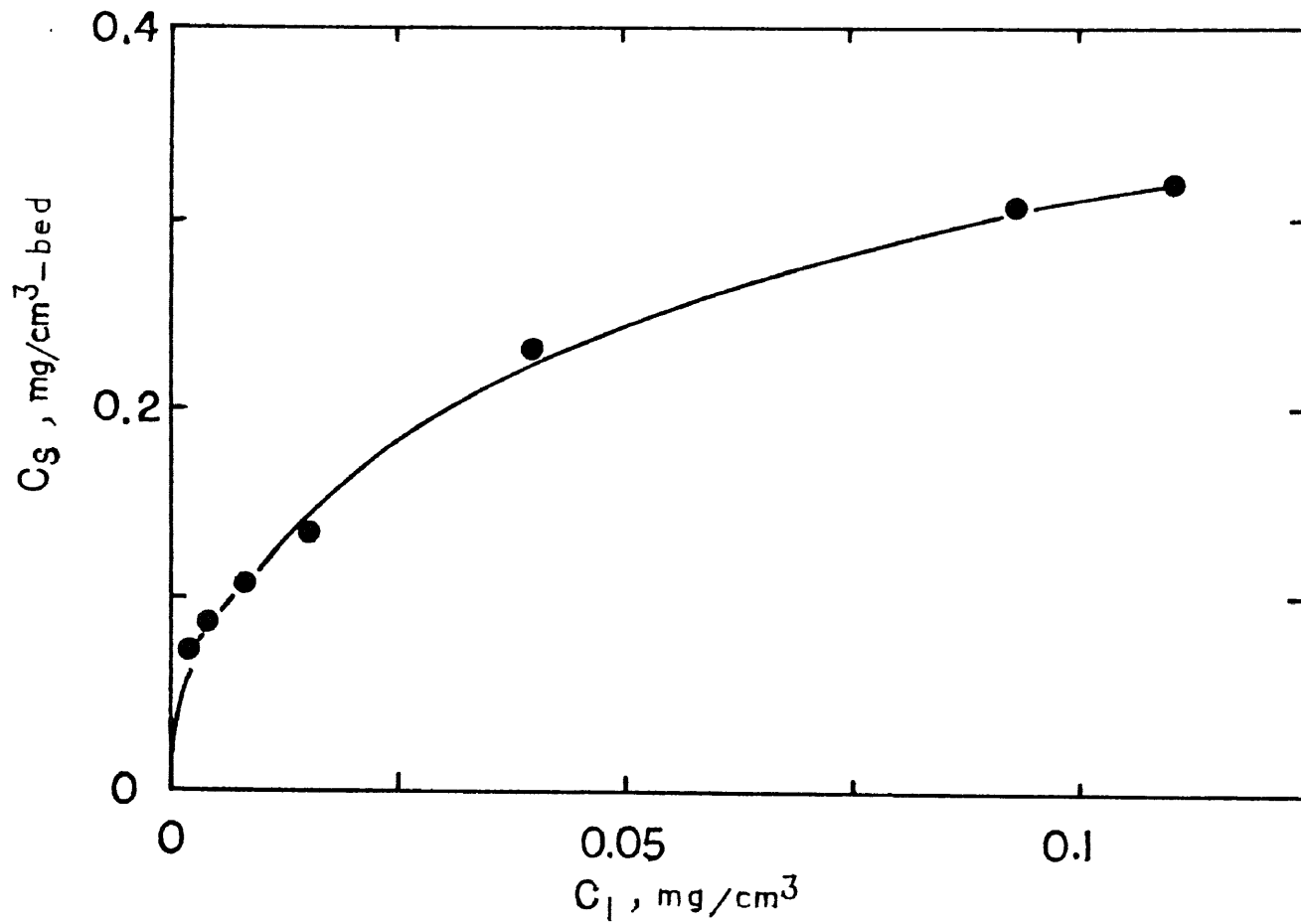
FIGURE   5.1
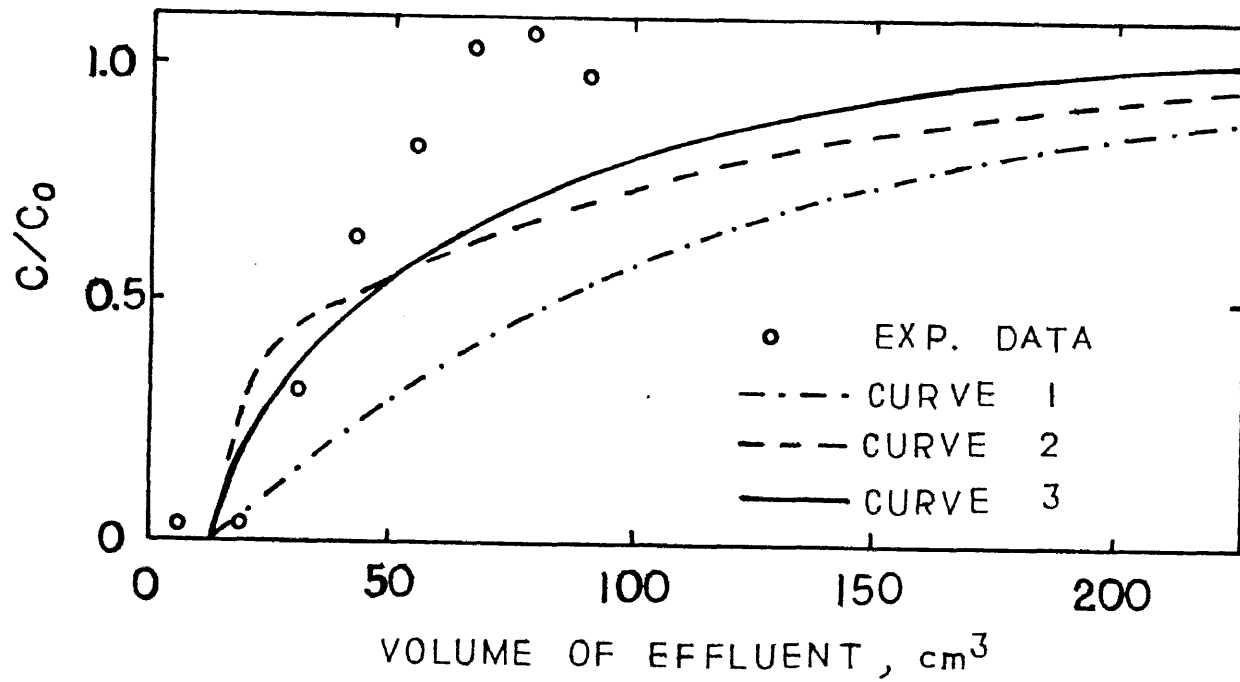
FIGURE   5.2

calculated by using the model B in Chapter III with the average equilibrium constant at C=0.5 C_O and axial eddy diffusivity is 0.8. Curve 3 is calculated by using the model B in Chapter III with various equilibrium constants and axial eddy diffusivity equals 0.8. In the calculation of curve 3, the solute concentration region is divided into twenty intervals such as C/C_O=0~0.05, 0.05~0.1, 0.1~0.15, etc. with equilibrium constants at C/C_O=0.05, 0.1, 0.15, etc. respectively.

As shown in Figure 5.2, the fitting of data by curves 1, 2, and 3 are progressively improved. Still, the measured breakthrough curve is somewhat steeper than the calculated curve 3. This probably results from the variations of the mass transfer coefficient, K_f, and effective contact area, a, with the progress of adsorption.

It must be noted that the goal of fitting experimental data is to apply these mathematical models to calculate nonlinear equilibrium systems by using a revised numerical program. As far as data fitting is concerned, further revision of the numerical program is recommended to take into account the variations of the mass transfer coefficient and effective contact area in the calculations.

NOTATION

a	contact area per unit packed column, cm^{-1}
C_A	bulk concentration in fluid, $mole/cm^3$
C_{AO}	inlet concentration in fluid, $mole/cm^3$
C_A^*	interfacial fluid concentration assumed to be in equilibrium with C_{AS}, $mole/cm^3$
C_{AS}	concentration in solid phase, $mole/cm^3$
D_S	diffusivity in fluid in intrapores, cm^2/min
E_D	longitudinal dispersion coefficient, cm^2/min
K_f	the fluid phase mass transfer coefficient cm/min
m	adsorption equilibrium constant, dimensionless
Q	flow rate, cm^3/min
r	radial distance from center of particle, cm
r_o	particle radius, cm
S	cross-sectional area of column, cm^2
t	time, min
v	interstitial velocity, cm/min
z	distance in flow direction, cm
ε	volume fraction of column occupied by liquid, dimensionless

APPENDIX I

A CALCULATION OF THE ELUTION PROFILE

(SIMPLE MODEL)

Material balance of solid phase:

$$(1-\epsilon)SdZ \frac{\partial C_{AS}}{\partial t} = k_f a(C_A - C_A^*)SdZ \qquad (AI-1)$$

Material balance of liquid phase:

$$\epsilon SdZ \frac{\partial C_A}{\partial t} = -Q \frac{\partial C_A}{\partial Z} dZ - k_f a(C_A - C_A^*)SdZ \qquad (AI-2)$$

Equilibrium relationship on solid surface:

$$C_A^* = mC_{AS} \qquad (AI-3)$$

Change variable:

Let $t' = t - Z(\frac{\epsilon S}{Q})$

and use Chain Rule transfer Eqs. (AI-1) and (AI-2) to

$$(\frac{\partial C_A}{\partial Z})_{t'} = \frac{-k_f aS}{Q} (C_A - C_A^*) \qquad (AI-4)$$

$$(\frac{\partial C_{AS}}{\partial t'})_Z = \frac{k_f a}{1-\epsilon} (C_A - C_A^*) \qquad (AI-5)$$

With B.C. 1: $t' = 0$, $C_{AS} = C_{AS0}$ for $Z > 0$

B.C. 2: $Z = 0$, $C_A = 0$ for $t' > 0$

Introducing dimensionless forms

$$Y = \frac{C_{AS}}{C_{AS0}} , \quad X = \frac{C_A}{mC_{AS0}} , \quad \zeta = \frac{k_f aZS}{Q} , \quad \tau = \frac{mt'k_f a}{1-\epsilon}$$

Then Eqs. (AI-4) and (AI-5) become:

$$\frac{\partial X}{\partial \zeta} = -(X - Y) \qquad (AI-6)$$

$$\frac{\partial Y}{\partial \tau} = X - Y \qquad (AI-7)$$

53

With B.C. 1: $\tau = 0$, $Y = 1$ for $\zeta > 0$

   B.C. 2: $\zeta = 0$, $X = 0$ for $\tau > 0$

Take the Laplace Transform of Eqs. (AI-6), (AI-7) and B.C. with respect to ζ

$$p\overline{X} = -\overline{X} + \overline{Y} \qquad\qquad (AI-8)$$

$$\frac{d\overline{Y}}{d\tau} = \overline{X} - \overline{Y} \qquad\qquad (AI-9)$$

Combine eqs. (AI-8) and (AI-9)

$$\frac{d\overline{Y}}{d\tau} = - \frac{p}{p+1}\, \overline{Y} \quad\text{or}$$

$$\int_{\overline{Y}=\frac{1}{p}}^{\overline{Y}} \frac{d\overline{Y}}{\overline{Y}} = - \frac{p}{p+1} \int_{\tau=0}^{\tau} d\tau \qquad\qquad (AI-10)$$

Integral above equation, one obtains

$$\overline{Y} = e^{-\tau}[\frac{e^{\frac{\tau}{p+1}}}{p+1} + \frac{1}{p}\frac{e^{\frac{\tau}{p+1}}}{p+1}] \qquad\qquad (AI-11)$$

Combine eqs. (AI-8) and (AI-11), then

$$\overline{X} = e^{-\tau}[\frac{1}{p} \cdot \frac{e^{\frac{\tau}{p+1}}}{p+1}] \qquad\qquad (AI-12)$$

After inverse of eqs. (AI-11) and (AI-12), the solutions are

$$Y(\zeta,\tau) = e^{-(\tau+\zeta)}J_O(i\sqrt{4\tau\zeta}) + \int_0^\zeta e^{-(\tau+\sigma)}J_O(i\sqrt{4\tau\sigma})\, d\sigma \qquad (AI-13)$$

and

$$X(\zeta,\tau) = \int_0^\zeta e^{-(\tau+\sigma)}J_O(i\sqrt{4\tau\sigma})\, d\sigma \qquad\qquad (AI-14)$$

The calculated elution profiles are given in Figures AI.1 to AI.5.

FIGURE A I.I

FIGURE   AI.2

FIGURE   AI.3

FIGURE   AI.4

Parameters shown in figure:

$K_f = 0.0001$ $Z = 10$ $\epsilon = 0.75$

$a = 300$ $S = 2$

$Q = 1$ (first curve, peak at $t = 15$)

$Q = 0.5$ (second curve, peak at $t = 30$)

Vertical axis: $\dfrac{C_A}{mC_{A30}}$

Horizontal axis: t

$$\frac{C_A}{C_{ASO}}$$

- - - - $m = 30$

——— $m = 10$

$K_f = 0.0001$
$a = 300$
$Z = 10$
$S = 2$
$Q = 0.5$
$\epsilon = 0.75$
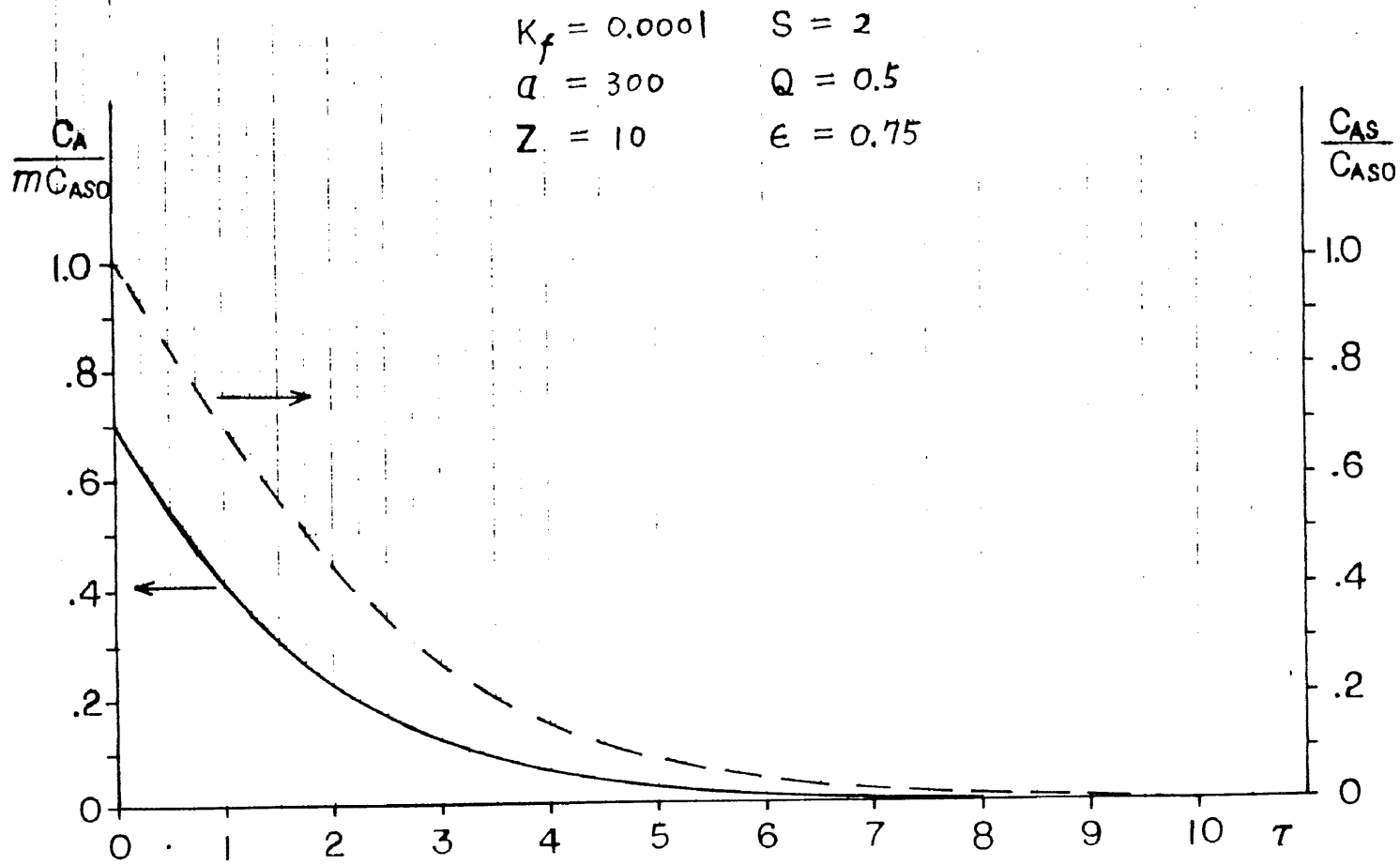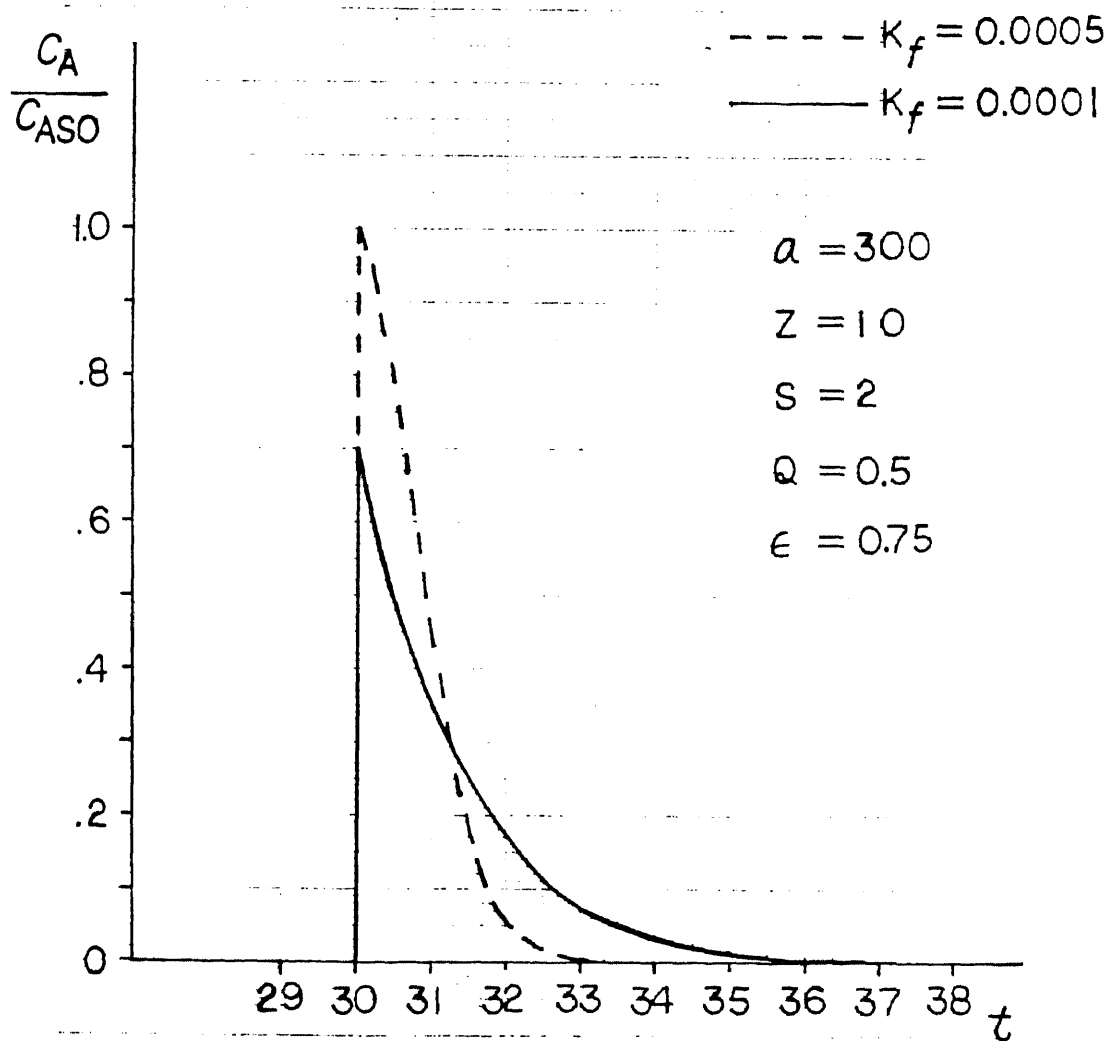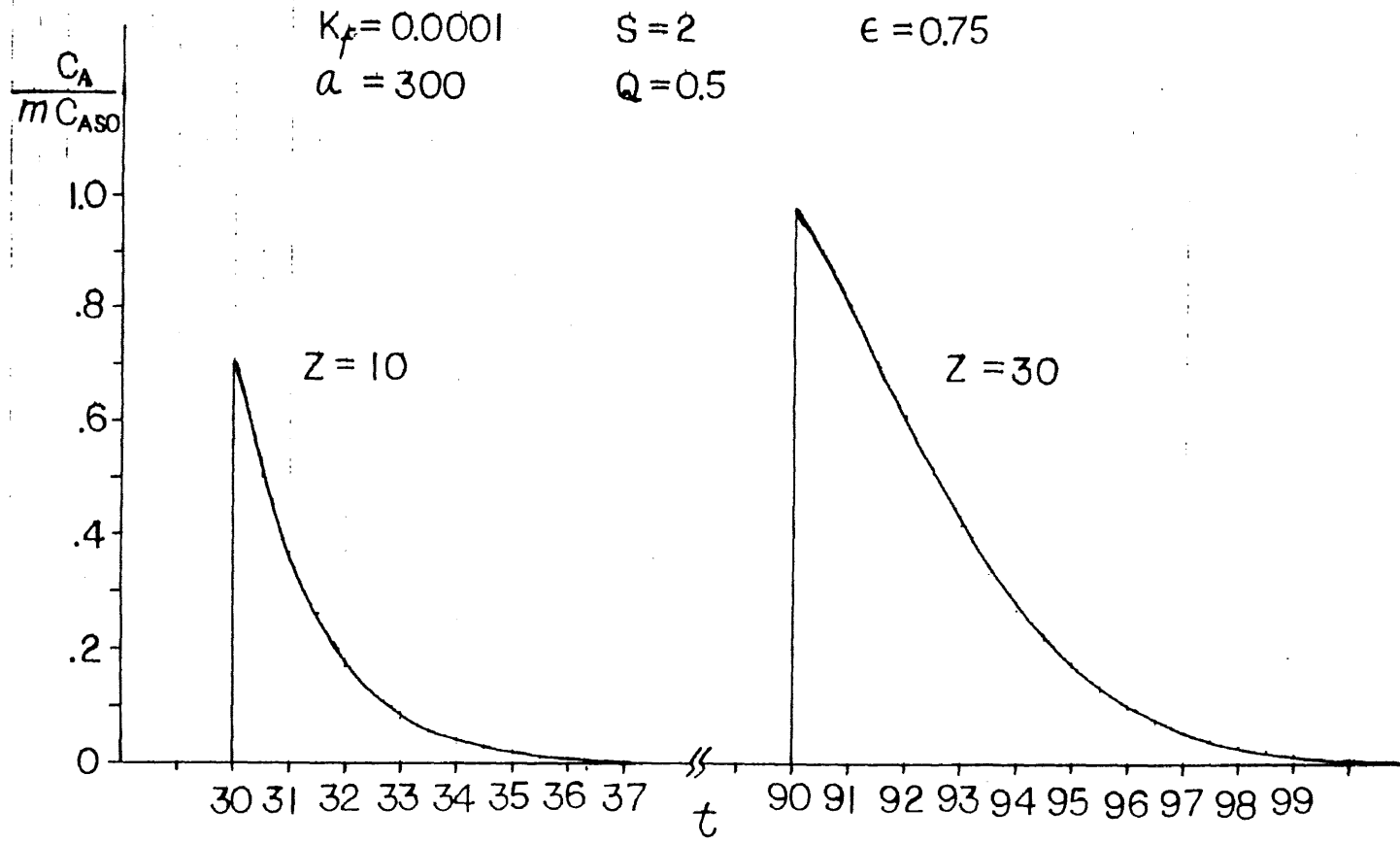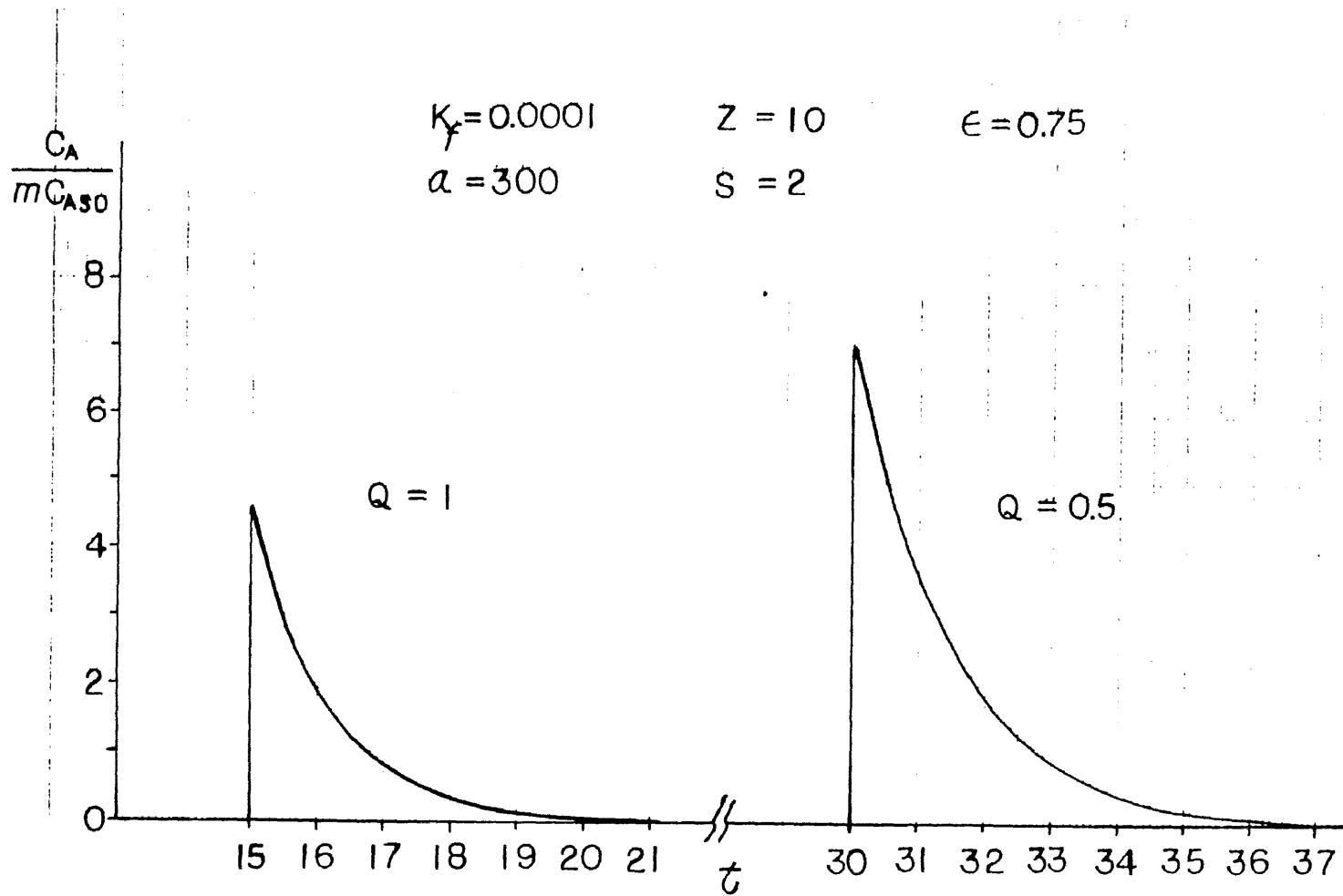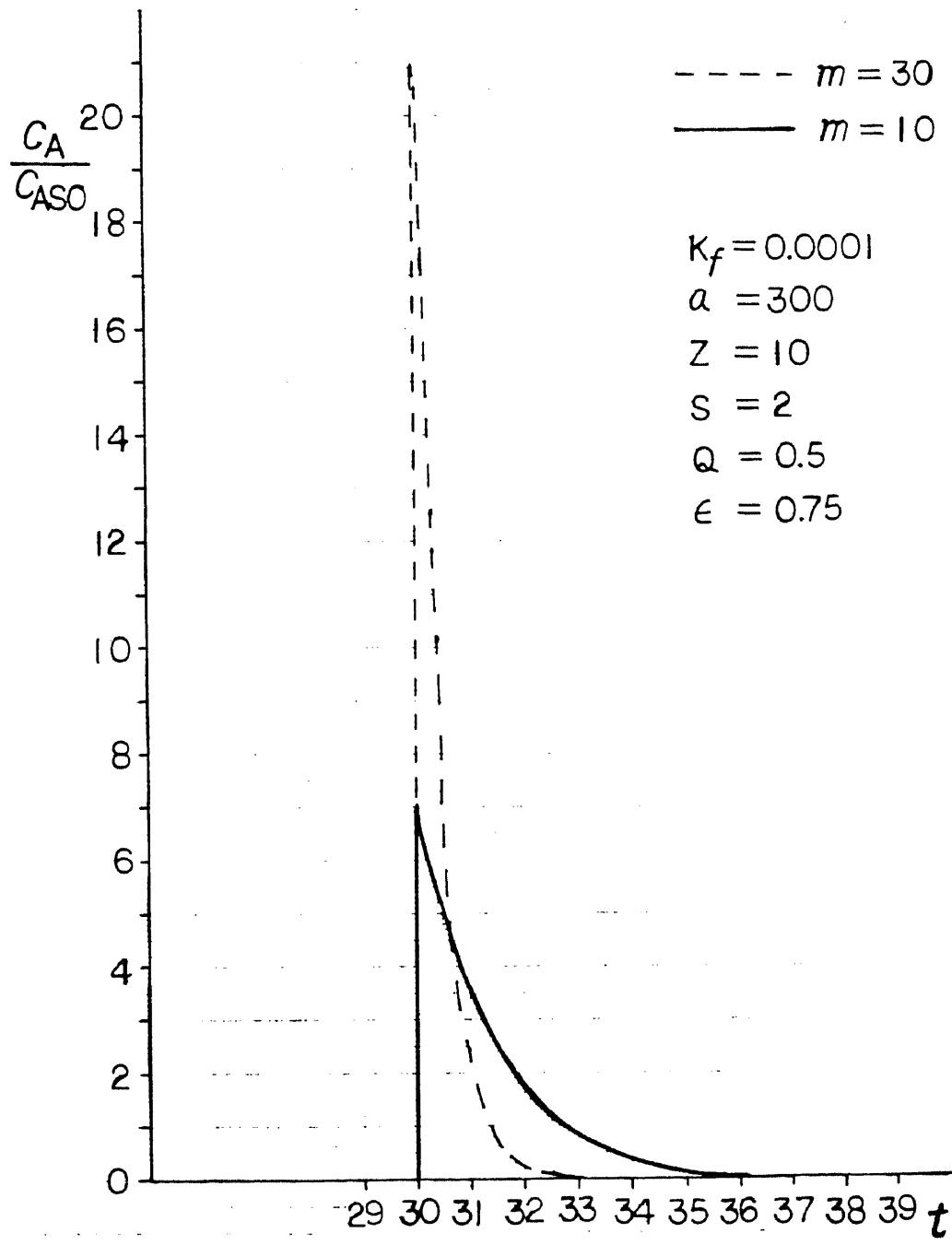
FIGURE   AI.5

APPENDIX II

WITH DIFFUSION IN PARTICLES AND LONGITUDINAL

DISPERSION IN BED

Material balance of liquid phase:

$$\varepsilon S \Delta Z \frac{\partial C_A}{\partial t} = Q C_A \Big|_{Z=Z} - Q C_A \Big|_{Z=Z+\Delta Z}$$

$$- \frac{S \Delta Z (1 - \varepsilon)}{\frac{4}{3} \pi r_o^3} 4 \pi r_o^2 k_f (C_A - C_A^*)$$

$$- \varepsilon S E_D \frac{\partial C_A}{\partial Z} \Big|_{Z=Z} + \varepsilon S E_D \frac{\partial C_A}{\partial Z} \Big|_{Z=Z+\Delta Z}$$

Divided by $\Delta Z \cdot \varepsilon \cdot S$; $\Delta Z \rightarrow 0$

$$\frac{\partial C_A}{\partial t} = - \frac{Q}{\varepsilon S} \frac{\partial C_A}{\partial Z} - \frac{1-\varepsilon}{\varepsilon} \frac{3}{r_o} k_f (C_A - C_A^*) + E_D \frac{\partial^2 C_A}{\partial Z^2} \qquad \text{(AII-1)}$$

Material balance on solid particles:

$$4 \pi r^2 N_{Ar} \Big|_r - 4 \pi (r+\Delta r)^2 N_{Ar} \Big|_{r+\Delta r} = 4 \pi r^2 \Delta r \frac{\partial C_{AS}}{\partial t}$$

divided by $4 \pi \Delta r$; $r \rightarrow 0$

$$- \frac{\partial (r^2 N_{Ar})}{\partial r} = r^2 \frac{\partial C_{AS}}{\partial t}$$

Since $N_{Ar} = -D_S \frac{\partial C_{AS}}{\partial r}$

$$\frac{\partial C_{AS}}{\partial t} = D_S \left(\frac{\partial^2 C_{AS}}{\partial r^2} + \frac{2}{r} \frac{\partial C_{AS}}{\partial r} \right) \qquad \text{(AII-2)}$$

Equilibrium relationship between solid phase and liquid phase

$$C_A^*(Z,t) = m C_{AS}(r = r_o, Z, t) \qquad \text{(AII-3)}$$

I.C. and B.C.

$$C_A(Z, \ t = 0) = C_{A,t_o} \tag{AII-4}$$

$$C_A^*(Z, \ t = 0) = C_{A,t_o} \tag{AII-5}$$

$$C_{AS}(Z, \ t = 0) = C_{AS,t_o} \tag{AII-6}$$

Note that $C_{AS,t_o} = C_{A,t_o}$

$$\frac{\partial C_{AS}}{\partial r} \ (r = 0, \ Z, \ t) = 0 \tag{AII-7}$$

$$D_S \ \frac{\partial C_{AS}}{\partial r}(r = r_o, \ Z, \ t) = k_f(C_A - C_A^*) \tag{AII-8}$$

Introduce dimensionless variables

$$C'_A = \frac{C_A - C_{A,t_o}}{C_{A0} - C_{A,t_o}} \ , \quad C'_A{}^* = \frac{C_A^* - C_{A,t_o}}{C_{A0} - C_{A,t_o}} \ , \quad C'_{AS} = \frac{C_{AS} - C_{A,t_o}}{C_{A0} - C_{A,t_o}}$$

Equations (AII-1), (AII-2) and (AII-3) become

$$\frac{\partial C'_A}{\partial t} = - \frac{Q}{\epsilon S} \frac{\partial C'_A}{\partial Z} - \frac{(1-\epsilon)3}{\epsilon r_o} k_f(C'_A - C'_A{}^*) + E_D \frac{\partial^2 C'_A}{\partial Z^2} \tag{AII-9}$$

$$\frac{\partial C'_{AS}}{\partial t} = D_S \left(\frac{\partial^2 C'_{AS}}{\partial r^2} + \frac{2}{r} \frac{\partial C'_{AS}}{\partial r} \right) \tag{AII-10}$$

$$C'_A{}^* = mC'_{AS} \text{ at } r = r_o \tag{AII-11}$$

With I.C.

$$C'_A(Z,t=0) = 0, \ C'_A{}^*(Z,t=0) = 0, \ C'_{AS}(Z,r,t=0) = 0$$

Take Laplace Transformation of Eqs. (AII-9), (AII-10),
and (AII-11) and use above I.C., then

$$p\overline{C}_A = - \frac{Q}{\epsilon S} \frac{d\overline{C}_A}{dZ} - \frac{(1-\epsilon)3}{\epsilon r_o} k_f(\overline{C}_A - \overline{C}_A^*) + E_D \frac{d^2\overline{C}_A}{dZ^2} \tag{AII-12}$$

$$p\overline{C}_{AS} = D_S(\frac{\partial^2 \overline{C}_{AS}}{\partial r^2} + \frac{2}{r}\frac{\partial \overline{C}_{AS}}{\partial r}) \tag{AII-13}$$

$$\overline{C}_A^* = m\overline{C}_{AS} \quad \text{at } r = r_o \tag{AII-14}$$

Equation (AII-13) identifies

$$r^2 \frac{\partial \overline{C}_{AS}}{\partial r^2} + 2r \frac{\partial \overline{C}_{AS}}{\partial r} - \frac{p}{D_S} r^2 \overline{C}_{AS} = 0 \tag{AII-15}$$

Since $r_o \ll L$, one can treat that $\overline{C}_{AS}$ is a function of r only in a small shell of the column (ΔZ is small). Therefore Eq. (AII-15) can be reduced to

$$r^2 \frac{d^2 \overline{C}_{AS}}{dr^2} + 2r \frac{d\overline{C}_{AS}}{dr} - \frac{p}{D_S} r^2 \overline{C}_{AS} = 0$$

From Mickley, Sherwood and Reed (p. 174) generalized Bessel's equation

$$\overline{C}_{AS} = r^{-1/2}[C_1 I_{\frac{1}{2}}(\sqrt{\frac{p}{D_S}}\ r) + C_2 I_{-1/2}(\sqrt{\frac{p}{D_S}}\ r)] \tag{AII-16}$$

Note that

$$I_{\frac{1}{2}}(\sqrt{\frac{p}{D_S}}\ r) = \frac{(p/D_S)^{1/4}}{2^{\frac{1}{2}} \cdot \frac{1}{2}!}\ r^{1/2} \quad \text{for small r}$$

$$I_{-\frac{1}{2}}(\sqrt{\frac{p}{D_S}}\ r) = \frac{2^{1/2}}{(-\frac{1}{2})!}\ (\frac{p}{D_S})^{-1/4}\ r^{-1/2} \quad \text{for small r}$$

From Eq. (AII-7)

$$C_{AS}(r = 0,\ Z,\ t) = \text{finite}$$

or

$$\overline{C}_{AS} = \frac{(C_{AS}-C_{AS,t_o})}{(C_{A0}-C_{A,t_o})p} = \text{finite at } r = 0$$

Therefore $C_2 = 0$, and Eq. (AII-16) becomes

$$\overline{C}_{AS} = C_1 r^{-1/2} I_{1/2}(\sqrt{\frac{p}{D_S}}\ r) \tag{AII-17}$$

Note that C_1 is a function of Z, since $\overline{C}_{AS}$ is a function of r and Z.

$$\frac{\partial \overline{C}_{AS}}{\partial r} = C_1 \sqrt{\frac{p}{D_S}}\ r^{-1/2}\ I_{3/2}\left(\sqrt{\frac{p}{D_S}}\ r\right) \qquad \text{(AII-18)}$$

From Eq. (AII-8)

$$D_S\ \frac{\partial \overline{C}_{AS}}{\partial r} = k_f(\overline{C}_A - \overline{C}_A{}^*)\ \text{at } r = r_0 \qquad \text{(AII-19)}$$

Put Eq. (AII-17) into Eq. (AII-14) to rid of $\overline{C}_{AS}$

$$\overline{C}_A{}^* = C_1 m r_0^{-1/2} I_{1/2}\left(\sqrt{\frac{p}{D_S}}\ r_0\right) \qquad \text{(AII-20)}$$

Put Eqs. (AII-18) and (AII-20) into Eq. (AII-19) to get C_1

$$C_1 = \frac{k_f \overline{C}_A}{\sqrt{D_S p}\ r_0^{-1/2} I_{3/2}\left(\sqrt{\frac{p}{D_S}}\ r_0\right) + k_f m r_0^{-1/2} I_{1/2}\left(\sqrt{\frac{p}{D_S}}\ r_0\right)} \qquad \text{(AII-21)}$$

Put Eq. (AII-21) into Eq. (AII-20) to rid of C_1

$$\overline{C}_A{}^* = \frac{k_f m I_{1/2}\left(\sqrt{\frac{p}{D_S}}\ r_0\right)\overline{C}_A}{\sqrt{D_S p}\ I_{3/2}\left(\sqrt{\frac{p}{D_S}}\ r_0\right) + k_f m I_{1/2}\left(\sqrt{\frac{p}{D_S}}\ r_0\right)} \qquad \text{(AII-22)}$$

Put Eq. (AII-22) into Eq. (AII-12) to obtain an ordinary differential equation of $\overline{C}_A$

$$\frac{d^2 \overline{C}_A}{dZ^2} - A\ \frac{d\overline{C}_A}{dZ} - F(p)\overline{C}_A = 0 \qquad \text{(AII-23)}$$

where,

$$A = \frac{Q}{\epsilon S E_D}\ ,\ F(p) = Bp + D(p),\ B = \frac{1}{E_D}$$

$$D(p) = \frac{3(1-\varepsilon)k_f\sqrt{D_S p}\; I_{3/2}(\sqrt{\frac{p}{D_S}}\, r_0)}{\varepsilon E_D r_0[\sqrt{D_S p}\; I_{3/2}(\sqrt{\frac{p}{D_S}}\, r_0) + k_f m I_{1/2}(\sqrt{\frac{p}{D_S}} r_0)]} \tag{AII-24}$$

$$\therefore\; \overline{C}_A = e^{\frac{A}{2}Z}\{C_3 \sinh \frac{\sqrt{A^2+4F(p)}}{2}\, Z + C_4\cosh \frac{\sqrt{A^2+4F(p)}}{2}\, Z\} \tag{AII-25}$$

Now we need to find out C_3 and C_4

Boundary Condition 1: shell mass balance at the inlet of the column

$$QC_{A0} - QC_A\Big|_{Z=\Delta Z} + S\varepsilon E_D \frac{\partial C_A}{\partial Z}\Big|_{Z=\Delta Z} = \Delta Z \cdot S \cdot \varepsilon\, \frac{\partial C_A}{\partial t} \tag{AII-26}$$

Divided by Q; let $\Delta Z \to 0$

$$C_{A0} - C_A\Big|_{Z=0} + \frac{S\varepsilon E_D}{Q}\, \frac{\partial C_A}{\partial Z}\Big|_{Z=\Delta Z} = 0 \tag{AII-27}$$

Introduce dimensionless variable C'_A and take Laplace Transformation, Eq. (AII-27) becomes

$$\frac{1}{A}\frac{d\overline{C}_A}{dZ}\Big|_{Z=0} - \overline{C}_A\Big|_{Z=0} + \frac{1}{p} = 0 \tag{AII-28}$$

Boundary Condition 2: Total material balance of column

$$Q\int_{t=0}^{t=t}(C_{A0} - C_A\Big|_{Z=L})dt = S\cdot\varepsilon\int_{Z=0}^{Z=L}(C_A - C_{A,t_0})dZ$$

$$+ \int_{Z=0}^{Z=L}\int_{r=0}^{r=r_0} \frac{(C_{AS} - C_{AS,t_0})}{\frac{4}{3}\pi r_0^3}\, 4\pi r^2(1-\varepsilon)S dr dZ \tag{AII-29}$$

Introduce dimensionless variables C'_A, C'_{AS} and take Laplace Transformation, above equation becomes

$$Q\frac{1}{p}(\frac{1}{p} - \overline{C}_A\Big|_{Z=L}) = S\varepsilon\int_{Z=0}^{Z=L}\overline{C}_A dZ + \frac{3(1-\varepsilon)S}{r_0^3}\int_{Z=0}^{Z=L}\int_{r=0}^{r=r_0}\overline{C}_{AS}r^2 dr dZ \tag{AII-30}$$

Substitute Eqs. (AII-17) and (AII-21) into Eq. (AII-30), Eq. (AII-30) becomes

$$Q \frac{1}{p}(\frac{1}{p} - \overline{C}_A\big|_{Z=L}) = S\epsilon \int_{Z=0}^{Z=L} \overline{C}_A dZ +$$

$$\frac{3(1-\epsilon)Sk_f}{r_o^{\frac{5}{2}}[\sqrt{D_S p}\ I_{\frac{3}{2}}(\sqrt{\frac{p}{D_S}}\ r_o)+k_f m I_{\frac{1}{2}}(\sqrt{\frac{p}{D_S}}\ r_o)]} \quad \int_{Z=0}^{Z=L} \overline{C}_A \int_{r=0}^{r=r_o} r^2 I_{\frac{1}{2}}(\sqrt{\frac{p}{D_S}}r)drdZ$$

$$(AII-31)$$

We now need to determine

$$\int_{r=0}^{r=r_o} r^{\frac{3}{2}} I_{\frac{1}{2}}(\sqrt{\frac{p}{D_S}}r)dr$$

$$\int_{r=0}^{r=r_o} r^{\frac{3}{2}} I_{\frac{1}{2}}(\sqrt{\frac{p}{D_S}}r)dr = \sqrt{\frac{D_S}{p}}\ r_o^{\frac{3}{2}}\ I_{\frac{3}{2}}(\sqrt{\frac{p}{D_S}}r_o) \qquad (AII-32)$$

$$(\text{since } \frac{d}{dx}[x^p I_p(\alpha x)] = \alpha x^p I_{p-1}(\alpha x))$$

Introduce Eq. (AII-32) into Eq. (AII-31), then

$$Q \frac{1}{p}(\frac{1}{p} - \overline{C}_A\big|_{Z=L}) = S\epsilon \int_{Z=0}^{Z=L} \overline{C}_A dZ +$$

$$\frac{3(1-\epsilon)Sk_f\sqrt{\frac{D_S}{p}}\ I_{\frac{3}{2}}(\sqrt{\frac{p}{D_S}}r_o)}{r_o[\sqrt{D_S p}\ I_{\frac{3}{2}}(\sqrt{\frac{p}{D_S}}r_o)+k_f m I_{\frac{1}{2}}(\sqrt{\frac{p}{D_S}}r_o)]} \int_{Z=0}^{Z=L} \overline{C}_A dZ \qquad (AII-33)$$

Multiply the above equation by $p/\epsilon SE_D$, then

$$A(\frac{1}{p} - \overline{C}_A\big|_{Z=L}) = F(p) \int_{Z=0}^{Z=L} \overline{C}_A dZ \qquad (AII-34)$$

From Eq. (AII-25)

$$\overline{C}_A\big|_{Z=0} = C_4 \qquad (AII-35)$$

$$\frac{d\overline{C}_A}{dZ}\big|_{Z=0} = \frac{A}{2} C_4 + C_3 \frac{\sqrt{A^2+4F(p)}}{2} \qquad (AII-36)$$

Substitute Eqs. (AII-35) and (AII-36) into Eq. (AII-28), one obtains

$$C_4 = \frac{\sqrt{A^2+4F(p)}}{A} C_3 + \frac{2}{p} \qquad \text{(AII-37)}$$

Also, from Eq. (AII-25)

$$\overline{C}_A\Big|_{Z=L} = e^{\frac{A}{2}L}\{C_3\sinh \frac{\sqrt{A^2+4F(p)}}{2}L + C_4\cosh \frac{\sqrt{A^2+4F(p)}}{2}L\} \qquad \text{(AII-38)}$$

$$\int_{Z=0}^{Z=L}\overline{C}_A dZ = \frac{-C_3 e^{\frac{A}{2}L}}{F(p)}\{\frac{A}{2}\sinh \frac{\sqrt{A^2+4F(p)}}{2}L - \frac{\sqrt{A^2+4F(p)}}{2}\cosh \frac{\sqrt{A^2+4F(p)}}{2}L$$

$$+ e^{-\frac{A}{2}L} \frac{\sqrt{A^2+4F(p)}}{2} - \frac{C_4 e^{\frac{A}{2}L}}{F(p)}\{\frac{A}{2}\cosh \frac{\sqrt{A^2+4F(p)}}{2}L - \frac{\sqrt{A^2+4F(p)}}{2}\sinh \frac{\sqrt{A^2+4F(p)}}{2}L$$

$$-e^{-\frac{A}{2}L} \frac{A}{2} \} \qquad \text{(AII-39)}$$

Put Eqs. (AII-38) and (AII-39) into Eq. (AII-33), then B.C. 2 becomes

$$e^{-\frac{A}{2}L} \frac{A}{p} +$$

$$C_3[-A\sinh \frac{\sqrt{A^2+4F(p)}}{2}L + \frac{A}{2}\sinh \frac{\sqrt{A^2+4F(p)}}{2}L - \frac{\sqrt{A^2+4F(p)}}{2}\cosh \frac{\sqrt{A^2+4F(p)}}{2}L$$

$$+ e^{-\frac{A}{2}L} \frac{\sqrt{A^2+4F(p)}}{2}] = C_4[A\cosh \frac{\sqrt{A^2+4F(p)}}{2}L - \frac{A}{2} \cosh \frac{\sqrt{A^2+4F(p)}}{2}L$$

$$+ \frac{\sqrt{A^2+4F(p)}}{2} \sinh \frac{\sqrt{A^2+4F(p)}}{2}L + \frac{A}{2} e^{-\frac{A}{2}L}] \qquad \text{(AII-40)}$$

Substitute Eq. (AII-37) into Eq. (AII-40), one obtains

$$C_3 = - \frac{A\cosh \frac{\sqrt{A^2+4F(p)}}{2}L + \sqrt{A^2+4F(p)} \sinh \frac{\sqrt{A^2+4F(p)}}{2}L}{p[\sqrt{A^2+4F(p)}\cosh \frac{\sqrt{A^2+4F(p)}}{2}L +(A + \frac{2F(p)}{A})\sinh \frac{\sqrt{A^2+4F(p)}}{2}L]}$$

(AII-41)

Combine Eq. (AII-37) with (AII-41)

$$C_4 = \frac{\sqrt{A^2+4F(p)} \cosh \frac{\sqrt{A^2+4F(p)}}{2}L + A \sinh \frac{\sqrt{A^2+4F(p)}}{2}L}{p[\sqrt{A^2+4F(p)} \cosh \frac{\sqrt{A^2+4F(p)}}{2}L +(A + \frac{2F(p)}{A})\sinh \frac{\sqrt{A^2+4F(p)}}{2}L]}$$

(AII-42)

Put Eqs. (AII-41) and (AII-42) into Eq. (AII-25)

$$\overline{C}_A = e^{\frac{A}{2}Z} \frac{j(p)}{p\,\ell(p)}$$

(AII-43)

where,

$$j(p) = A\sinh \frac{(L-Z)\sqrt{A^2+4F(p)}}{2} + \sqrt{A^2+4F(p)} \cosh \frac{(L-Z)\sqrt{A^2+4F(p)}}{2}$$

(AII-44)

$$\ell(p) = \sqrt{A^2+4F(p)} \cosh \frac{\sqrt{A^2+4F(p)}}{2}L +(A+ \frac{2F(p)}{A})\sinh \frac{\sqrt{A^2+4F(p)}}{2}L$$

(AII-45)

Next: check poles and singularities, Eq. (AII-43) can be expressed as

$$\overline{C}_A = \frac{e^{\frac{A}{2}Z} \sum_{n=0}^{\infty} [\frac{(\frac{L-Z}{2})^{2n}}{2n!} + A\frac{(\frac{L-Z}{2})^{2n+1}}{(2n+1)!}](A^2+4F(p))^n}{p \sum_{n=0}^{\infty} [\frac{(\frac{L}{2})^{2n}}{2n!}+(A+ \frac{2F(p)}{A}) \frac{(\frac{L}{2})^{2n+1}}{(2n+1)!}](A^2+4F(p))^n}$$

(AII-46)

So there is no singularity in $\overline{C}_A(p)$. However, there are simple poles at p=0 and at $\ell(p)=0$. By using the Residue Theorem,

$$L^{-1}[\overline{C}_A] = \Sigma \text{ residues of } e^{pt} \cdot \overline{C}_A(p) \text{ at poles} \qquad (AII-47)$$

The residue at simple pole p=0 is

$$\lim_{p \to 0} p \cdot [e^{pt} \cdot \overline{C}_A(p)] = 1 \qquad (AII-48)$$

The other simple poles are eigenvalues which make

$\ell(p) = 0$ or

$$\frac{-\sqrt{A^2+4F(p)}}{(A+ \frac{2F(p)}{A})} = \tanh \frac{\sqrt{A^2+4F(p)}}{2}L \qquad (AII-49)$$

let $\qquad \sqrt{A^2+4F(p)} = i\beta_n \qquad (AII-50)$

then $\tanh \dfrac{\sqrt{A^2+4F(p)}}{2}L = \tanh i\beta_n \dfrac{L}{2} = i \tan \beta_n \dfrac{L}{2} \qquad (AII-51)$

and $\qquad F(p) = \dfrac{-\beta_n^2 - A^2}{4} \qquad (AII-52)$

Put Eqs. (AII-50), (AII-51) and (AII-52) into Eq. (AII-49),
Eq. (AII-49) becomes

$$\tan \beta_n \frac{L}{2} = \frac{-2A\beta_n}{A^2-\beta_n^2} \qquad (AII-53)$$

So β_n can be solved numerically. From Eq. (AII-52), knowing the values of β_n, p_n(n=2,3,4,...) can be obtained numerically. Also, from Eq. (AII-52), p_n(n=2,3,4,...) should be negative quantities or zero. Once p_n are known, the next step is to find out the residues at p_n.

The residues at poles p_n are

$$\lim_{p \to p_n} (p - p_n) \cdot [e^{pt} \cdot \overline{C}_A(p)]$$

$$= \lim_{p \to p_n} (p - p_n) e^{pt}\, e^{\frac{A}{2}Z}\, \frac{j(p)}{p\ell(p)}$$

$$= \{\lim_{p \to p_n} \frac{(p - p_n)}{\ell(p)}\}\{\lim_{p \to p_n} e^{\frac{A}{2}Z}\, \frac{j(p)}{p}\, e^{pt}\}$$

$$= \{\lim_{p \to p_n} \frac{\frac{d}{dp}(p-p_n)}{\frac{d}{dp}\ell(p)}\}\{e^{\frac{A}{2}Z}\, \frac{j(p_n)}{p_n}\, e^{p_n t}\} = e^{\frac{A}{2}Z}\, \frac{j(p_n)}{p_n \ell'(p_n)}\, e^{p_n t} \qquad \text{(AII-54)}$$

Now to calculate $\ell'(p)$

$$\ell'(p) = \frac{d}{dp}\left[\sqrt{A^2+4F(p)}\, \cosh \frac{\sqrt{A^2+4F(p)}}{2}L + (A + \frac{2F(p)}{A})\sinh \frac{\sqrt{A^2+4F(p)}}{2}L\right]$$

$$= \cosh \frac{\sqrt{A^2+4F(p)}}{2}L\, \frac{d}{dp}\sqrt{A^2+4F(p)} + \sqrt{A^2 4F(p)}\, \frac{d}{dp}\cosh \frac{\sqrt{A^2+4F(p)}}{2}L$$

$$+ \sinh \frac{\sqrt{A^2+4F(p)}}{2}L\, \frac{d}{dp}(A + \frac{2F(p)}{2}) + (A + \frac{2F(p)}{A})\frac{d}{dp}\sinh \frac{\sqrt{A^2+4F(p)}}{2}L$$

$$\qquad \text{(AII-55)}$$

$$\frac{d}{dp}\sqrt{A^2+4F(p)} = \frac{2(\frac{1}{E_D} + \frac{dD(p)}{dp})}{\sqrt{A^2+4F(p)}} \qquad \text{(AII-56)}$$

Since

$$\frac{d}{dx}[xI_p(\alpha x)] = (1-p)I_p(\alpha x) + \alpha x I_{p-1}(\alpha x)$$

$$\frac{d}{dx}[I_p(\alpha x)] = \alpha I_{p-1}(\alpha x) - \frac{p}{x} I_p(\alpha x)$$

$$I_{p-1}(\alpha x) = \frac{2p}{\alpha x} I_p(\alpha x) + I_{p+1}(\alpha x)$$

Then

$$\frac{d}{dp}\left[\sqrt{p}\ I_{\frac{3}{2}}\left(\frac{r_0}{\sqrt{D_S}}\sqrt{p}\right)\right] = \frac{d\left[\sqrt{p}\ I_{\frac{3}{2}}\left(\frac{r_0}{\sqrt{D_S}}\sqrt{p}\right)\right]}{d\sqrt{p}} \cdot \frac{d\sqrt{p}}{dp}$$

$$= \left[-\frac{1}{2}\ I_{\frac{3}{2}}\left(\frac{r_0}{\sqrt{D_S}}\sqrt{p}\right) + \frac{r_0}{\sqrt{D_S}}\sqrt{p}\ I_{\frac{1}{2}}\left(\frac{r_0}{\sqrt{D_S}}\sqrt{p}\right)\right]\cdot\frac{1}{2}\cdot\frac{1}{\sqrt{p}} \qquad \text{(AII-57)}$$

$$\frac{d}{dp}\left[I_{\frac{1}{2}}\left(\frac{r_0}{\sqrt{D_S}}\sqrt{p}\right)\right] = \frac{d\left[I_{\frac{1}{2}}\left(\frac{r_0}{\sqrt{D_S}}\sqrt{p}\right)\right]}{d\sqrt{p}} \cdot \frac{d\sqrt{p}}{dp}$$

$$= \left[\frac{r_0}{\sqrt{D_S}}\ I_{-\frac{1}{2}}\left(\frac{r_0}{\sqrt{D_S}}\sqrt{p}\right) - \frac{1}{2\sqrt{p}}\ I_{\frac{1}{2}}\left(\frac{r_0}{\sqrt{D_S}}\sqrt{p}\right)\right]\cdot\frac{1}{2}\cdot\frac{1}{\sqrt{p}}$$

$$= \left[\frac{r_0}{2\sqrt{D_S}p}\left[\frac{\sqrt{D_S}}{r_0\sqrt{p}}\ I_{\frac{1}{2}}\left(\frac{r_0}{\sqrt{D_S}}\sqrt{p}\right) + I_{\frac{3}{2}}\left(\frac{r_0}{\sqrt{D_S}}\sqrt{p}\right)\right] - \frac{1}{4p}\ I_{\frac{1}{2}}\left(\frac{r_0}{\sqrt{D_S}}\sqrt{p}\right)\right.$$

$$= \frac{r_0}{2\sqrt{D_S}p}\ I_{\frac{3}{2}}\left(\frac{r_0}{\sqrt{D_S}}\sqrt{p}\right) + \frac{1}{4p}\ I_{\frac{1}{2}}\left(\frac{r_0}{\sqrt{D_S}}\sqrt{p}\right) \qquad \text{(AII-58)}$$

From Eqs. (AII-24), (AII-57) and (AII-58)

$$\frac{dD(p)}{dp} = \frac{3(1-\epsilon)k_f}{\epsilon E_D r_0}\left[\frac{k_f m r_0}{2}\left(I_{\frac{1}{2}}\left(\sqrt{\frac{p}{D_S}}\ r_0\right)\right)^2 - \frac{k_f m r_0}{2}\left(I_{\frac{3}{2}}\left(\sqrt{\frac{p}{D_S}}\ r_0\right)\right)^2\right.$$

$$- \frac{k_f m}{2}\sqrt{\frac{D_S}{p}}\ I_{\frac{1}{2}}\left(\sqrt{\frac{p}{D_S}}\ r_0\right)I_{\frac{3}{2}}\left(\sqrt{\frac{p}{D_S}}\ r_0\right)\right]/\left(\sqrt{D_S p}\ I_{\frac{3}{2}}\left(\sqrt{\frac{p}{D_S}}\ r_0\right)\right.$$

$$+ k_f m I_{\frac{1}{2}}\left(\sqrt{\frac{p}{D_S}}\ r_0\right)\Big]^2$$

$$= G(p) \qquad \text{(AII-59)}$$

Put Eq. (AII-59) into Eq. (AII-56), Eq. (AII-56) then becomes

$$\frac{d}{dp}\sqrt{A^2+4F(p)} = 2[\frac{1}{E_D} + G(p)]/\sqrt{A^2+4F(p)} = H(p) \qquad \text{(AII-60)}$$

$$\frac{d}{dp}\cosh\frac{\sqrt{A^2+4F(p)}}{2}L = \frac{d(\cosh\frac{\sqrt{A^2+4F(p)}}{2}L}{d(\frac{\sqrt{A^2+4F(p)}}{2}L)}\frac{\frac{L}{2}d(\sqrt{A^2+4F(p)})}{dp}$$

$$= \frac{L}{2}H(p)\sinh\frac{\sqrt{A^2+4F(p)}}{2}L \qquad \text{(AII-61)}$$

$$\frac{d}{dp}(A + \frac{2F(p)}{A}) = \frac{2}{A}\cdot\frac{d}{dp}[\frac{p}{E_D} + D(p)] = \frac{2}{A}[\frac{1}{E_D} + G(p)] = \frac{\sqrt{A^2+4F(p)}}{A}H(p)$$

$$\text{(AII-62)}$$

$$\frac{d}{dp}\sinh\frac{\sqrt{A^2+4F(p)}}{2}L = \frac{L}{2}H(p)\cosh\frac{\sqrt{A^2+4F(p)}}{2}L \qquad \text{(AII-63)}$$

Substitute Eqs. (AII-60), (AII-61), (AII-62) and (AII-63)

into Eq. (AII-55); then one obtains

$$\ell'(p)=H(p)[\frac{2A+LA^2+2LF(p)}{2A}\cosh\frac{\sqrt{A^2+4F(p)}}{2}L + \sqrt{A^2+4F(p)}(\frac{L}{2}+\frac{1}{A})\sinh\frac{\sqrt{A^2+4F(p)}}{2}L$$

$$\text{(AII-64)}$$

The inverse of $\overline{C}_A$ is

$$C'_A(Z,t) = 1 + e^{\frac{A}{2}Z}\sum_{n=2}^{\infty}\frac{j(P_n)}{P_n\ell'(P_n)}e^{P_nt} \qquad \text{(AII-65)}$$

Since $\sqrt{A^2+4F(p)} = i\beta_n$, $F(p) = \frac{-\beta_n^2 - A^2}{4}$,

$$\sinh(ix) = i\sin x,$$

$$\cosh(ix) = \cos x$$

Equation (AII-65) can be reduced to

$$C'_A(Z,t) = 1 - e^{\frac{A}{2}Z} \sum_{n=2}^{\infty} \frac{\beta_n[A\sin\frac{(L-Z)\beta_n}{2} + \beta_n\cosh\frac{(L-Z)\beta_n}{2}]}{p_n2[\frac{1}{E_D} + G(p_n)]Q(\beta_n)} e^{p_nt}$$

(AII-66)

where

$$Q(\beta_n) = (1 + \frac{LA}{4} - \frac{L\beta_n^2}{4A})\cos\frac{L\beta_n}{2} - \beta_n(\frac{L}{2} + \frac{1}{A}) \sin \frac{L\beta_n}{2}$$

The calculations of Eq. (AII-66) are given in Figs. AII.1 and AII.2.

$$Q = 0.5 \qquad m = 0.5$$
$$\epsilon = 0.75 \qquad K_f = 0.0001$$
$$S = 2. \qquad D_S = 0.05$$
$$Z = 10. \qquad Y_0 = 0.1$$

C'_A

- - - - $E_D = 0.2$
- · - · - $E_D = 0.5$
· · · · · $E_D = 0.6$
———— $E_D = 1.0$

time

FIGURE   A II . I

$Q = 0.5$

$\epsilon = 0.75$

$S = 2.$

$Z = 10.$

$m = 0.5$

$K_f = 0.0001$

$D_S = 0.05$

$E_D = 0.2$

C_A'

1.0

.8

.6

.4

.2

0

30   40   50   60   70   *time*   80   90

$Y_0 = 0.01$

$Y_0 = 0.5$
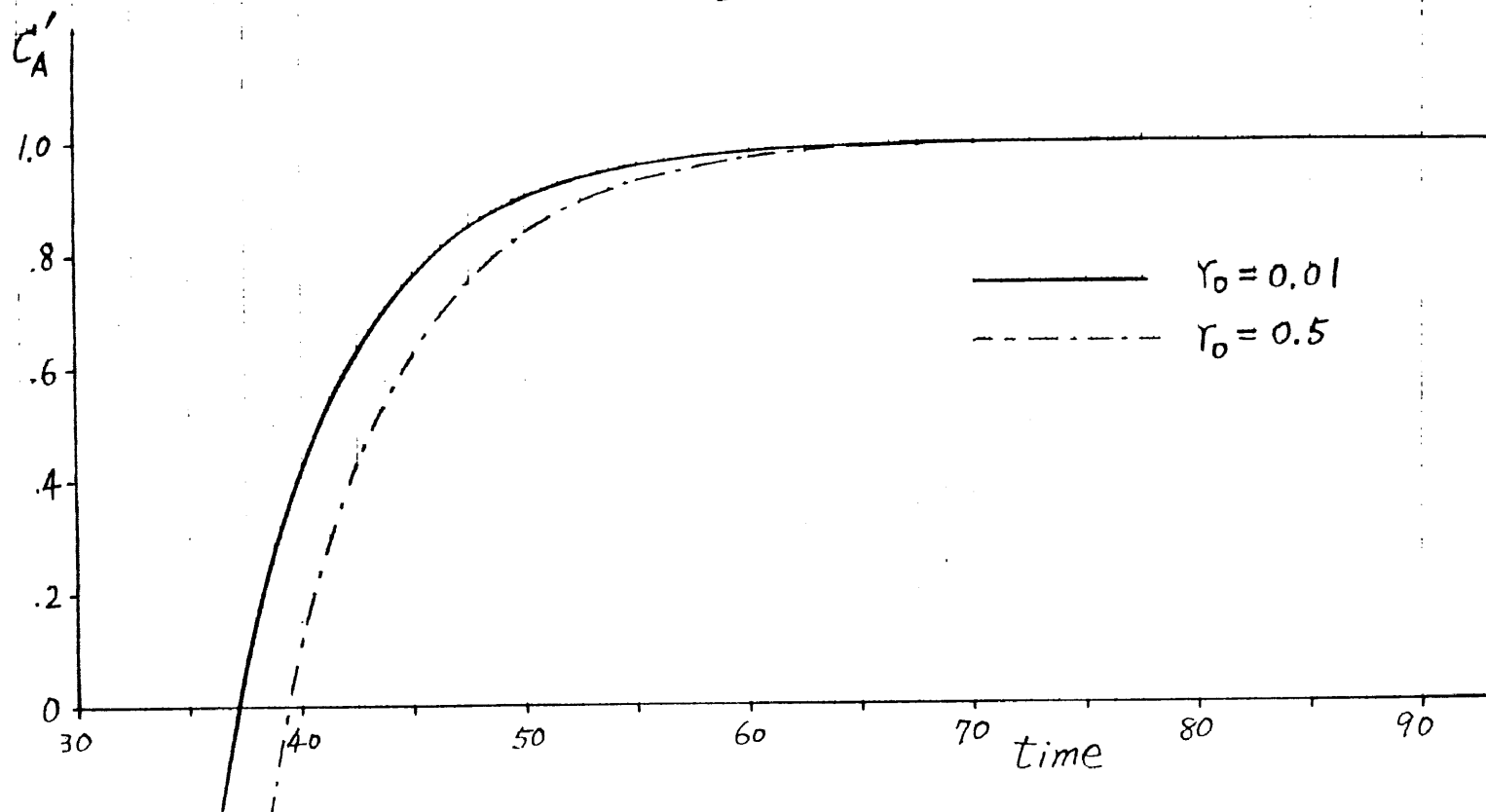
FIGURE   A II .2

APPENDIX III

A CALCULATION OF PARAMETRIC PUMPING

The batch parametric pumping system shown in Figure AIII.1 consists of a column packed with a particulate adsorbent and has reservoirs attached to each end. As shown in Figure AIII.1, there are four steps within each cycle, namely, 1) forward adsorption, 2) circulation for reaching equilibrium at $m=m_1$, 3) backward desorption, 4) circulation for reaching equilibrium at $m=m_2$. The initial conditions and boundary conditions required for a calculation are as follows.

Initial Conditions:

Column: $m(z,0) = m_2$

$$C_A = m_2 C_{AS} = C_{A0}$$

Top Reservoir: $m = m_1$

$$C_A = C_{A0}$$

Bottom Reservoir: $m = m_2$

$$C_A = C_{A0}$$

Boundary Conditions:

1. Column: (a) $n\tau < t < n\tau + t_1 + t_2$

$$m(0,t) = m_1$$

$$C_A(0,t) = C_{ATR}$$

$$m(L,t) = finite$$

$$C_A(L,t) = finite$$

(b) $n\tau + t_1 + t_2 < t < (n+1)\tau$

$$m(0,t) = finite$$

$$C_A(0,t) = finite$$
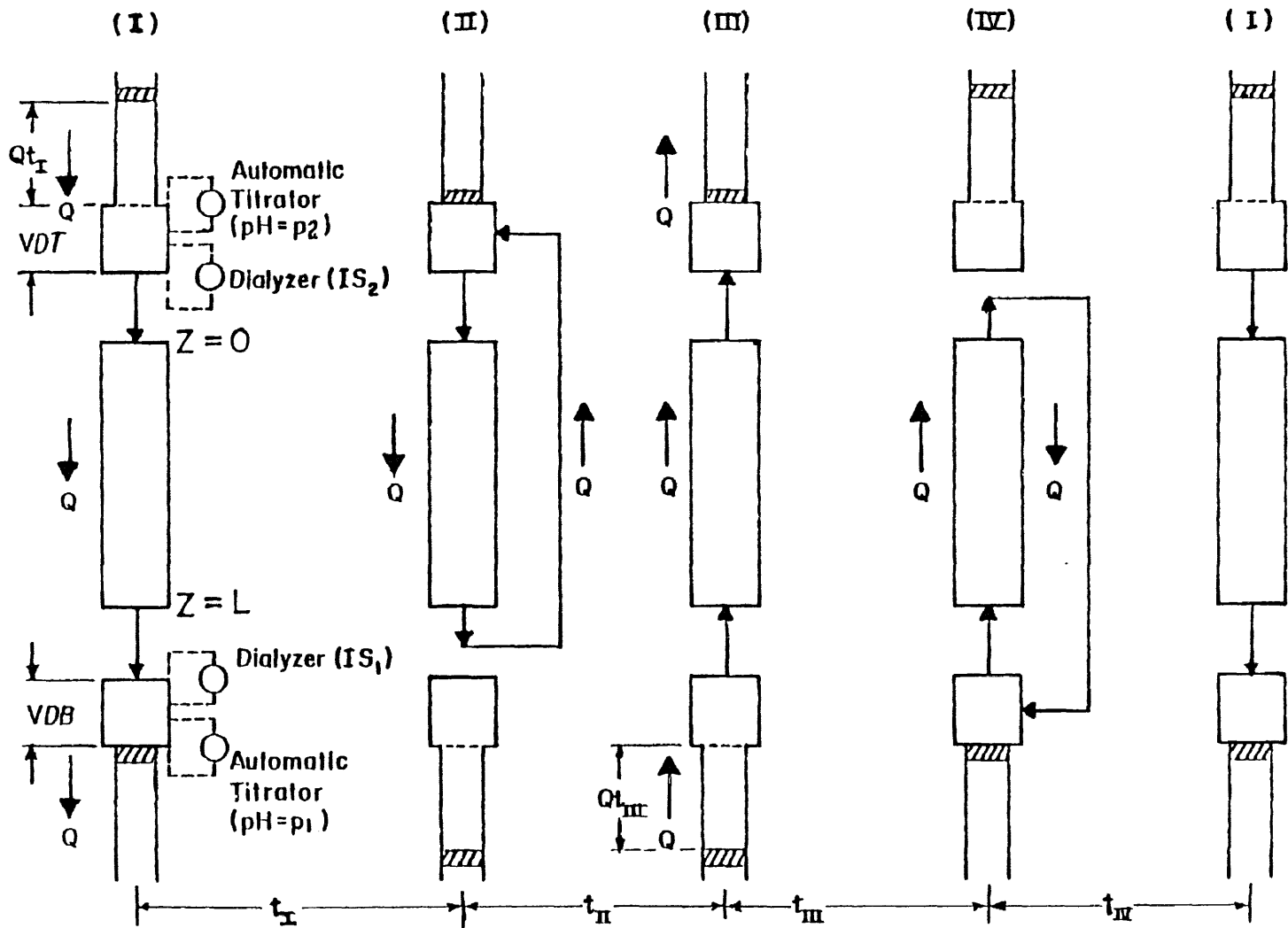
FIGURE   A III.I

$$m(L,t) = m_2$$

$$C_A(L,t) = C_{ABR}$$

2. Top Reservoir: $m = m_1$

   (a) $n\tau + t_1 < t < n\tau + t_1 + t_2$

$$\frac{\partial C_{ATR}}{\partial t} = \frac{Q(t)}{V_d} [C_A(L,t) - C_{ATR}(t)]$$

   (b) $n\tau + t_1 + t_2 < t < n\tau + t_1 + t_2 + t_3$

$$C_{ATR}(t) = \frac{V_d \cdot C_{ATR}(n\tau+t_1+t_2) + \int_{n\tau+t_1+t_2}^{t} Q(t) \cdot C_A(0,t)dt}{V_d + \int_{n\tau+t_1+t_2}^{t} Q(t)dt}$$

   (c) $n\tau + t_1 + t_2 + t_3 < t < (n+1)\tau + t_1$

$$C_{ATR} = C_{ATR}(n\tau + t_1 + t_2 + t_3)$$

3. Bottom Reservoir: $m = m_2$

   (a) $n\tau < t < n\tau + t_1$

$$C_{ABR}(t) = \frac{V_d \cdot C_{ABR}(n\tau) + \int_{n\tau}^{t} Q(t) \cdot C_A(z,t)dt}{V_d + \int_{n\tau}^{t} Q(t)dt}$$

   (b) $n\tau + t_1 < t < n\tau + t_1 + t_2 + t_3$

$$C_{ABR} = C_{ABR}(n\tau + t_1)$$

   (c) $n\tau + t_1 + t_2 + t_3 < t < (n+1)\tau$

$$\frac{\partial C_{ABR}}{\partial t} = \frac{Q(t)}{V_d} [C_A(0,t) - C_{ABR}(t)]$$

The calculated concentrations at the top reservoir and bottom reservoir versus the number of cycles are given in Figure AIII.2 and AIII.3.

$VDT = VDB = VE = Qt_1 = Qt_{III}$

① $m_1 = 0.2$, $m_2 = 10$

② $m_1 = 1$, $m_2 = 100$

③ $m_1 = 1$, $m_2 = 10$
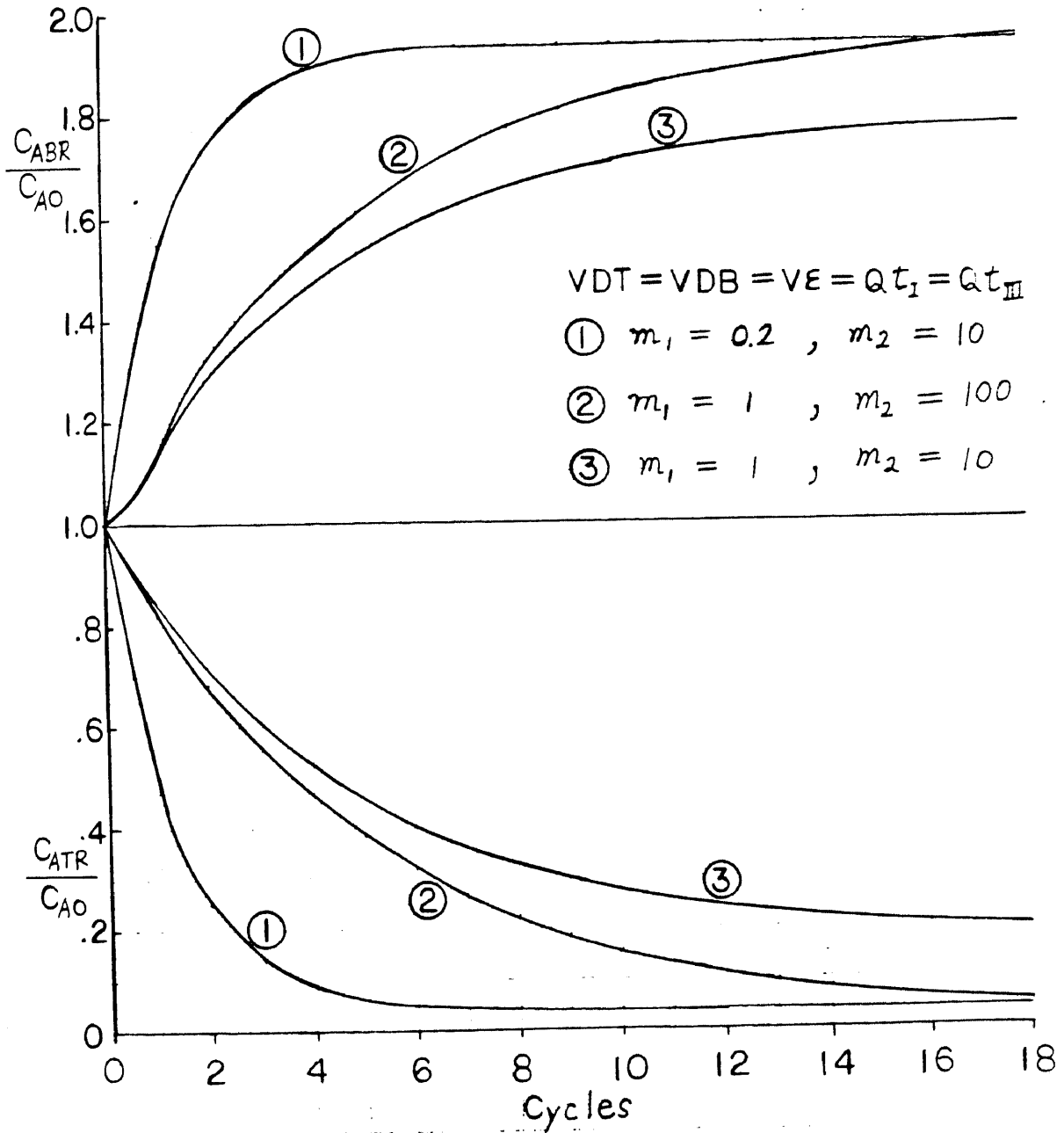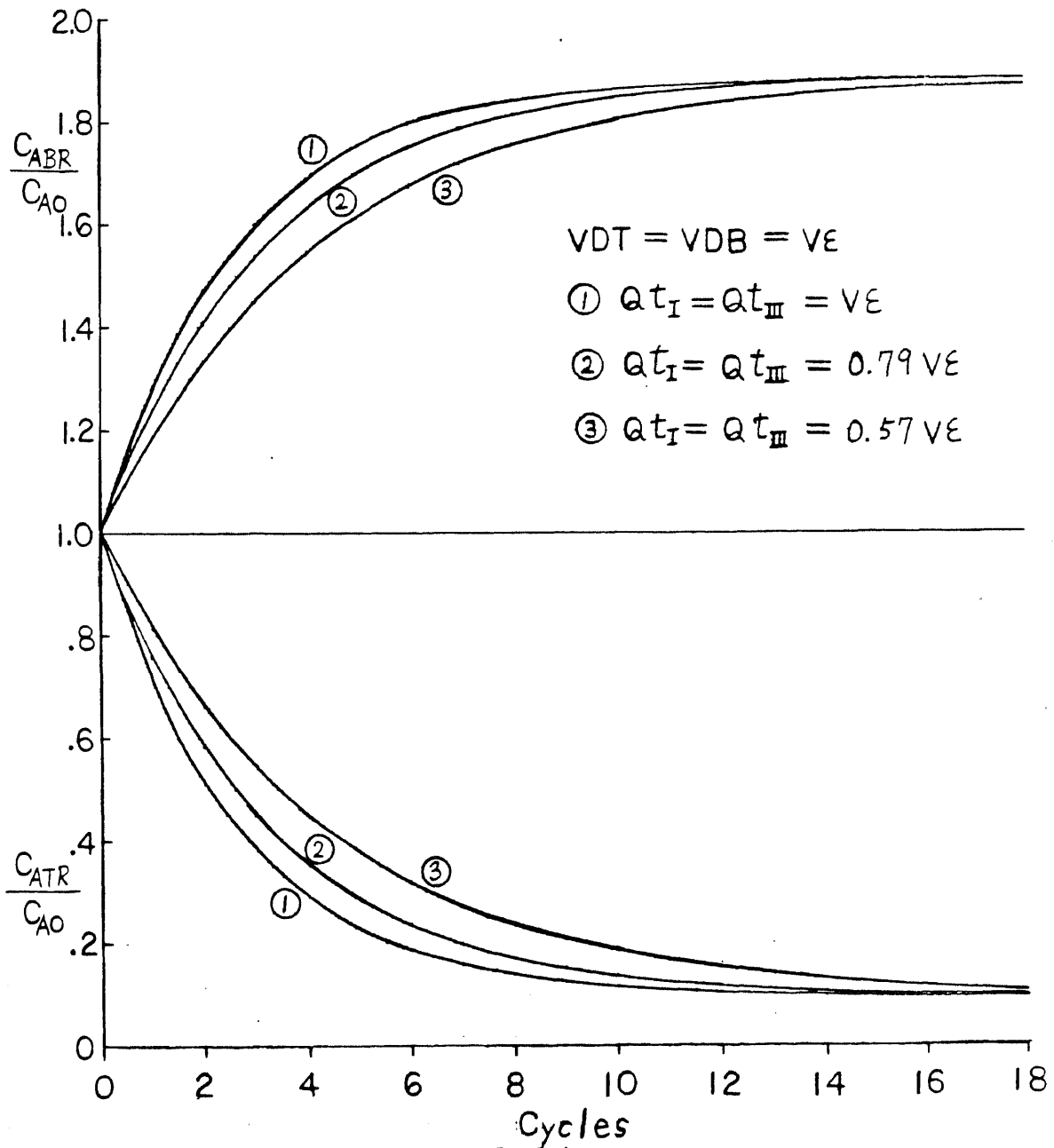
FIGURE   A III. 2

FIGURE A III .3

APPENDIX IV

Cycling Zone Electrophoresis

Jen-Fu Chao, Helen C. Hollein[1], and Ching-Rong Huang[*]

Department of Chemical Engineering and Chemistry
New Jersey Institute of Technology
Newark, New Jersey 07102

December, 1982

---

[*] Author to whom correspondence should be addressed.

[1] Present address, Manhattan College, Riverdale, N.Y. 10471.

ABSTRACT

The cycling zone separation principle has been applied to preparative polyacrylamide gel electrophoresis by incorporating cyclic variation of electric field strength. Experimental evidence is presented, based on the separation of a mixture of human hemoglobin and human serum albumin. Three cycles of operation are shown with fresh feed being added in each cycle and a continuous product stream being withdrawn. Cyclic operation eliminates the time-consuming gel preparation step which is an intrinsic part of the conventional process.

INTRODUCTION

Protein purification and separation is currently a focus of interest in the new field of genetic engineering. Typical separation methods depend on scale-up of conventional analytical techniques such as affinity chromatography, gel permeation chromatography, and electrophoresis (Donnelly, 1982). This communication examines the potential for polyacrylamide gel electrophoresis to be operated as a continuous cyclic separation process.

Pigford and co-workers introduced cycling zone adsorption as a new separation process in 1969. The separation in cyclic processes depends on periodic variation of a thermodynamic variable such as temperature, pressure, or solution pH. Appropriate intensive variables for protein separations are solution pH, solution ionic strength, electric field strength, and molecular affinity. We have recently investigated cyclic processes for the separation and purification of proteins, lectines, and enzymes using these particular intensive variables to institute adsorption and desorption in packed beds of ion exchangers and affinity resins (Hollein et al., 1982; Chao et al., 1982; Chen et al., 1981).

For comparison purposes, we have also studied the separation and purification of proteins and enzymes by polyacrylamide gel electrophoresis (PAGE). PAGE is traditionally operated batch-wise. New gel is prepared for each run, and a small sample of a given

protein mixture is separated for analytical purposes. Preparative-
scale electrophoresis systems such as the LKB UNIPHOR 7900 or the
Buchler Poly-Prep 200 handle larger feed samples than analytical
systems, but also require new gel for each batch. In the present
study, a continuous product stream was generated in preparative-
scale equipment by periodically removing the spent raffinate and
adding fresh feed in sequence with cyclic variation of the field
strength. The gel has been reused up to seven times with no
apparent degradation of physical properties. Elimination of
the time-consuming gel preparation step considerably increases
the unit production rate capability of this equipment.

Nelson et al., 1978, have examined cycling zone separations
of various mixtures using temperature, feed concentration, or
feed pH as the cyclic variables. The thermodynamic variable is
set at one level for adsorption and changed to a second level
for desorption, and the procedure is repeated in successive
cycles. The separation can be optimized by setting the cycle
time so that it tends to amplify the concentration waves of the
component species of the mixture. These processes have the
advantage of continuous operation, yielding more product per
unit time than a batch operation in the same equipment.

Thompson and Bass, 1974, and Oren and Soffer, 1978, have
used electric field as the intensive variable in electrochemical
parapumping processes for the desalination of water. The
separation principle in parametric pumping is similar to cycling
zone adsorption, but the former process incorporates an oscillating

direction of fluid flow, while the flow in the latter process is unidirectional. Electrochemical parametric pumping uses cyclic variation of electric field strength for adsorption and desorption.

The separation in cycling zone electrophoresis, however, is based on the fact that different proteins move at different velocities in the presence of an applied electric field. The proteins move from the feed solution through the polyacrylamide gel into the effluent solution. The basic requirement for cyclic separation processes is the existence of a two-phase system where the distribution of a given component between the phases is altered by changing an appropriate intensive variable. Wankat, 1973, has shown that this principle can be extended to non-adsorptive separations such as liquid-liquid extraction. The cycling zone separation principle is applied to conventional electrophoresis in the present study.

Experimental studies on the purification of the enzyme, alkaline phosphatese, via PAGE (to be published in subsequent papers) indicate that significant improvements in purification can be achieved by optimizing the operating conditions with respect to field strength, feed volume, solution ionic strength, solution pH, etc. The impurities associated with alkaline phosphatese are undesired proteins, the exact composition of which is unknown. In order to better evaluate the phenomena behind electrophoretic separations, an arbitrary mixture of known proteins (human serum albumin plus human hemoglobin) was chosen as the model system for this investigation.

EXPERIMENTAL SECTION

A preparative-scale PAGE system, the Buchler Poly-Prep 200, was used for the experimental work. The system was maintained at $278^\circ K$ by circulation of cooling water through the inner and outer cooling jackets. A Buchler 3-1500 power supply was used for a direct current source. The power supply was set at constant wattage for the duration of an experimental run, and the voltage and amperage were recorded. A multistaltic pump (manufactured by Buchler) was used to circulate the buffer solution through the anode and cathode compartments to an external buffer reservoir (1 liter volume). The buffer was titrated to maintain constant pH. A second multistaltic pump was used to pump pre-cooled elution buffer through the elution chamber.

Prior to the start of each experimental run, the polyacrylamide gel is polymerized directly in the PAGE system. The composition of the gel was 5 weight % acrylamide, 0.13 weight % N,N'-methylene bis acrylamide, 0.15 weight % ammonium persulfate, plus 0.07 volume % TEMED (Rodbard and Chrambach, 1972). The gel solution was titrated to a pH of 8.6. A gel height of 8.3 cm was used for all experimental runs. After allowing several hours for polymerization, the Poly-Prep system was assembled and filled with buffer solution. The power supply was set at constant voltage (200 volts), and the system was run for 6 hours to remove ultraviolet detectable materials from the gel.

For all experimental runs, the buffer solution was a mixture of Tris plus glycine (0.05 M each) at a pH of 8.6. The

feed was made-up by adding 0.05 weight % total proteins plus 10.0 weight % sucrose to the buffer solution. The added sucrose makes the feed solution denser than the buffer solution. The feed is pumped into the upper compartment and forms a separate layer directly above the gel and directly below the circulating buffer. The dense feed layer remains in place throughout an experimental run. For cyclic operation, the spent feed is periodically removed and fresh feed solution is pumped into the system.

Product samples from the elution chamber were collected at either 15 or 30 minute time intervals. These samples were analyzed using a Bausch and Lomb spectrophotometer. Hemoglobin concentration was determined by ultraviolet adsorbance at a wavelength of 403 μm and total protein was determined at a wavelength of 595 μm. Albumin concentration was then determined by difference.

RESULTS AND CONCLUSIONS

Typical elution profiles for PAGE separations of protein or enzyme mixtures show the total protein eluted as a function of time or fraction number (Righetti and Secchi, 1972). This type of data is sufficient for the analysis of protein mixtures and generates a series of peaks which can be related to the various components in the original mixture. If electrophoresis is to be used for protein separation, however, a detailed analysis of the composition of each peak is required.

The electrophoretic separation of a mixture of hemoglobin and albumin is shown in the figures below. The concentration of the individual proteins is indicated, rather than simply reporting the total protein in each peak. The experimental operating conditions are listed in Table I.

All proteins carry both negatively and positively charged functional groups (COO^- and NH_3^+), with a net charge of zero at the isoelectric point. Human hemoglobin and human serum albumin have isoelectric points of $I_A = 6.7$ and $I_B = 4.7$, respectively. The pH of the feed solutions was set at $P = 8.6$ for all of the experimental runs. This pH is higher than the isoelectric points of both proteins, so both proteins carry a net negative charge and move towards the cathode in the presence of an applied electric field. Since hemoglobin and albumin are both globular proteins with similar physical properties except for their isoelectric points and since $(P - I_B) > (P - I_A)$, the albumin molecules have a greater net negative charge at $P = 8.6$ and

move at a greater velocity than the hemoglobin molecules in the experimental runs below. Thus in Figures 1-3, the albumin peak exits the PAGE system in a shorter period of time than the hemoglobin peak in all cases.

Electrophoresis of either pure albumin or pure hemoglobin yields a relatively simple elution profile as shown in Figure 1A. Albumin is known to contain several species and may give multiple peaks (Righetti and Secchi, 1972). The heterogenity of the albumin sample is evidenced by the irregular shape of the trailing portion of the albumin peak in Figure 1A, but multiple peaks were not obtained for the pure components under the operating conditions used for the present studies.

When a mixture of hemoglobin and albumin is separated, however, multiple peaks are observed for hemoglobin. A small hemoglobin peak is eluted with the albumin peak as seen in Figure 1B. The reddish-brown color of the hemoglobin allowed visual confirmation of the experimental data. Two hemoglobin bands were observed moving through the polyacrylamide gel -- a faint narrow leading band and a dark broader trailing band. Some of the hemoglobin apparently "sticks to" the albumin.

Steiner, 1953, reported association complexes between serum albumin and lysozyme due to electrostatic attraction at pH's intermediate between the isoelectric points of the two proteins. A similar association complex between serum albumin and hemoglobin would account for the double hemoglobin peaks in Figures 1B, 2, and 3, only if the pH inside the gel were between I_A and I_B so that negatively charged albumin molecules and

positively charged hemoglobin molecules would be attracted to each other. The pH of the feed and elution solutions is above both I_A and I_B, but the pH inside the gel during the experiment is not known. It is known, however, that the pH increases in the vicinity of the anode and decreases in the vicinity of the cathode in the presence of an applied electric field. Since the gel is nearer the cathode, the pH inside the gel is some value less than $P = 8.6$. The protein-protein interaction, as indicated by the double peaks in Figures 1B, 2, and 3, is not well-understood and will be studied in more detail in future work.

The separation of the mixture is compared at several different field strengths in Figure 2. As the power increases from 3 watts to 10 watts, the cycle or batch time decreases from 13 hours to 8 hours. An experiment was attempted at 20 watts in order to further decrease the cycle time, but serious degradation of the gel due to overheating was observed. The field strengths corresponding to these wattages are listed in Table I.

The separations obtained in the various runs are also listed in Table I. The eluted protein is divided into two product fractions at the crossover point of the elution profiles for the individual solutes. Fraction 1 is richer in albumin and fraction 2 is richer in hemoglobin. The separation factor for the batch or cycle is defined as follows,

$$S.F. = \frac{(mg. \ Al)_1 \ (mg. \ Hb)_2}{(mg. \ Al)_2 \ (mg. \ Hb)_1} \tag{1}$$

Comparison of runs 4 and 5 in Table I shows that the separation factor increases from 6 to 13 when the field strength decreases from 331 volts to 231 volts. Comparison of runs 5 and 6, however, shows that the separation factor decreases from 13 to 11 when the field strength decreases from 231 volts to 170 volts. Thus the observed separation goes through an optimum somewhere around 5 watts.

Comparison of runs 3 and 5 in Table I indicates that better separation is obtained for a feed volume of 10 cc than for a feed volume of 30 cc. This result is reasonable since the concentration bands are proportionally smaller for a smaller feed quantity, leading to less overlapping of the side portions of the peaks.

Cycling zone electrophoresis is shown in Figure 3. In order to minimize the batch or cycle time while still maintaining good separation, the albumin rich fraction was collected at 5 watts to maximize purity, then the power was increased to 10 watts to remove the remaining protein in the minimum time. After the major portion of the hemoglobin rich fraction had exited the PAGE system, the spent feed solution was pumped out and a 10 cc pulse of fresh feed was added. The power was simultaneously reduced to 5 watts.

Three cycles of operation are indicated for run 7 in Figure 3. Each cycle yields two product fractions and includes a feed step plus periods of operation at low and high fields. Cycles 2 or 3 begin at the time when the effluent stream becomes richer in albumin. The separation factors for run 7 are given

in Table I.   The separation in the first cycle of run 7 is
comparable to the batch experiments with the identical operating
conditions, i.e., runs 4 and 5.   The separation in cycles 2 and
3 of run 7 is slightly lower than in cycle 1 (6-7 versus 9).
This is due to the fact that the hemoglobin rich peak has a
long tail, part of which extends into the succeeding albumin
rich peak of the next cycle.   The separation factor of approxi-
mately seven can be maintained from cycle 2 ad infinitum.

All of the data in Figures 1-3 was obtained using the
Buchler Poly-Prep 200 electrophoresis system.   Similar batch
data was obtained in a LKB UNIPHOR 7900 electrophoresis system
by using the same conditions for power, pH, gel height, and
buffer composition while reducing the feed volume from 10 cc
to 3 cc in order to compensate for the smaller cross-sectional
area of the LKB system.   The Buchler system was much more
successful, however, in long-term reusage of the polyacrylamide
gel for cyclic operation.

Another cycling zone electrophoresis experiment was
conducted at P = 5.7 with 0.05M Tris-maleate plus 0.05M NaOH
buffer solution.   Under these conditions, the albumin molecules
are negatively charged and the hemoglobin molecules are positively.
charged.   The cathode was first placed at the bottom of the PAGE
system and the albumin rich fraction was collected.   The polarity
of the electric field was then switched in order to collect the
hemoglobin rich fraction, but the hemoglobin was not recovered
in this case.   Visual observation indicated that during the
first part of the low pH experiment, the hemoglobin had migrated

upward from the dense feed layer through the buffer layer towards the anode where the hemoglobin was destroyed. A cloudy,foamy substance was observed in the region of the anode and was attributed to the presence of denatured proteins.

In conclusion, the cyclic operation of a preparative-scale PAGE system has been demonstrated. The electric field strength is cycled between 231 volts and 331 volts, and a 10 cc pulse of fresh feed is added in each cycle. Cycling zone electrophoresis appears to be a promising technique for protein separation and enzyme purification.

ACKNOWLEDGMENT

NOMENCLATURE

Al : albumin

Hb : hemoglobin

I_A : isoelectric point of hemoglobin

I_B : isoelectric point of albumin

P : pH of feed, buffer, and elution solutions

PAGE : polyacrylamide gel electrophoresis

S.F. : separation factor, defined by equation 1

y_F : concentration of solute in feed, kg mol / m^3

y_P : concentration of solute in product, kg mol / m^3

Subscripts

1 : fraction 1

2 : fraction 2

LITERATURE CITED

Chao, J.F., Huang, J.J., Huang, C.R., "Continuous Multiaffinity
    Separation of Proteins: Cyclic Processes," AIChE Symposium
    Series, in press.

Chen, H.T., Ahmed, Z.M., Rollan, V., Ind. Eng. Chem. Fundam.,
    1981, 20, 171.

Donnelly, L.W., Chem. Eng. Prog., 1982, 78, no. 11, 21.

Hollein, H.C., Ma, H.C., Huang, C.R., Chen, H.T., Ind. Eng. Chem.
    Fundam., 1982, 21, 205.

Nelson, W.C., Silarski, D.F., Wankat, P.C., Ind. Eng. Chem.
    Fundam., 1978, 17, 32.

Oren, Y., Soffer, A., J. Electrochem. Soc., 1978, 125, 869.

Pigford, R.L., Baker, B., Blum, D.E., Ind. Eng. Chem. Fundam.,
    1969, 8, 848.

Righetti, P., Secchi, C., J. Chromatogr., 1972, 72, 165.

Rodbard, D., Chrambach, A., Anal. Biochem., 1971, 40, 95.

Steiner, R.F., Arch. Biochem. Biophys., 1953, 47, 56.

Thompson, D.W., Bass, D., Canadian J. Chem. Engr., 1974, 52, 345.

Wankat, P.C., Ind. Eng. Chem. Fundam., 1973, 12, 372.

TABLE I.   EXPERIMENTAL PARAMETERS & RESULTS

Run	Cycle	Feed (cc)	Watts	Volts	Feed, weight % Albumin	Feed, weight % Hemoglobin	S.F.
1	--	30	5	234	0.050	--	--
2	--	30	5	233	--	0.050	--
3	--	30	5	230	0.025	0.025	5.1
4	--	10	10	331	0.025	0.025	5.5
5	--	10	5	231	0.025	0.025	12.6
6	--	10	3	170	0.025	0.025	11.3
7	1	10	5 / 10	224 / 321	0.025	0.025	9.4
"	2	10	5 / 10	224 / 321	0.025	0.025	6.9
"	3	10	5 / 10	224 / 321	0.025	0.025	6.3

Buffer = 0.05M Tris + 0.05M Glycine,   pH = 8.6,   Gel Height = 8.3 cm,

Elution Rate = 20 cc / hr,   Cooling Water Temperature = 278 °K.

FIGURE CAPTIONS

Figure 1. Evidence for protein-protein interaction in the
           separation of protein mixtures.

Figure 2. Effect of electric field strength on the separation
           of a mixture of albumin and hemoglobin via polyacryl-
           amide gel electrophoresis.

Figure 3. Cycling zone electrophoresis (run 7).

FIGURE I

run 4 (10 watts)
Albumn ——
Hemoglobin - - -

run 5 (5 watts)

run 6 (3 watts)

hours
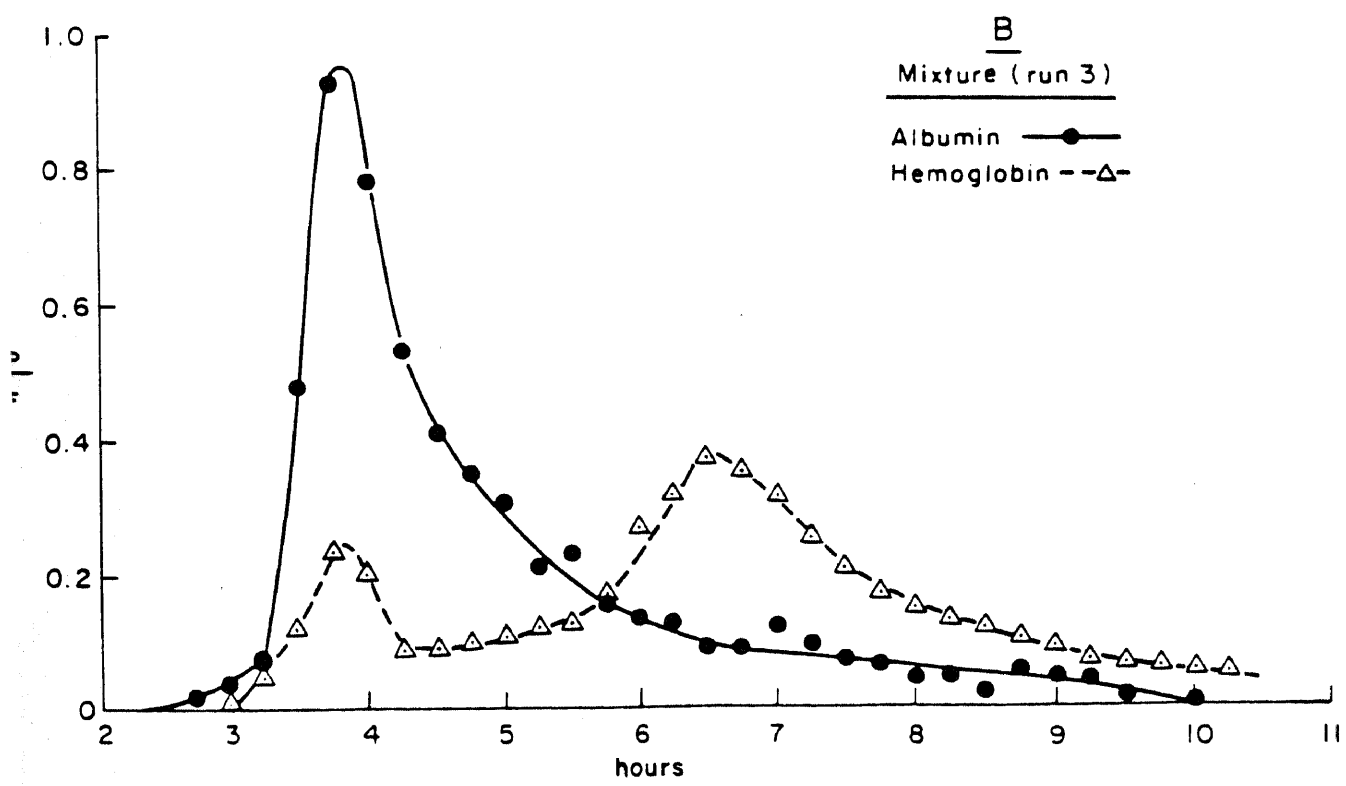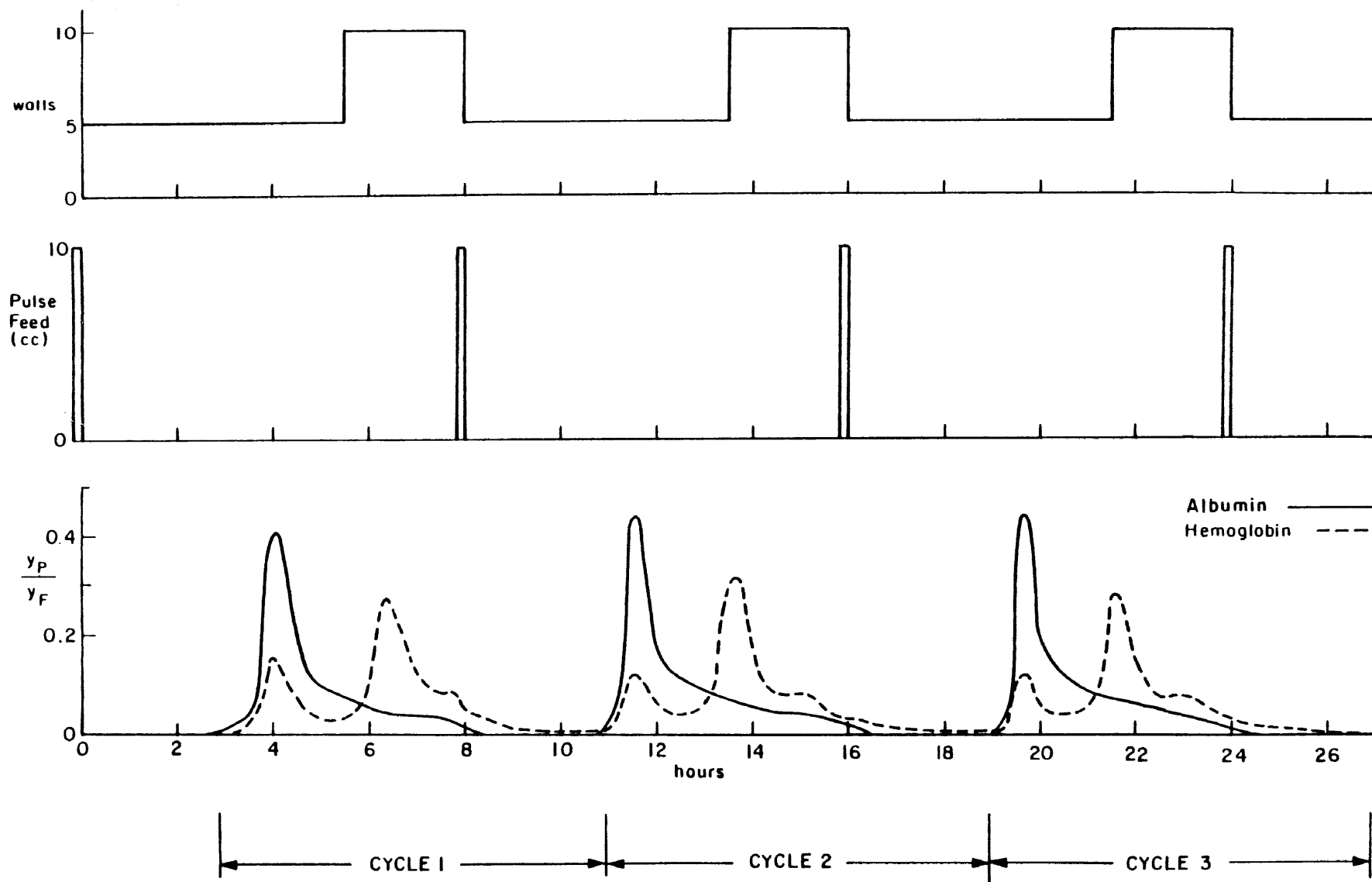
FIGURE 2

FIGURE 3
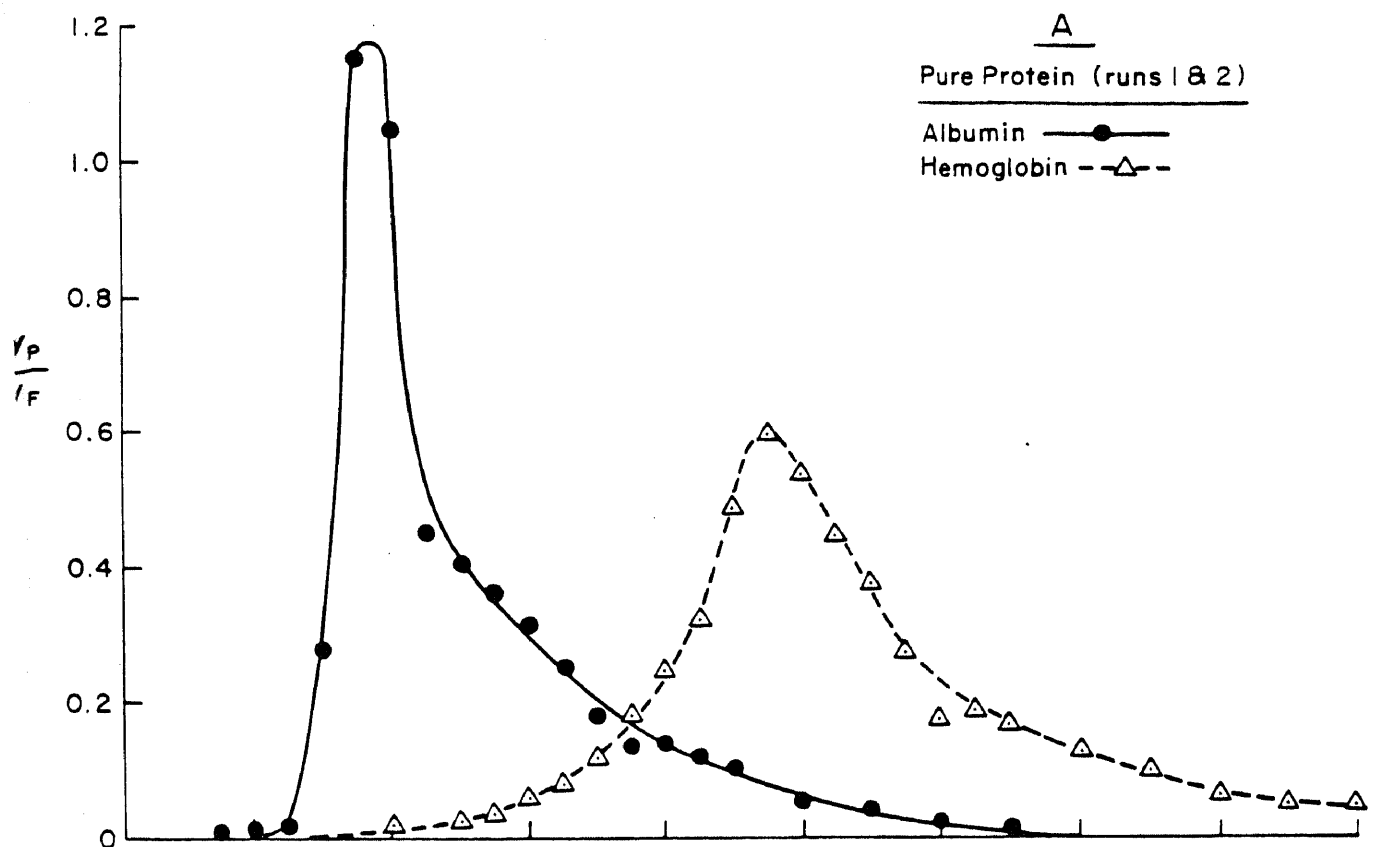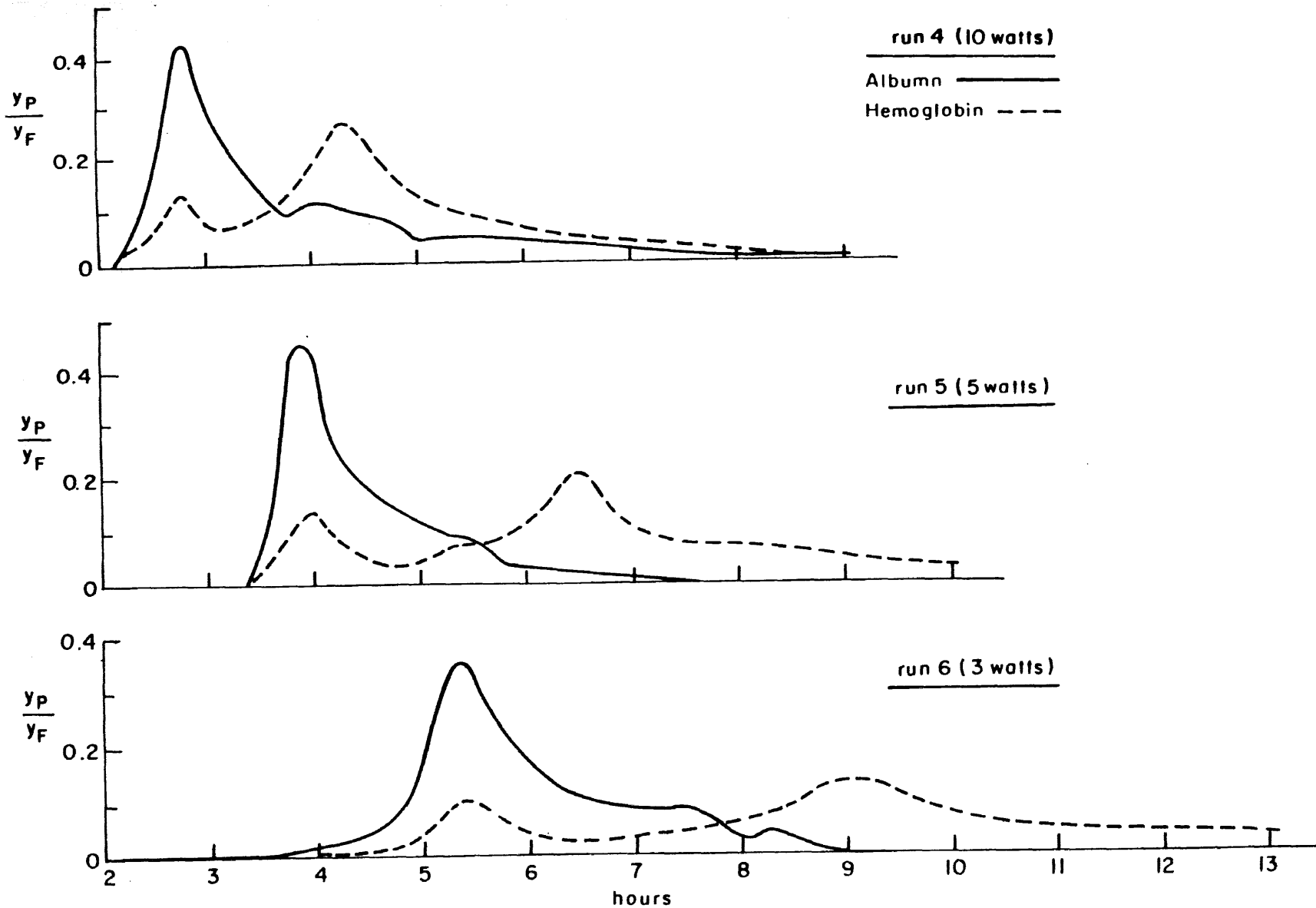
APPENDIX V

ENZYME PURIFICATION

A Comparison of prep-PAGE with Cyclic Processes

J.F. Chao, V.P. Rollan, H.C. Hollein[+], and C.R. Huang[*]

Department of Chemical Engineering and Chemistry
New Jersey Institute of Technology
Newark, New Jersey 07102

March, 1983

[*] Author to whom correspondence should be addressed.

[+] Present address, Manhattan College, Riverdale, New York 10471

ABSTRACT

Enzyme purification has been investigated in a preparative-scale polyacrylamide gel electrophoresis system, the Buchler Poly-Prep 200. Experimental results are presented for the optimization of this process using human placental alkaline phosphatase as a typical enzyme. The varibles considered are electric field strength, feed concentration, buffer ionic strength, and buffer pH. Enzymes may also be purified by adsorption/desorption onto an ion exchange resin such as DEAE Sepharose in either of two cyclic processes -- parametric pumping or cycling zone adsorption. Comparison of the three processes indicates that polyacrylamide gel electrophoresis has the highest purification factor and the greatest enzyme activity recovered, but also the lowest rate of production.

INTRODUCTION

In our recent study of enzyme purification via parametric pumping [1], the question was posed as to how this new process compares with conventional separation techniques for enzymes -- specifically with regard to purification, enzyme activity recovered, and rate of production. Enzymes are difficult to purify and generally require a series of purification steps [2 - 4]. The enzyme, human placental alkaline phosphatase (HPAP), typifies the separation problems encountered in enzyme purification. There are six different forms of the enzyme HPAP, and the crude enzyme mixture contains protein impurities such as human placental albumin with isoelectric points and molecular weights close to the values for HPAP, thus making these impurities difficult to remove [3,5,6].

A typical purification procedure is given by Seargeant and Stinson for human liver alkaline phosphatase [4]. Their procedure includes butanol extraction and acetone precipitation, followed by ion-exchange and/or affinity chromatography on resins such as DEAE Sephadex, Concanavalin A Sepharose, Phosphonic acid Sepharose, and Sephadex G-200. Ghosh and Fishman [3] have proposed continuous paper curtain electrophoresis in addition to Sephadex G-200 gel filtration and DEAE cellulose anion-exchange chromatography as the final steps in a large-scale purification scheme for human placental alkaline phosphatase. The crude enzyme mixture can be easily separated from the placental homogenate by extraction and precipitation or dialysis [3,4]. In our previous experiments with HPAP, parametric pumping was investigated as a replacement for the final more-difficult chromatographic steps. In the present work,

preparative-scale polyacrylamide gel electrophoresis (prep-PAGE) is proposed as an alternative in the final purification steps.

Parametric pumping is a semicontinuous separation process developed from common chromatographic procedures such as ion-exchange chromatography [1] or affinity chromatography [7]. Semicontinuous processing tends to minimize processing time and, therefore, has the dual advantage of maximizing rate of production and minimizing time-dependent degradation of sensitive compounds like enzymes which are generally not very stable.

Parametric pumping is a member of a group of cyclic separation processes, including cycling zone adsorption, which depend on a change in some thermodynamic variable for adsorption and desorption. For purification of HPAP on DEAE Sepharose anion exchanger [1], the adsorption/desorption cycle has three major steps involving changes in ionic strength and pH as the intensive variables: (I) adsorption of all proteins at high pH and low ionic strength, pH = 7.4 and I.S. = 0.1 M; (II) selective desorption of the desired enzyme at high pH and high ionic strength, pH = 7.4 and I.S. = 0.6 M; and (III) desorption of protein impurities at low pH and low ionic strength, pH = 4.0 and I.S. = 0.1 M. In parametric pumping, an oscillating direction of fluid flow is coupled to the change in the thermodynamic variable. The oscillating fluid flow tends to amplify the concentration waves giving better separation or purification than one-way processes. Cycling zone adsorption is similar to parametric pumping except that the flow in unidirectional. Chen et al. [1] compared parametric pumping and cycling zone adsorption for the purification of HPAP and showed that the former process yields a

larger percentage of the total enzyme activity recovered and greater purification while the latter process yields a higher rate of production. These processes are compared with prep-PAGE below.

We have recently demonstrated that prep-PAGE can be operated in a semicontinuous manner, i.e., cycling zone electrophoresis, for protein separations [8]. PAGE has previously been used for analytical separations of HPAP samples [9,10]. The disc gel patterns show excellent resolution, thus indicating a strong potential for the use of cycling zone prep-PAGE in enzyme purification.

Polyacrylamide gel was introduced as a new stabilizing medium for electrophoresis by two independent groups of researchers in 1959, Raymond and Weintraub [11] and also Davis and Ornstein [12]. The sharpness of the individual protein bands and the number of separate bands observed were reported to be superior compared to preexisting electrophoretic procedures such as starch gel, agar gel, or paper electrophoresis. Reviews of the development of the procedures and equipment for both analytical-scale and preparative-scale PAGE are available in the literature [13-16].

A Buchler Poly-Prep 200 preparative-scale electrophoresis system was used in the current investigation. This apparatus is based on the design by Chrambach and co-workers [13,17]. Note that the term "preparative-scale" implies load capacities in the order of one milligram per square centimeter of cross-sectional area of gel. Righetti and Secchi [18] have used prep-PAGE for separation of protein mixtures in a LKB UNIPHOR 7900 electrophoresis system. Because of the limited capacity of this milligram-scale equipment, prep-PAGE is only recommended as one of the final process

steps after the quantity of starting material has been considerably reduced.

Righetti and Secchi [18] studied the optimal conditions for the separation of proteins such as bovine serum albumin, ovalbumin, lysozyme, and cytochrome C via prep-PAGE. They recommended gel strengths ranging from 4 to 8% acrylamide, gel heights of 5 - 10 cm, elution buffer rates of 12 - 25 ml / h, and buffer ionic strengths of 0.02 - 0.03 M. An optimization problem occurs in electrophoretic separations with respect to the length of time required for the individual proteins to move through the gel. If the product elution time is too short, successive concentration peaks will not be completely developed, resulting in poor separation. On the other hand if the time period is too long, axial diffusion will tend to broaden the individual peaks leading to overlapping of successive bands and to poor separation. In order to maximize the separation, the variables such as gel height, buffer ionic strength, buffer pH, and electric field strength which control the total time for protein movement through the gel must be optimized. The optimal conditions are dependent on the nature of the components of each mixture to be separated, and must be determined experimentally.

EXPERIMENTAL

HPAP with a specific activity of 3.0 units per milligram of solid was purchased from Sigma Biochemicals. By definition, one unit of enzyme activity will hydrolyze 1 μmole of p-nitrophenyl phosphate per minute at 303°K and at a pH of 10.15 [6]. The activity of pure HPAP is approximately 1171 units per milligram [4]. The detailed composition of the impurities in the Sigma HPAP is not known, but the major impurity is probably human placental albumin [4]. The electrophoretic elution profiles for the major impurity in the experiments below closely match the elution profiles for human serum albumin under identical operating conditions.

The experimental set-up is shown in Figure 1. The electro-phoresis system includes the Buchler Poly-Prep 200 apparatus, two Buchler multistaltic pumps, and a Buchler 3-1500 direct current power supply. One multistaltic pump was used to circulate the buffer solution through the cathode and anode compartments to an external buffer reservoir (1 liter volume). The buffer was titrated in the external reservoir to maintain the desired pH. A second multistaltic pump was used to pump pre-cooled elution buffer into the elution chamber and up through the central elution capillary tube to the product stream. The Buchler Poly-Prep system was maintained at 278°K by circulation of cooling water through the inner and outer cooling jackets.

The Buchler Poly-Prep apparatus has two main parts. The upper section contains the electrophoresis column, the upper electrode chamber, the central elution capillary, and the inner and outer cooling jackets. The lower section contains the lower

electrode chamber and the elution chamber, separated by a semi-permeable glass membrane. Prior to the start of each experiment, the polyacrylamide gel is polymerized directly in the prep-PAGE system. When the two sections of the Buchler Poly-Prep apparatus are assembled, the bottom of the self-supporting gel forms the upper boundary of the elution chamber. The gel has an annular cross-sectional area of 18 cm^2. A gel height of 8.3 cm was used for all of the experimental runs.

The gel must be meticulously prepared in order to obtain reproducible data. The composition of the gel was 5 weight % acrylamide, 0.13 weight % N,N'-methylene bis acrylamide, 0.15 weight % ammonium persulfate, plus 0.07 volume % TEMED [19]. The gel solution was titrated to a pH of 8.6 with 0.10 M Tris buffer solution, then filtered and poured slowly into the column being careful to avoid formation of air bubbles. A thin layer of distilled water was gently layered onto the surface of the gel solution in order to prevent the formation of a miniscus on top of the gel during polymerization. After allowing the gel to polymerize completely (approximately thirty minutes), the surface of the gel was rinsed with fresh water and the Buchler Poly-Prep apparatus was assembled and filled with buffer solution. The power supply was set at constant voltage (200 volts), and the system was run for six hours to remove ultraviolet detectable materials from the gel.

The buffer was prepared by mixing solutions of Tris and glycine of the same molarities. In the experiments below, the buffer ionic strength was varied from 0.05 M to 0.20 M and the

pH was varied from 8.0 to 9.5 as shown in Table I. The feed solution was prepared by adding 0.02 - 0.05 weight % Sigma HPAP and 10.0 weight % sucrose to the Tris/glycine buffer solution. The added sucrose makes the feed solution denser than the buffer solution. The feed is pumped into the upper compartment through the feed layering tube. The feed solution forms a distinct layer directly above the gel and directly below the circulating buffer solution. The dense feed layer remains in place throughout an entire experimental run. We have previously shown that the gel can be reused a number of times [8]. In cycling zone electrophoresis, the spent feed is periodically removed and fresh feed is pumped into the system.

Product samples were collected at equal time intervals at a product elution rate of 20 ml/h. These samples were analyzed using a Bausch and Lomb spectrophotometer. Bio-Rad protein assay was used to determine total protein concentration at a wavelength of 595 nm and $293^{o}K$. The enzyme activity of the product was determined by measuring the increase in absorbance after reaction with p-nitrophenyl phosphate at 405 nm and $303^{o}K$ as described in the Worthington Enzyme Manual [6].

RESULTS AND DISCUSSION

The experimental operating conditions for thirteen runs on HPAP are listed in Table I. Tris/glycine buffer was used for all of the experiments. Rodbard and Chrambach suggest using different buffer components for the circulating buffers in the upper and lower electrode chambers and also for the gel preparation [19]. The operation of the prep-PAGE system is simplified in the present work by the use of only one buffer solution.

The power settings in the various experiments vary from 2 watts to 10 watts. An experiment was attempted at 20 watts, but serious degradation of the gel occurred due to overheating. The electric power generates heat and the cooling capacity of the Buchler Poly-Prep system is mechanically limited.

Ahmed et al. studied paper electrophoresis of HPAP using veronal, borate, and phosphate buffers and achieved the best resolution with phosphate buffer [20]. In the present work, preliminary runs were made with phosphate buffer (NaH_2PO_4 plus Na_2HPO_4), Tris-maleate plus NaOH buffer, and Tris plus glycine buffer. The migration velocities of the various proteins are directly proportional to the strength of the applied electric field, and higher voltages were obtained at a given wattage with the Tris/glycine buffer. At 10 watts constant power, the voltage was approximately 120 volts in 0.05 M phosphate buffer, 210 volts in 0.05 M Tris-maleate/NaOH buffer, and 360 volts in 0.05 M Tris/glycine buffer. The Tris/glycine buffer carries less current and thus generates less heat at the higher voltage, because it consists of two organic components which are only

partially ionized.

A typical experimental run is shown in Figure 2. The ratio of the concentration y_i of total protein in each product sample to the feed concentration y_F is plotted at the top of the figure. Two major peaks were resolved. By comparison with the activities plotted at the bottom of the figure, it is seen that the protein in the first peak has nearly zero enzyme activity a_i, where a_i is expressed in international units per volume of sample. The protein in the second peak has a high enzyme activity. The second peak is, therefore, identified as the desired enzyme and the first peak is identified as the major impurity. Other minor components of the crude enzyme mixture appear as minor peaks on the shoulders of the two major peaks.

The protein with high activity is taken as the product and is indicated by the hatched areas in Figure 2. The purification factor P.F. is defined as the ratio of the activity per milligram of product to the activity per milligram of feed or the ratio of the hatched areas in Figure 2.

$$\text{P.F.} = \frac{\sum a_i v_i / \sum y_i v_i}{a_F / y_F} = \frac{\text{AREA I}}{\text{AREA II}} \qquad (1)$$

The percent enzyme activity recovered ψ is the ratio of the total enzyme activity in the product to the total enzyme activity in the feed.

$$\psi = \frac{\sum a_i v_i}{a_F F} \text{ X } 100\% \qquad (2)$$

The purification factors vary from 1.9 to 3.5 and the recoveries

vary from 37% to 98% in the experiments in Table I.

In previous experiments with human hemoglobin and human serum albumin in the Buchler Poly-Prep system, better separation was obtained for a feed volume of 10 cc than for a feed volume of 30 cc [8]. Figure 3 compares the separation obtained for 10 cc of 0.05 weight % HPAP feed (run 13) versus 10 cc of 0.02 weight % HPAP feed (run 8). The enzyme activity peaks are identical in both runs, but the lower feed concentration in run 8 gives a much sharper peak for the impurity and, therefore, a significant improvement in purification. A 10 cc volume of 0.02 weight % HPAP feed was used in the remaining experiments.

Righetti and Secchi give a value for the maximum sample load in prep-PAGE of 10 milligrams of protein per cm^2 per protein band, and recommend that the load be reduced to 2 milligrams of protein per cm^2 per protein band for mixtures whose components give closely adjacent bands [18]. The much smaller loading in the present work of 0.056 milligram of crude enzyme per cm^2 per protein band is necessitated by the difficulty of separating HPAP from the accompanying impurities.

The effect of increased power and voltage on the separation is studied in Figure 4. As the power and voltage increase, both the impurity and the enzyme move at a faster rate through the gel and exit the prep-PAGE system in a shorter time. The sharpest peaks for the concentrations of the impurity and the enzyme and also for the activity of the enzyme occur at 5 watts or 250 volts (run 2). As seen in Figure 5, the purification factor is maximized at 5 watts. At higher wattages, the peaks are too

close together giving poor separation. At lower values than
5 watts, the residence time in the system is too long giving
broad diffuse peaks and poor separation.

The recovery as a function of power is also plotted in
Figure 5. The recovery is excellent up to 6 watts, but drops
off drastically at 8 - 10 watts. As seen in the bottom of
Figure 4, the area under the enzyme activity peak is much
smaller at 10 watts than at the lower fields. In our previous
experiments with human hemoglobin and human serum albumin, the
separation also went through an experimental optimum around 5 watts,
but the recovery was good up to 10 watts [8]. The enzymes are
evidently more sensitive to degradation than globular proteins.

The effect of pH on purification and recovery is examined
in Figures 6 and 7. All proteins carry both negatively and
positively charged functional groups (COO^- and NH_3^+). The pH at
which the net charge on the protein molecule is neutral is called
the isoelectric point. At pH's above the isoelectric point, the
protein molecule carries a net negative charge and is attracted
towards the cathode in an applied electric field. HPAP has an
isoelectric point I_A of 4.6 [21]. As $|pH-I_A|$ increases, the
net charge on the protein molecule increases and thus the migra-
tion velocity in the presence of an applied electric field
increases.

As seen in Figure 6, the concentration and activity peaks
move at a faster rate through the gel at higher pH values as
expected. The enzyme activity peaks are approximately the same
shape at different pH's, but the concentration peaks are sharper
at higher pH values. The best purification is obtained at an

operating pH of about 8.6 (Figure 7). The recoveries are approximately constant in the pH range of 8.0 to 9.5. Ahmed et al. reported the best separations in paper electrophoresis of various types of alkaline phosphatase at pH values of 8.0 to 8.6, some separation at pH values of 7.2, and poor separation at pH values of 4.6 to 6.8 [20]. Preliminary experiments in the Buchler Poly-Prep system gave very poor results at pH 7.2.

The effect of buffer ionic strength on the purification and recovery of HPAP is shown in Figures 8 and 9. The electrophoretic elution curves in Figure 8 show very little change when the ionic strength is increased at constant power. Since the 0.20 M buffer carries more current at 5 watts than the 0.05 M buffer, the voltage is decreased and the peaks are slightly delayed in run 7 as compared with run 2. For the two runs at constant voltage (run 2 versus run 9), the concentration and activity peaks exit the prep-PAGE system much earlier at the higher buffer molarity -- the reason for this phenomena is not clear.

The purification factor increases very slightly as the ionic strength increases from 0.05 M to 0.20 M as shown in Figure 9. At 5 watts constant power, the recovery is approximately constant. At 250 volts constant field, however, the power along with the inherent heating effects increase as the buffer molarity increases causing a decrease in recovery.

The recoveries and purification factors are summarized in Table I. The best results were obtained in runs 2 and 7 with purification factors of 3.3 to 3.4 and enzyme recoveries of 97% to 98%. Table II compares these results with the results obtained by Chen et al. for parametric pumping and cycling-zone

adsorption [1]. The purification and recovery for prep-PAGE are superior to the values obtained for the cyclic processes, but the rate of production is quite low. DEAE Sepharose anion exchanger was used in the cyclic processes, so the results in Table II are relevant to replacement of one of the chromatographic steps in a typical enzyme purification scheme.

CONCLUSIONS

Prep-PAGE has been demonstrated to be a feasible process step for enzyme purification. Optimum results were obtained at 5 watts power, at a buffer pH of 8.6, and at a feed loading of 10 cc of 0.02 weight % crude enzyme. A gel strength of 5 weight % acrylamide, a gel height of 8.3 cm, and an elution buffer rate of 20 ml/h were used for all of the experiments. The buffer ionic strength had little effect on the experimental results over the range of 0.05 M to 0.20 M using a Tris/glycine buffer solution. The experimental results obtained via prep-PAGE are superior to the results achieved via DEAE type anion exchangers for the purification and recovery of HPAP.

ACKNOWLEDGMENT

NOMENCLATURE

a_i :   activity of product sample, international units / ml

a_F :   activity of feed solution, international units / ml

F   :   volume of feed, ml

HPAP   :   human placental alkaline phosphatase

I.S.   :   ionic strength or molarity of buffer solution

P.F.   :   purification factor defined by equation 1

prep-PAGE :   preparative-scale polyacrylamide gel electrophoresis

v_i :   volume of product sample, ml

y_i :   concentration of product sample, mg / ml

y_F :   concentration of feed, mg / ml

Greek Letters

ψ :   % enzyme activity recovered

REFERENCES

1. H.T. Chen, Z.M. Ahmed and V.P. Rollan, Ind. Eng. Chem. Fundam., 20 (1981) 171.

2. Z. Ahmed and E.J. King, Biochim. Biophys. Acta., 40 (1960) 320.

3. N.K. Ghosh and W.H. Fishman, Biochem. J., 108 (1968) 779.

4. L.E. Seargeant and R.A. Stinson, J. Chromatogr., 173 (1979) 101.

5. E.B. Robson and H. Harris, Nature, 207 (1965) 1257.

6. Worthington Enzyme Manual, Freehold, New Jersey: Worthington Biochemical Corporation, 1977, p. 143 & p. 289.

7. J.F. Chao, J.J Huang and C.R. Huang, "Continuous Multiaffinity Separation of Proteins: Cyclic Processes," AIChE Symposium Series (1983) in press.

8. J.F. Chao, H.C. Hollein and C.R. Huang, "Cycling Zone Electrophoresis," Ind. Eng. Chem. Fundam. (1983) submitted for publication.

9. H.H. Sussman and A.J. Gottlieb, Biochim. Biophys. Acta., 194 (1969) 170.

10. G.J. Doellgast and W.H. Fishman, Biochem. J., 141 (1974) 103.

11. S. Raymond and L. Weintraub, Science, 130 (1959) 711.

12. B.J. Davis and L. Ornstein, "A High Resolution Electrophoresis Method," delivered at the Society for the Study of Blood at the New York Academy of Medicine, March 24, 1959.

13. A. Chrambach and D. Rodbard, Science, 172 (1971) 440.

14. S. Raymond, Ann. N.Y. Acad. Sci., 121 (1964) 350.

15. B.J. Davis, Ann. N.Y. Acad. Sci., 121 (1964) 404.

16. L. Ornstein, Ann. N.Y. Acad. Sci., 121 (1964) 321.

17. T. Jovin, A. Chrambach and M.A. Naughton, Anal. Biochem., 9 (1964) 351.

18. P. Righetti and C. Secchi, J. Chromatogr., 72 (1972) 165.

19. D. Rodbard and A. Chrambach, Anal. Biochem., 40 (1971) 95.

20. Z. Ahmed, M.A.M. Abul-Fadl and E.J. King, Biochim. Biophys. Acta., 36 (1959) 228.

21. P.G. Righetti and T. Caravaggio, J. Chromatogr., 127 (1976) 1.

TABLE I. Experimental Conditions and Results

run	volts	current (mA)	watts	I.S.	pH	feed weight %	P.F.	ψ, %
CONSTANT POWER RUNS								
1	140	14	2	0.05 M	8.6	0.02	2.04	98
2	250	20	5	0.05 M	8.6	0.02	3.25	98
3	277	22	6	0.05 M	8.6	0.02	2.54	95
4	312	26	8	0.05 M	8.6	0.02	2.07	69
5	360	28	10	0.05 M	8.6	0.02	1.86	37
6	203	25	5	0.10 M	8.6	0.02	3.32	94
7	180	28	5	0.20 M	8.6	0.02	3.42	97
CONSTANT VOLTAGE RUNS								
8	250	28	7	0.10 M	8.6	0.02	3.26	93
9	250	36	9	0.20 M	8.6	0.02	3.49	89
10	250	18	4.5	0.10 M	8.0	0.02	2.54	89
11	250	28	7.0	0.10 M	9.0	0.02	2.92	86
12	250	19	4.8	0.10 M	9.5	0.02	2.49	88
13	250	34	8.5	0.10 M	8.6	0.05	2.03	92

TABLE II

Comparison of prep-PAGE with Cyclic Processes

	prep-PAGE	parametric[a] pumping	cycling zone[a] adsorption
purification factor, P.F.	3.4	2.8	1.6
% enzyme activity recovered, ψ	97%	75%	59%
rate of production, international units per cm^2 per hour	0.027	1.9	3.6

(a) data from Chen et al., 1981 [1].

FIGURE CAPTIONS

Figure 1. Experimental apparatus.

Figure 2. Determination of purification factor (run 2).

Figure 3. Effect of feed concentration on elution profiles.

Figure 4. Effect of power on elution profiles.

Figure 5. Optimization of enzyme activity recovered (top) and purification factor (bottom) with respect to power.

Figure 6. Effect of buffer pH on elution profiles.

Figure 7. Optimization of enzyme activity recovered (top) and purification factor (bottom) with respect to buffer pH.

Figure 8. Effect of buffer ionic strength on elution profiles.

Figure 9. Optimization of enzyme activity recovered (top) and purification factor (bottom) with respect to buffer ionic strength.
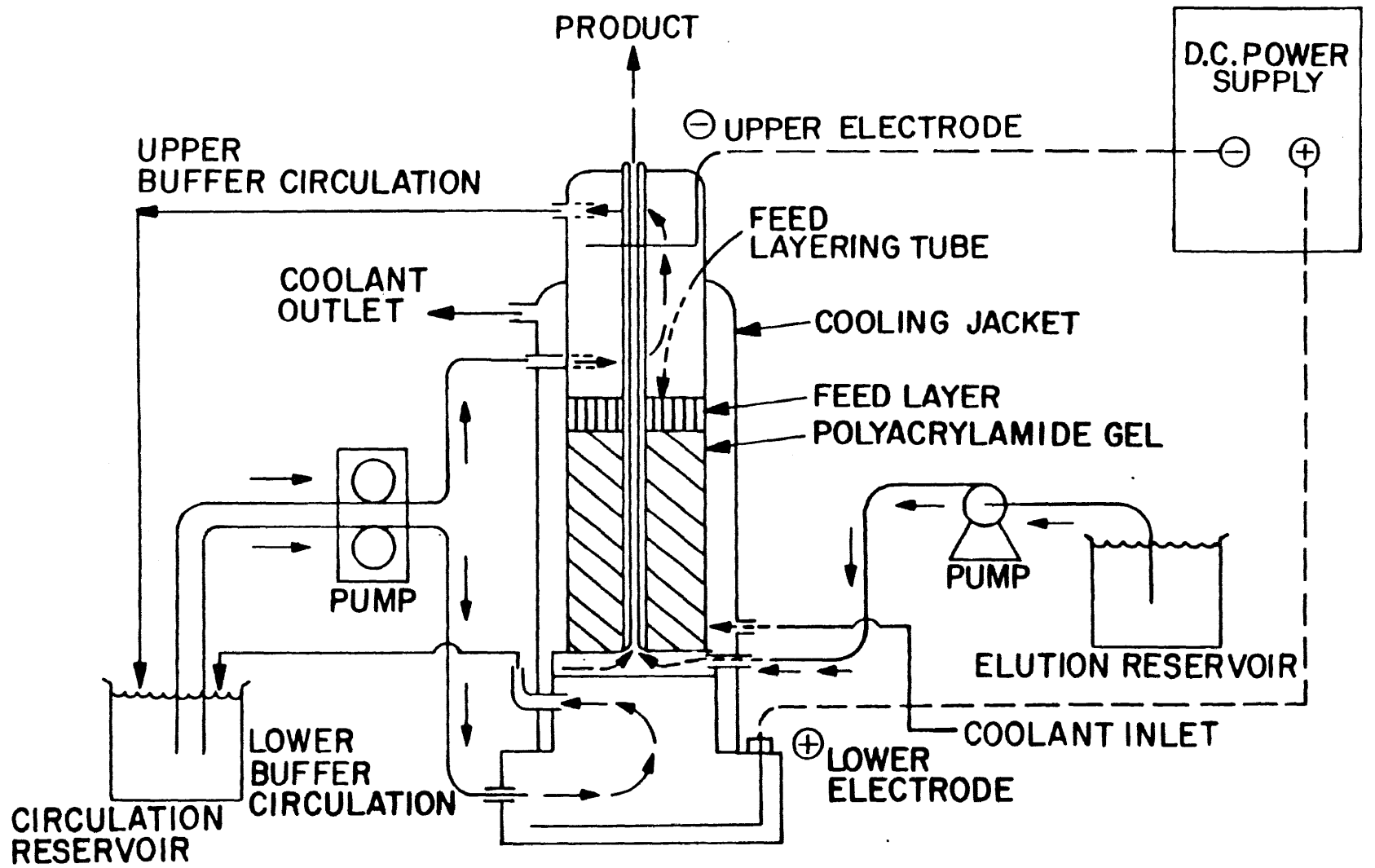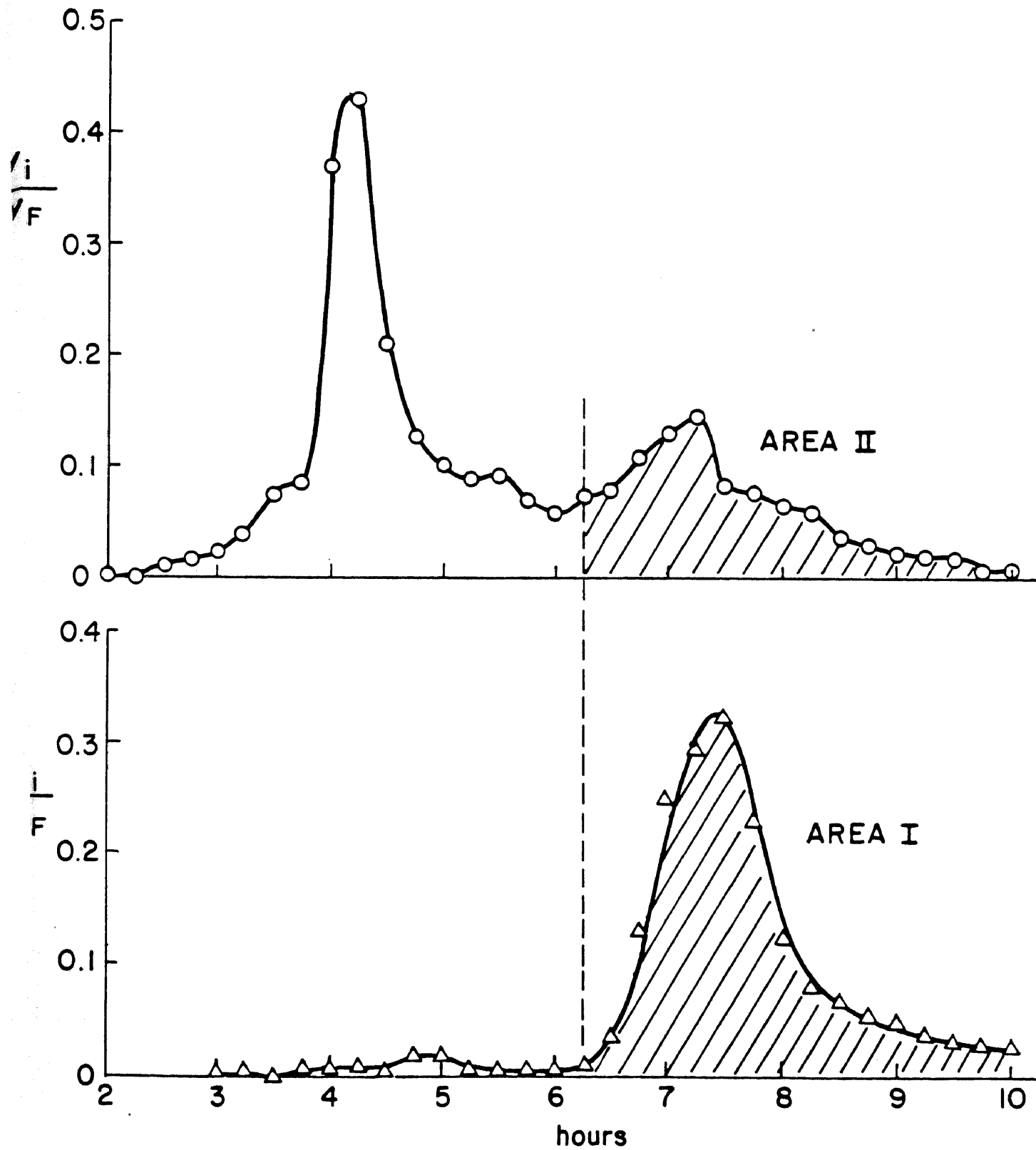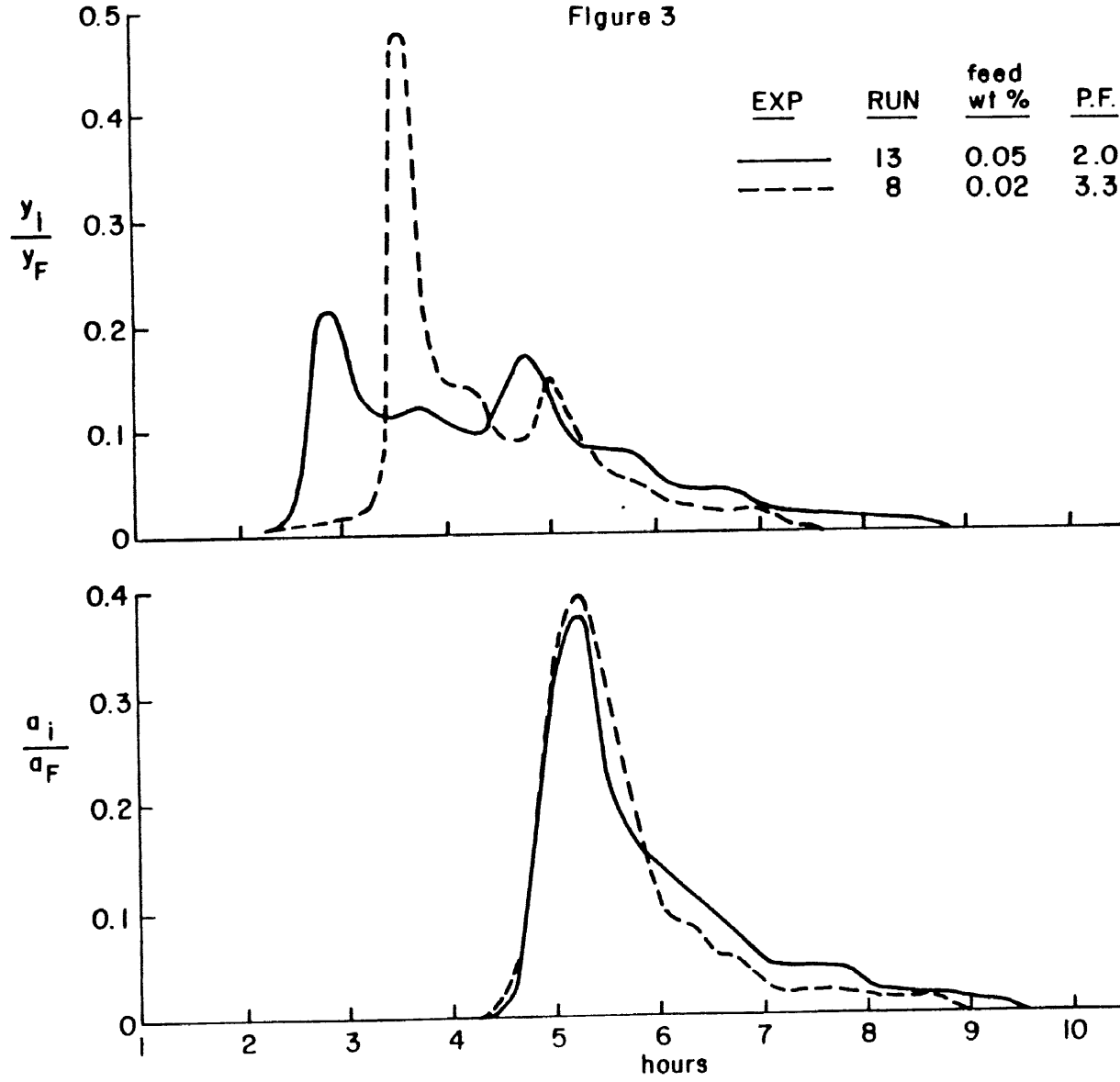
PRODUCT
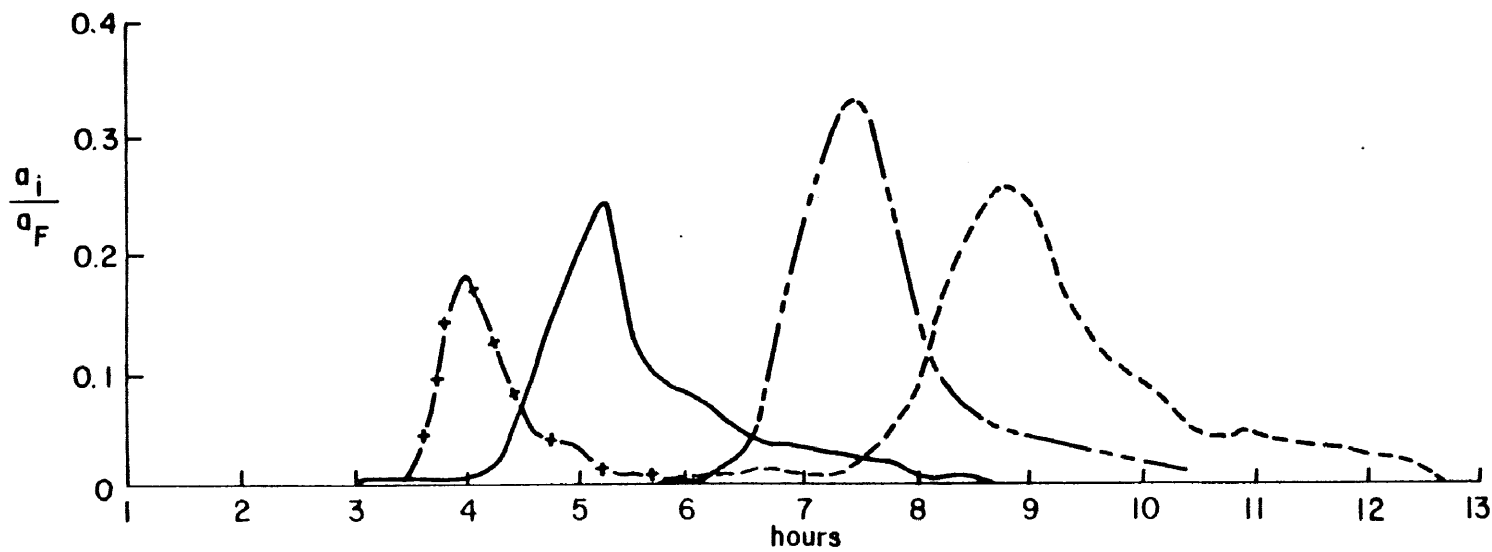
UPPER BUFFER CIRCULATION

⊖ UPPER ELECTRODE

D.C. POWER SUPPLY

⊖ ⊕

FEED LAYERING TUBE

COOLANT OUTLET

COOLING JACKET

FEED LAYER

POLYACRYLAMIDE GEL

PUMP

PUMP

ELUTION RESERVOIR

COOLANT INLET

⊕ LOWER ELECTRODE

LOWER BUFFER CIRCULATION

CIRCULATION RESERVOIR

Figure I

Figure 2

Figure 3

EXP	RUN	feed wt %	P.F.
——	13	0.05	2.0
- - -	8	0.02	3.3

Figure 4

EXP	RUN	watts	volts
+——+—	5	10	360
——	4	8	312
———	2	5	250
-------	1	2	140

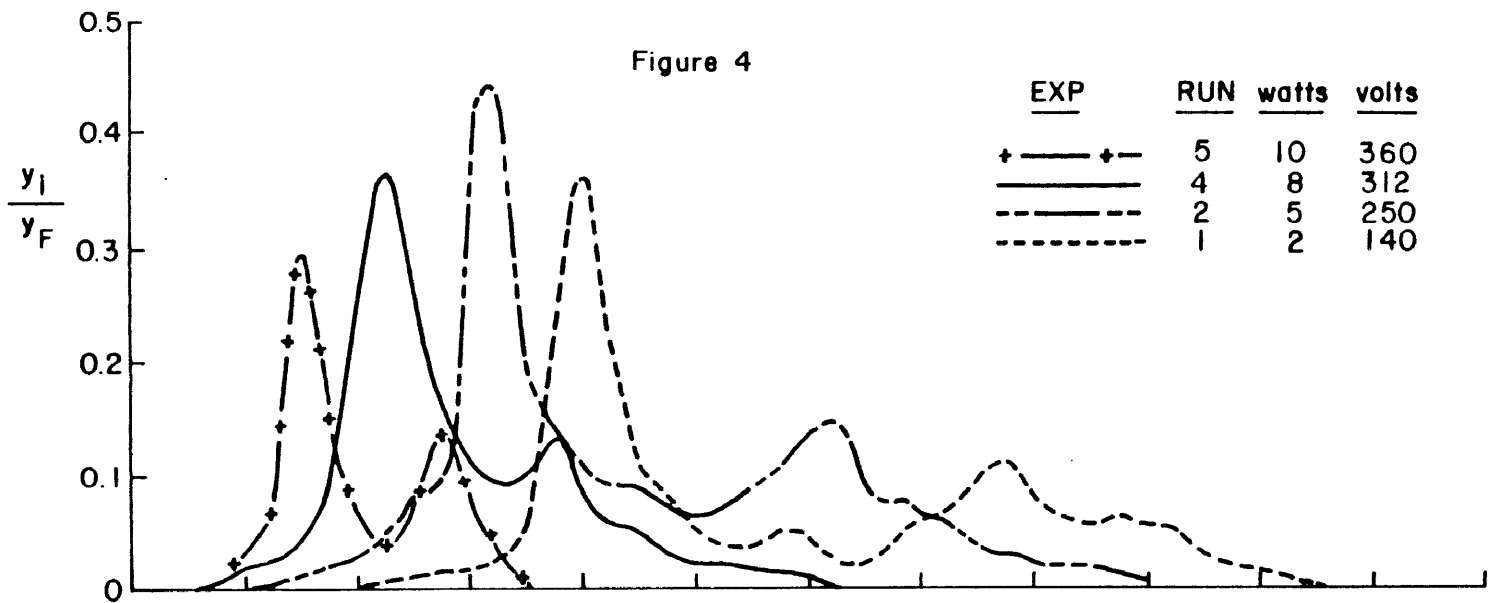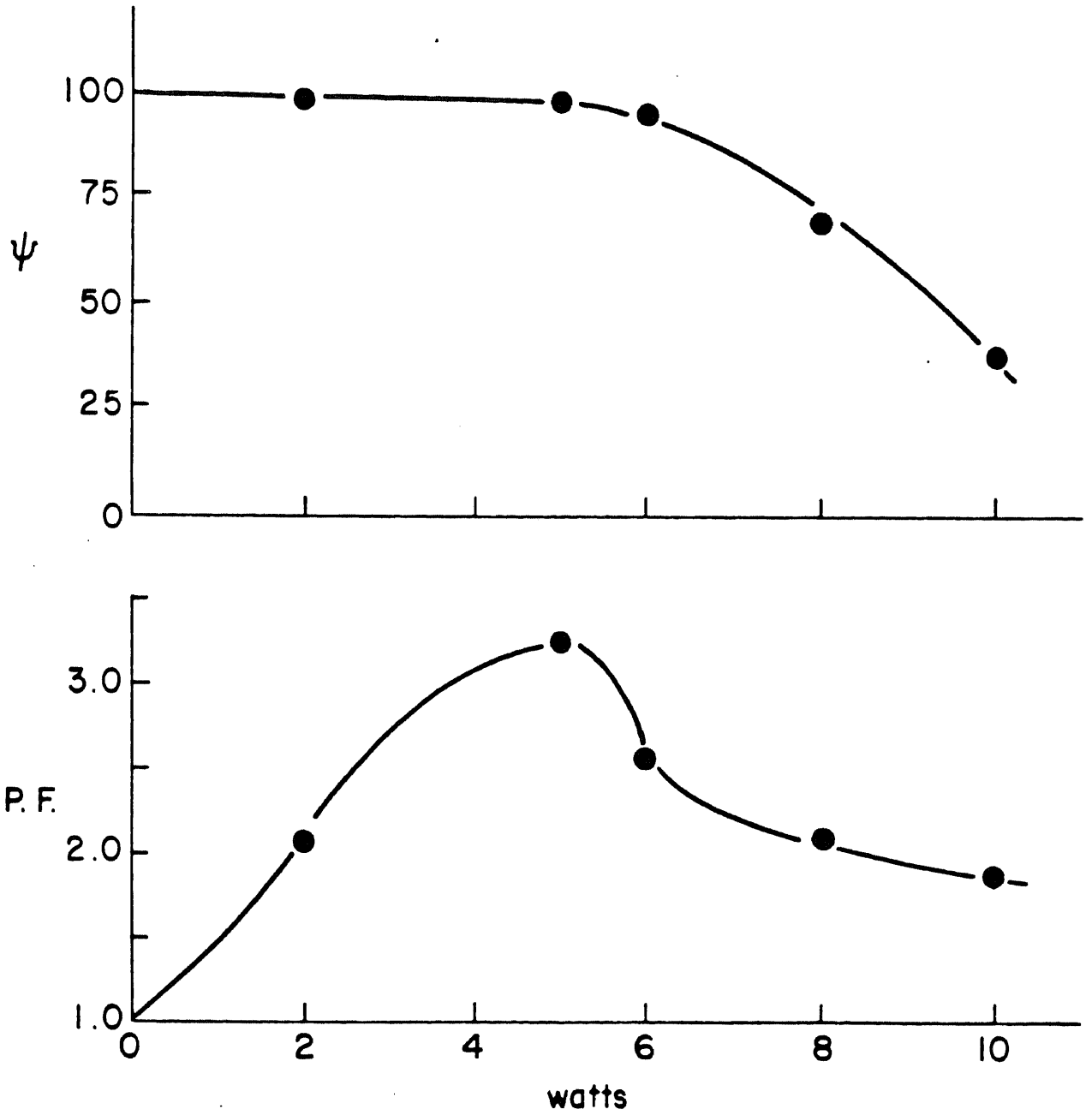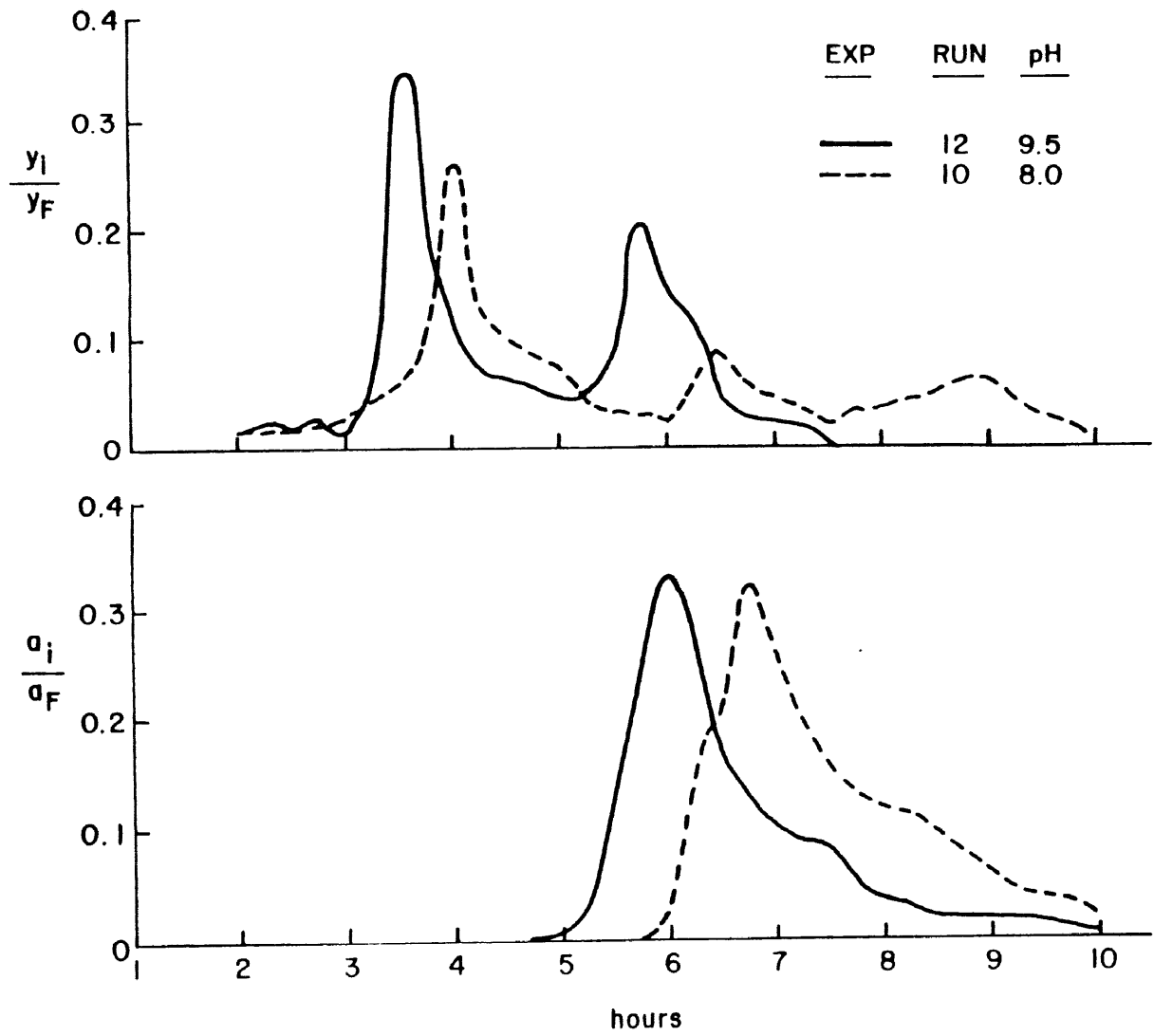Figure 5

Figure 6

Figure 7

Figure 8

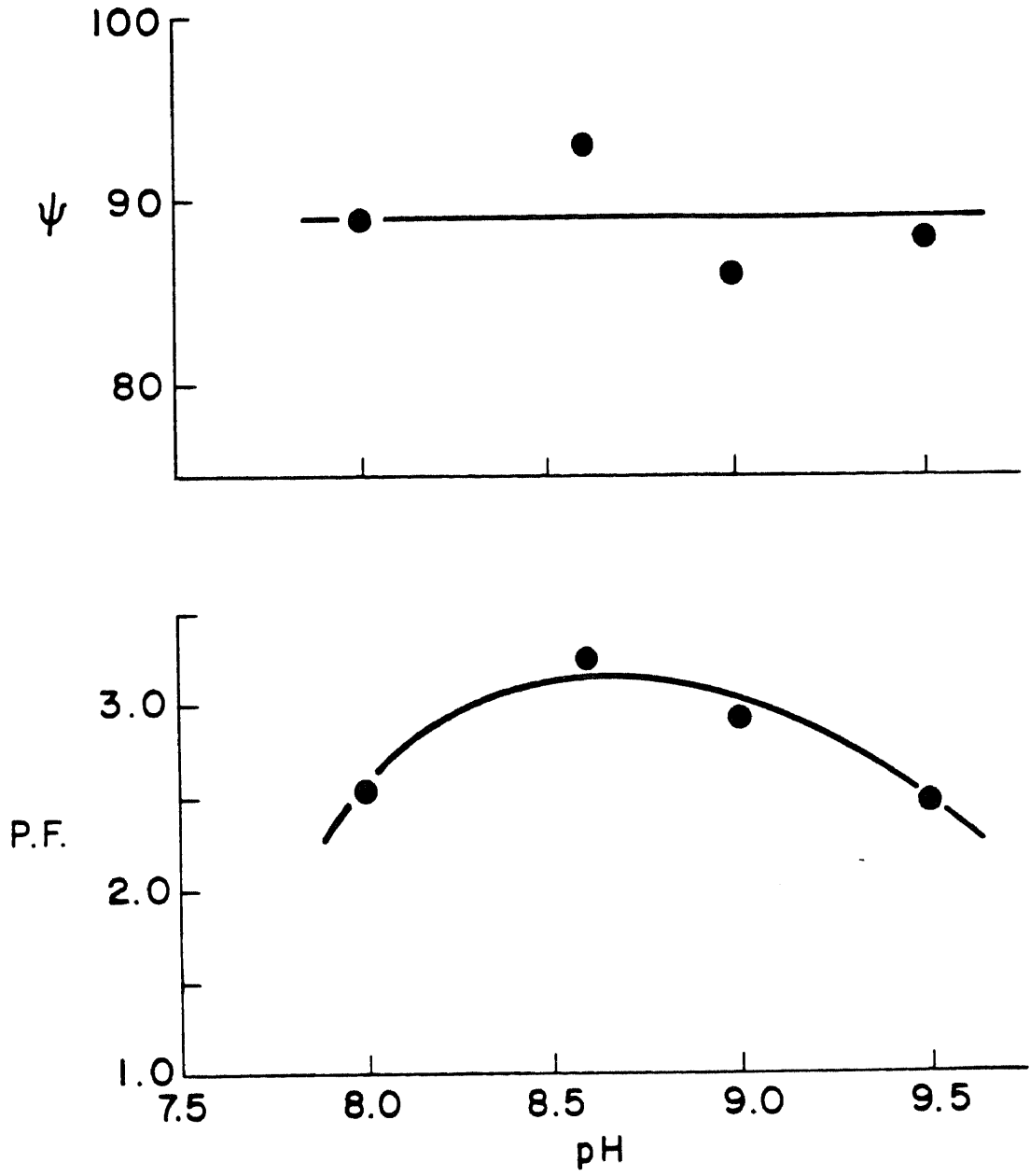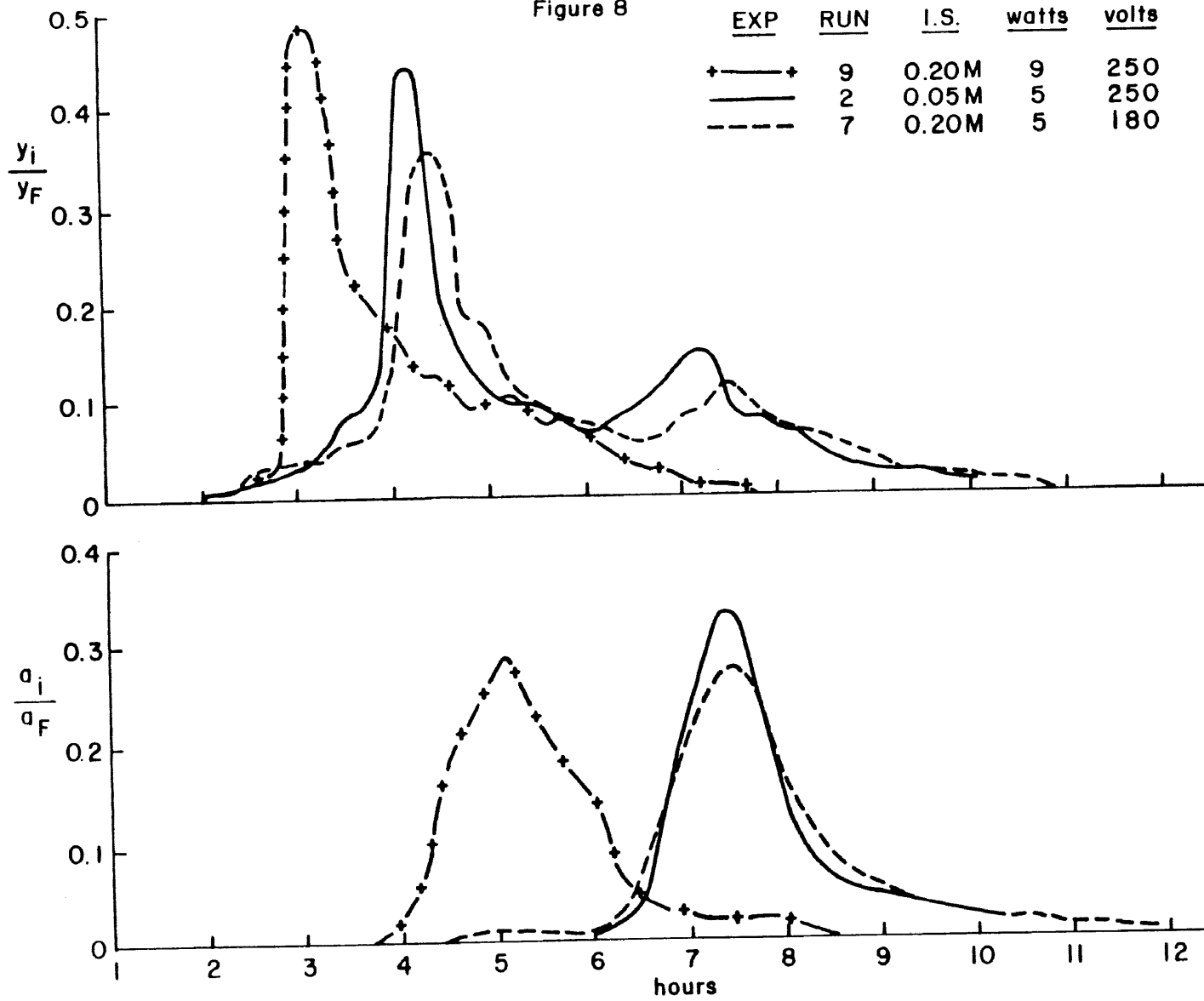| EXP	RUN	I.S.	watts	volts
+——+	9	0.20 M	9	250
——	2	0.05 M	5	250
- - - -	7	0.20 M	5	180

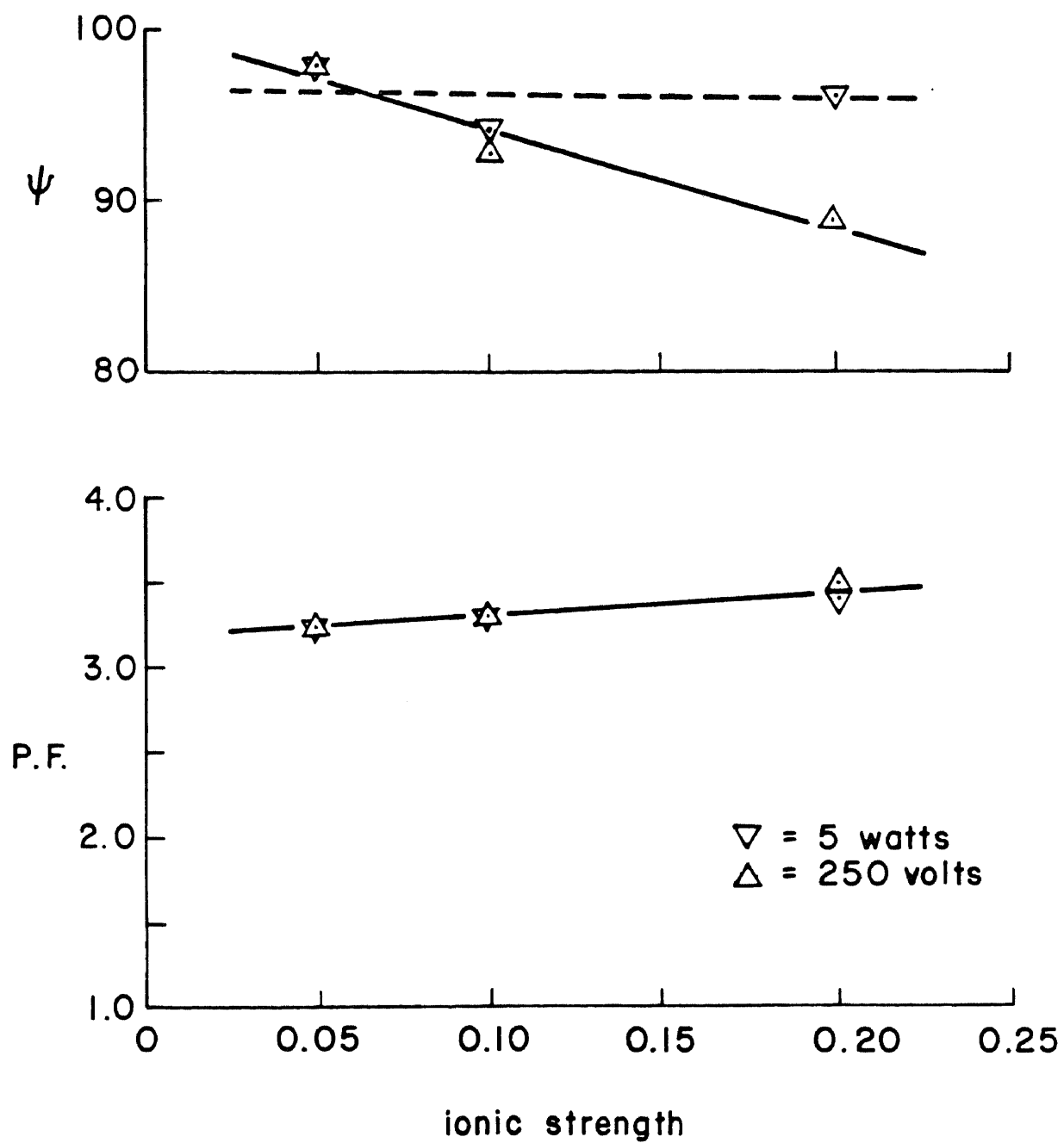Figure 9

CONTINUOUS MULTIAFFINITY SEPARATION OF

PROTEINS: CYCLIC PROCESSES

J.F. Chao, J.J. Huang and C.R. Huang

Department of Chemical Engineering & Chemistry
New Jersey Institute of Technology
Newark, New Jersey   07102

Correspondence concerning this paper should be addressed to C.R. Huang.

ABSTRACT

Separations of protein mixture by multiaffinity chromatography combined with cyclic operation are presented. The system consists of a series of columns packed with insoluble polymers or gels to which specific ligands have been covalently attached. A protein mixture is cycled over the bed to achieve splitting proteins from each other.

Two cyclic methods are considered: parametric pumping and simulated moving bed operation. The basic principle of parametric pumping is to utilize the coupling of periodic changes in flow direction to force the separation. The second approach is to simulate the movement of gel by periodically changing the feed and product locations.

The separation capability of multiaffinity chromatography is experimentally demonstrated for the system of Convanavalin A(Con)A-Ricinus Communis Agglutinin I (RCA_{120})-Sephadex G-150-Sepharose 4B. A comparison of the two cyclic processes with the batch process is also made.

SCOPE

The cyclic process was initially considered in order to eliminate the undesirable characteristics of a batch process. Since the composition of the effluent liquids vary continuously during each cycle, problems of control to ensure uniformity of products from each cycle were anticipated. In the batch process, large surge tanks would have been required to damp out fluctuation in compositions of feed to the subsequent fractionators in which desorbent was recovered.

To obtain a continuous steady state operation, the application of dynamic adsorption principles and technologies for the separation have been adapted to cyclic operation of fixed beds, especially from the principle of parametric pumping (Wilhelm and co-worker 1968). By using this concept, Chen et al. (1979, 1980) have obtained separation with semicontinuous product withdrawal. The parapump consists of a series of columns packed alternately with two kinds of ion exchangers, through which the protein solution to be separated flows. Also, their results indicate that the bi-functional two-column system has a higher separation capability than two single-columns which are packed with the same ion exchanger.

Another approach to continuous fractionation is a simulated moving bed operation which is adapted from Broughton et al. (1968, 1970). In the process, the bed is divided by the positions of the external streams into several zones, each of which performs a different function (adsorption, desorption). All the process aspects of movement of stationary phase past

fixed positions of liquid feed and withdrawal can be duplicated by movement of the position of feed and withdrawal past a fixed bed. A shift of these positions in the direction of liquid flow simulates movement of solid in the opposite direction.

Both the parametric pumping process and the moving bed operation are periodic separation techniques which represent an alternative to cycling zone adsorption processes. The difference between parametric pumping and moving bed operation is that the relative motion of the stationary and mobile phases reverses periodically in the former, while the relative motion between two phases is unidirectional in the latter. Both of these concepts require a solute/adsorption system in which some controllable thermodynamic variable affects the solute equilibrium distribution between the liquid and stationary phases. The thermodynamic intensive variables employed experimentally were pressure (Chan, 1981), temperature (Rice, 1981), ionic strength (Chen, 1980), and electrical potential (Oren, 1978). More or less experimental and theoretical works have already been done on cyclic separation methods which utilize the thermodynamic variables above. On the contrary, very few cyclic processes have been reported (Shaffer, 1975) which are based on affinity binding as the driving force for separation.

Applications of biospecific affinity chromatography involving the separation of valuable substances, such as proteins, may be very attractive and profitable to investigate. The separation method is based on the principle that proteins have different binding properties toward different ligands. The

adsorbed component can be subsequently eluted with a solution which weakens the particular protein-ligand interaction. To illustrate, the present study combined affinity chromatography and the two cyclic processes, were used for protein mixture separation. Emphasis is placed on the fact that these two processes are open-system operations and, compared with batch operation, the product composition fluctuation is eliminated.

CONCLUSIONS AND SIGNIFICANCE

The adaptation of the affinity chromatography principle to parametric pumping and moving bed operation is extended to separation of more complex protein systems such as lectin mixtures. The experiments show that after an initial transient state, the product concentrations and purifications reach a limiting condition and remain constant as the number of cycles increases. Thus, as long as the systems operate, the product streams remain on steady state. This offers advantages over the batch system for which no benefit results by operating an additional number of cycles. Furthermore, the proposed separation chromatography is of interest for engineering applications because: first, separation is based on specific protein-gel interactions, so high purity products are readily obtained; secondly, multiple gels can be used simultaneously, thus different proteins can be purified simultaneously; third, without pH change, this comparatively mild operation permits high recovery of viable proteins.

EXPERIMENTAL

System Selection

Lectins are proteins which bind in a specific manner to sugars (Sharon, 1972). One method for the isolation and purification of lectins is based on their specific conformation, which can couple to certain gels which contain specific ligands. The desorption of lectins from the gels is accomplished by elution with some sugars which possess the same structural features required for the interaction of lectins with the gels. Because of their low molecular weight, the sugars can readily diffuse into the gel matrix and compete with gel for the combining sites on the lectins. The mechanism of adsorption-desorption could be expressed as follows:

$$\text{Gel-Lectin + Sugar} \underset{k_2}{\overset{k_1}{\rightleftharpoons}} \text{Gel + Lectin-Sugar}$$

The remaining procedure for displacing sugars from the purified protein solutions can be treated either by gel filtration or with the aid of a membrane separator due to the molecular weight difference between them.

Based on the above information, a two-component lectin mixture of concanavalin A (M.W. 104,000, I.E. 5.5, Sigma Chem. Co. product) and Ricinus Communis Agglutinin I (M.W. 120,000, I.E. 5.2-5.5, Vector Laboratories, Inc. product) which can be biospecifically adsorbed on the Pharmacia Fine Chemical made Sephadex G-150 gel and Sepharose 4B gel respectively, which was chosen as the model system. The desorbent for washing out the adsorbed Con A from the chromatographic bed is D-glucose (M.W.

180.16), while, for the RCA_{120} the desorbent is β-lactose (M.W. 360.32). The buffer solution was a mixture of 0.05M monobasic and 0.05M dibasic sodium phosphate, plus 0.2M sodium chloride with a constant pH = 7.3 throughout the processes. The chosen pH value permits the lectins to have approximately maximum biological activities.

Processes Description

Parametric pumping--Experimental studies were made for two-column parapumps. A schematic diagram of the experimental procedures is shown in Figure 1. The system was maintained at $278^O K$ by the use of a refrigeration unit which circulated cooling water through the jackets of the two columns (0.016m inside diameter) and of the four reservoirs (T.R., B.R. and two M.R.). The top column was packed with Sephadex G-150 (0.08m high) and the bottom column packed with Sepharose 4B (0.08m high). Reciprocating flow within the columns at a flow rate of 0.5 cc/min was produced by two peristalic pumps. The pumps were wired to a dual timer to have flow direction reversed auto-matically at the end of each half cycle. Initially, the top column is saturated with D-glucose buffer solution by cir-culation the fluid with T.R. and the bottom column is saturated with β-lactose buffer by circulating the fluid with B.R. The operation of one complete cycle contains two distinct stages as outlined below.

(I) Forward Adsorption: The feed with Volume V_e from the

M.R. 1 enters the bottom of the top column, and the solution, with D-glucose, initially in the column, is displaced out from the top of the column into the top reservoir for time t_I. At the same time, the respective V_e of feed enters the top of the bottom column, and the β-lactose solution is displaced out from the bottom of the column into the bottom reservoir. As the feeds pass through, adsorptions are taking place in each of two columns.

(II) Backward Elution (Desorption): The D-glucose buffer and β-lactose buffer are pumped individually from the T.R. into the top of the top column and from the B.R. into the bottom of the bottom column respectively. The optimum volumes for the elution flow were experimentally determined, which were determined by desorbent solution concentrations and were found to be approximately 1.3 V_e.

In stage (IIA), the solution from the top column (first 0.7 V_e), which is enriched with unadsorbed component RCA_{120}, is pumped into the M.R. 2. Similarly, the first 0.7 V_e outlet from the bottom column, which is enriched with unadsorbed component Con A, is collected in the M.R. 1. The advantage of this step is that the separation efficiency of sequential cycle can be accumulated by the operation of previous cycles. In stage (IIB), the subsequent oncoming stream from the top column, enriched with desorbed component Con A, can be taken as the top product. Similarly, the subsequent elution stream from the

bottom column, enriched with RCA_{120}, is the bottom product. The product volume from each column is $0.6\ V_e$. Up to this point, one cycle is completed and stage I of the second cycle begins. Note that before continuing the next cycle, a $0.3\ V_e$ feed should make up the consumption of each M.R. Also, $0.3\ V_e$ of D-glucose buffer and $0.3\ V_e$ of β-lactose buffer should be added to T.R. and B.R. respectively as needed.

Simulated Moving Bed Operation--The mode of operation is depicted in Figure 2. The whole bed is divided into four zones in order to make each one perform a different function. Each zone has 0.016m diameter by 0.08m high. The system was maintained at 278°K. Equal flow rates of 0.5 cc/min were instituted by a multichannel peristaltic pump for the four external streams. The flow rates for liquid streams within the zones are alternately equal to 0.5 or 1.0 cc/min. Initially, the system is saturated with buffer solution by circulating the buffer via the feed and withdrawal ports. Each feed and withdrawal position shifts four times in one cycle. After every feed and withdrawal stream shifts back to the original position on the bed, one cycle is completed. The function of each zone is described below:

Zone I: The function of this zone is to adsorb A from the liquid. The liquid entering the top of this zone contains A and B. As the liquid stream flows downward, component A is transferred from the liquid stream to the solid.

Zone II: This zone performs the preliminary desorption of A. The liquid entering the top of this zone consists of A-D and some residue of D. A small part of A is desorbed in this zone.

Zone III: The function of this zone is to desorb A completely from the gel. As the fresh desorbent enters the top of this zone, component A is transferred to the liquid stream and leaves from the bottom of this zone.

Zone IV: This zone performs as a regeneration zone in which the desorbent liquid is displaced out by the entering liquid containing component B. By the displacement of D, the gel can adsorb component A effectively after the next shift in the function of the zones.

From Figure 2 it can be seen that the liquid flow rate in each zone is different because of the addition or withdrawal of various net streams. Also shown in Figure 2 is the position of these four zone shifts loopwise so that the adsorbent can be treated in an annual bed.

RESULTS AND DISCUSSION

Parametric pumping separation experiments for the typical runs were carried out in the mode depicted in Figure 1. Figure 3 shows the concentration transients for the top and bottom products. For the top product, the enriched component is Con A. However, for the bottom product, the main component is RCA_{120}. The separation factor, S.F., is defined as the ratio

of enriched component A to the lean component B in a product stream:

$$<S.F.>_n = \frac{[<Y_s>_n/Y_F]A}{[<Y_s>_n/Y_F]B}$$

As shown in Figure 3, at steady state the S.F. of the top product is 2.79 and the S.F. of the bottom product is 3.78.

The two column parapump system described above can be modified to improve the product qualities, concentration and S.F. by refluxing part of the product streams. The results for this effort are given in Figure 4.

A comparison on separation and concentration between with reflux and without reflux operations is listed in Table 1. The results indicate that the reflux parapump system improves the S.F. about 14% and increases the concentration about 30%.

Figure 5 shows the results for the simulated moving bed operation. There are four extract streams and four raffinate withdrawals in each cycle. When the system works on Sepharose 4B gel, the extract streams enriched with adsorbed component RCA_{120}, while the main composition in raffinates is unadsorbed component Con A. After reaching steady state, the S.F. of extract is approximately 3.26. The S.F. of raffinate is 8.75 (Figure 5A). A result for the study on Sephadex G-150 gel is also obtained (Figure 5B).

The batch operation consists simply of charging step inputs of feed and desorbent alternately to a fixed bed (Figure 6). As the feed components pass through the bed, they gradually sepa-

rate into distinct bands, which travel through the bed at different times and are withdrawn alternately as raffinate and extract. These bands broaden as they travel down the column under the influence of axial diffusion and finite transfer rates. The unadsorbed component develops as the leading peak and the adsorbed component develops as a second peak with a long tail. This long tail concentration profile is especially magnified when the adsorbed component is eluted by a weak desorbent. A second increment of feed must be delayed long enough to ensure that the unadsorbed component does not overtake the strongly adsorbed component in the first increment.

Consider the feed increment and desorbent increment introduced alternately into a fixed bed from different ends by periodically changing flow directions as in the parapumping process. The desorbent is consumed as it passes through the bed from the other end. Before washing out the adsorbed component completely, the desorption step stops and the feed step of the next cycle begins. Thus, the long tail commonly associated with a desorbed component concentration profile does not appear, and the extract product has less variance in composition. Also consider that the moving bed continuous operation is not simply equivalent to numbers of batch operations offset in time to simulate continuity. In the continuous process, composition is almost invariant at each level in the bed. However, in the batch process the composition undergoes a cyclic change at every level in the bed. A comparison of the three processes is listed in Table 2.

This article deals with the consideration of influencing the choice of process schemes by extending cyclic processes to more complex protein mixtures, such as a lectin mixture, separation. Many protein separation processes are operated batchwise. Parametric pumping, as described here, offers a semicontinuous process. The simulated moving bed operation presents a continuous process. Thereby, these two processes tend to minimize both processing time, desorbent consumption, and protein degradation. Furthermore, the application of bioaffinity separation in these cyclic processes will be an advantage in separating components, especially proteins which share similar molecular weight, isoelectric point or solubility. With a multiaffinity separation, more than one product can be separated simultaneously.

ACKNOWLEDGEMENT

NOTATION

D:	desorbent
I.E.:	isolectric point
k_1, k_2:	equilibrium constants
M.W.:	molecular weight
S.F.:	separation factor
t:	duration, min.
V_d:	dead volume in each reservoir
V_e:	column void volume, cc
Y:	concentration
< >:	average value

Subscripts

B:	bottom product
E:	extract
F:	feed
n:	nth cycle
R:	raffinate
s:	samples
T:	top product
∞:	steady state

TABLE 1

Comparison Between With Reflux and Without Reflux
Parapump System

	with Reflux	without Reflux
Reflux	0.33	0
$[\dfrac{<Y_T>_\infty + <Y_B>_\infty}{Y_F}]_{Con\ A}$	127.40%	96.83%
$[\dfrac{<Y_T>_\infty + <Y_B>_\infty}{Y_F}]_{RCA_{120}}$	127.25%	93.35%
$[<S.F.>_\infty]_T$	3.07	2.79
$[<S.F.>_\infty]_B$	4.47	3.78

TABLE 2

A Comparison of Batch, Parametric Pumping and Moving Bed Operation

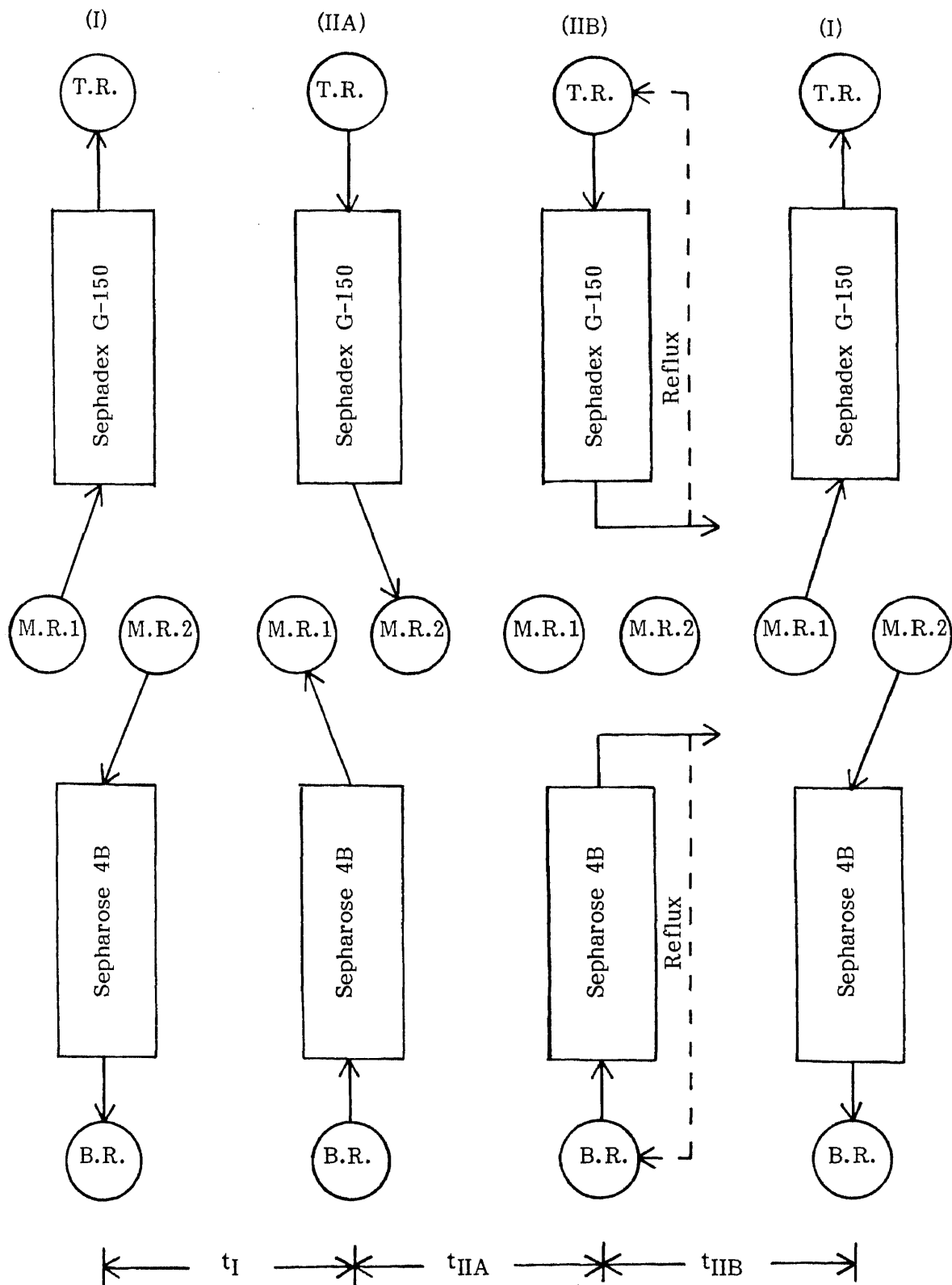|	Batch	Parametric Pumping	Moving Bed Operation
Separation Characteristics	Separation is governed by the wave propagation properties of the bed.	Separation factor increased cycle by cycle to reach a constant.	Separation capability increased by simultaneous adsorption and desorption in adjacent zones.
Control Variables	Adsorbent inventory.	Adsorbent inventory.	Adsorbent inventory.
	Flow rate.	Flow rate.	Flow rate.
	Ratio of desorbent to feed.	Ratio of desorbent to feed.	Ratio of desorbent to feed.
		Direction of flow.	Adsorbent circulating rate.
Advantages	Easy to operate.	Desorbent used more efficiently.	Desorbent used more efficiently.
		Product composition fluctuation during each cycle is eliminated.	Product composition fluctuation during each cycle is eliminated.
			Adsorbent used more efficiently.
Disadvantages			Process complexity.

FIGURE CAPTIONS

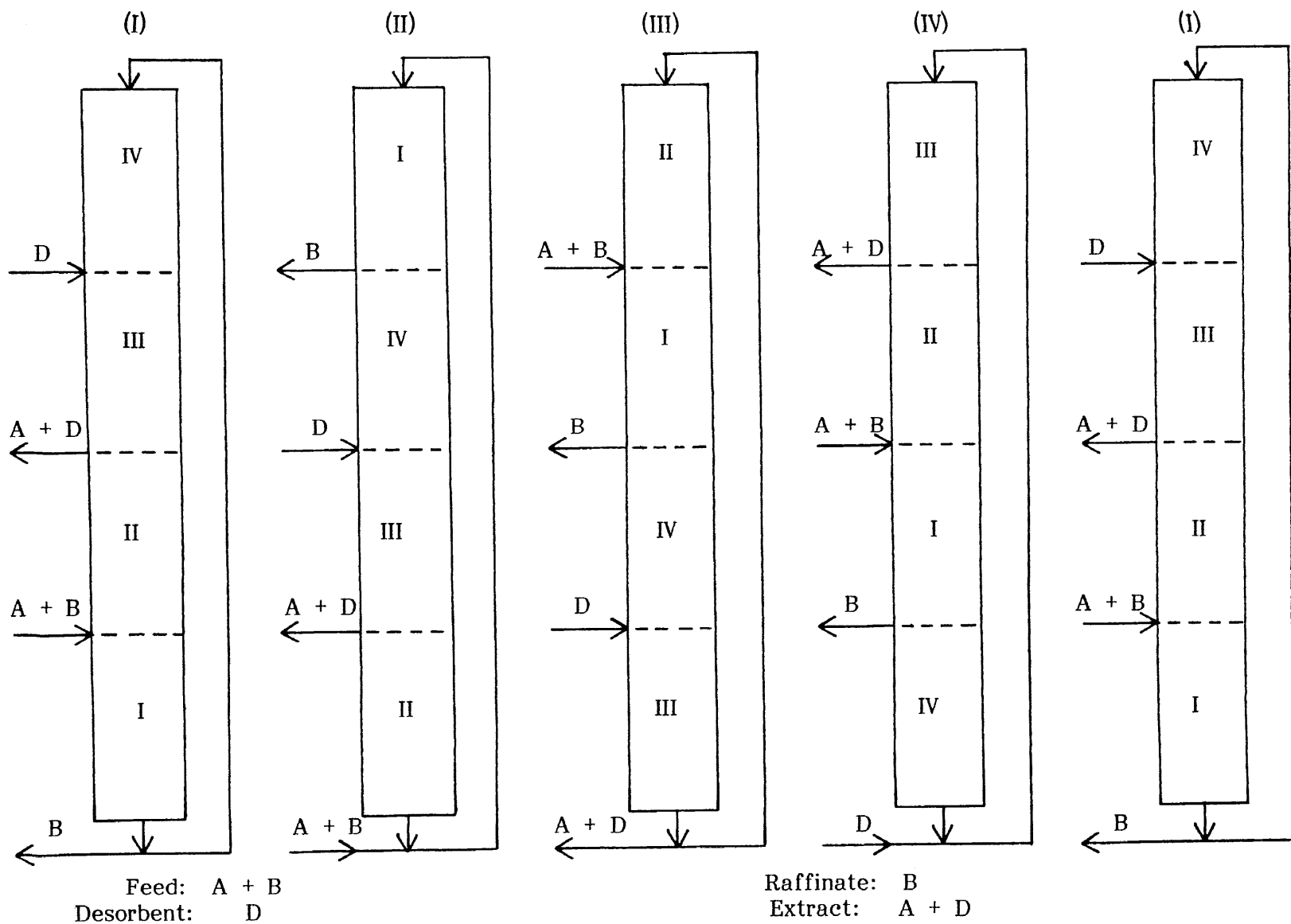Figure 1.   Schematic of two-column parametric pumping system

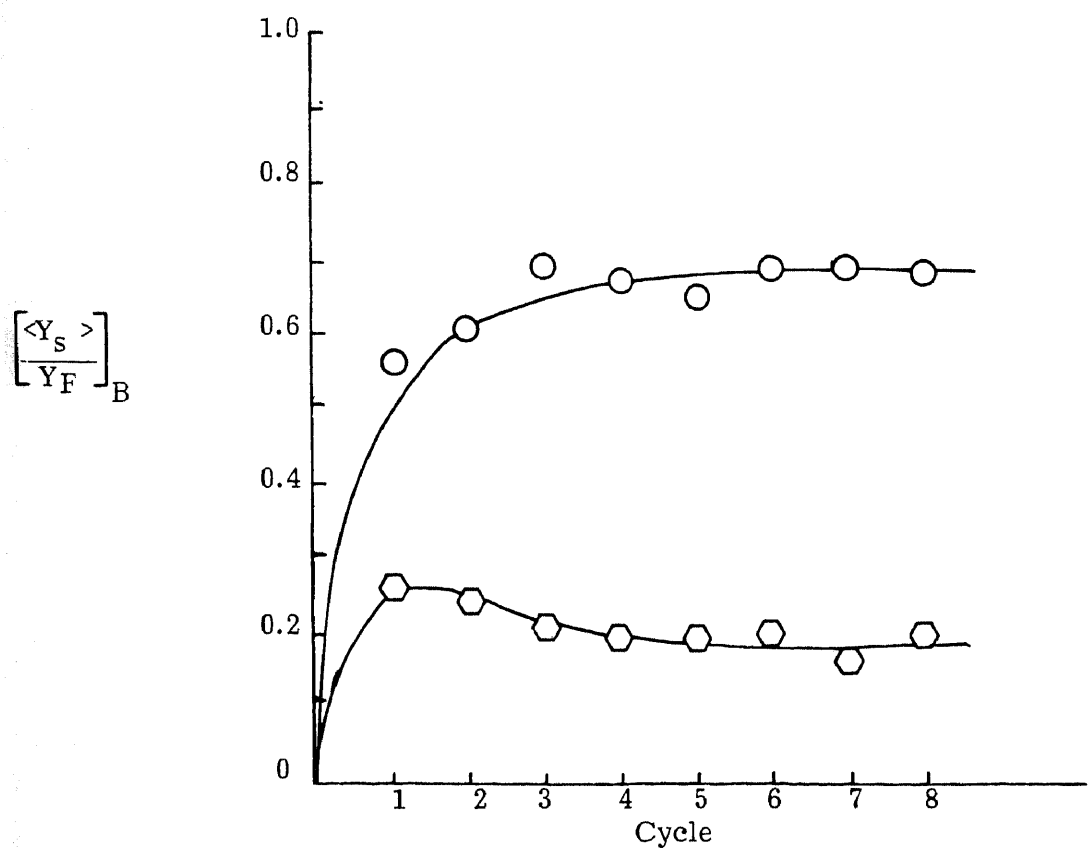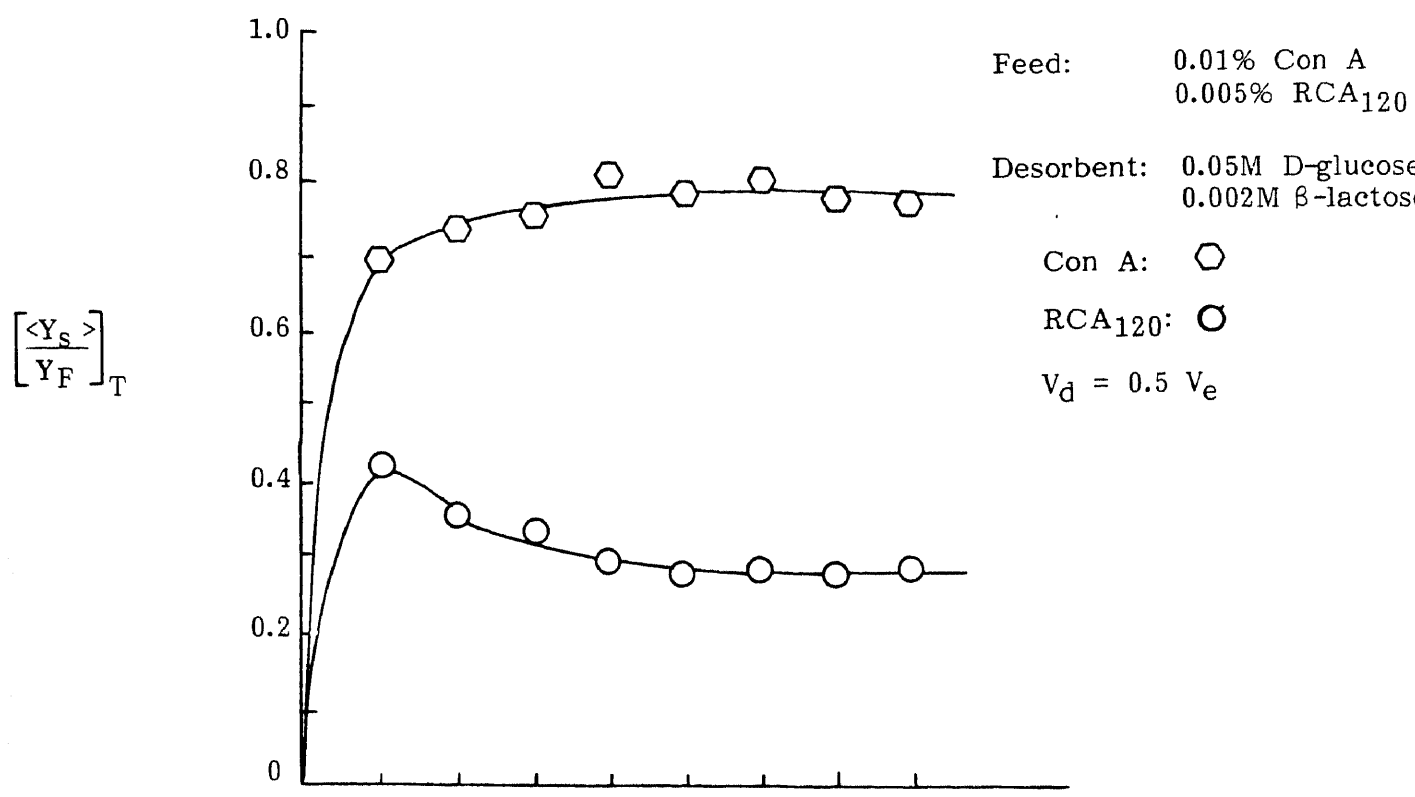Figure 2.   Schematic of the simulated moving bed operation

Figure 3.   Experimental results for the parametric pumping
system (without reflux)

Figure 4.   Experimental results for the practical reflux
parametric pumping system

Figure 5.   Experimental results for the simulated moving bed
operation

Figure 6.   Illustration for batch operation

FIGURE 1.

Schematic of Two-Column Parametric Pumping System

FIGURE 2.

Schematic of the Simulated Moving Bed Operation

FIGURE 3.

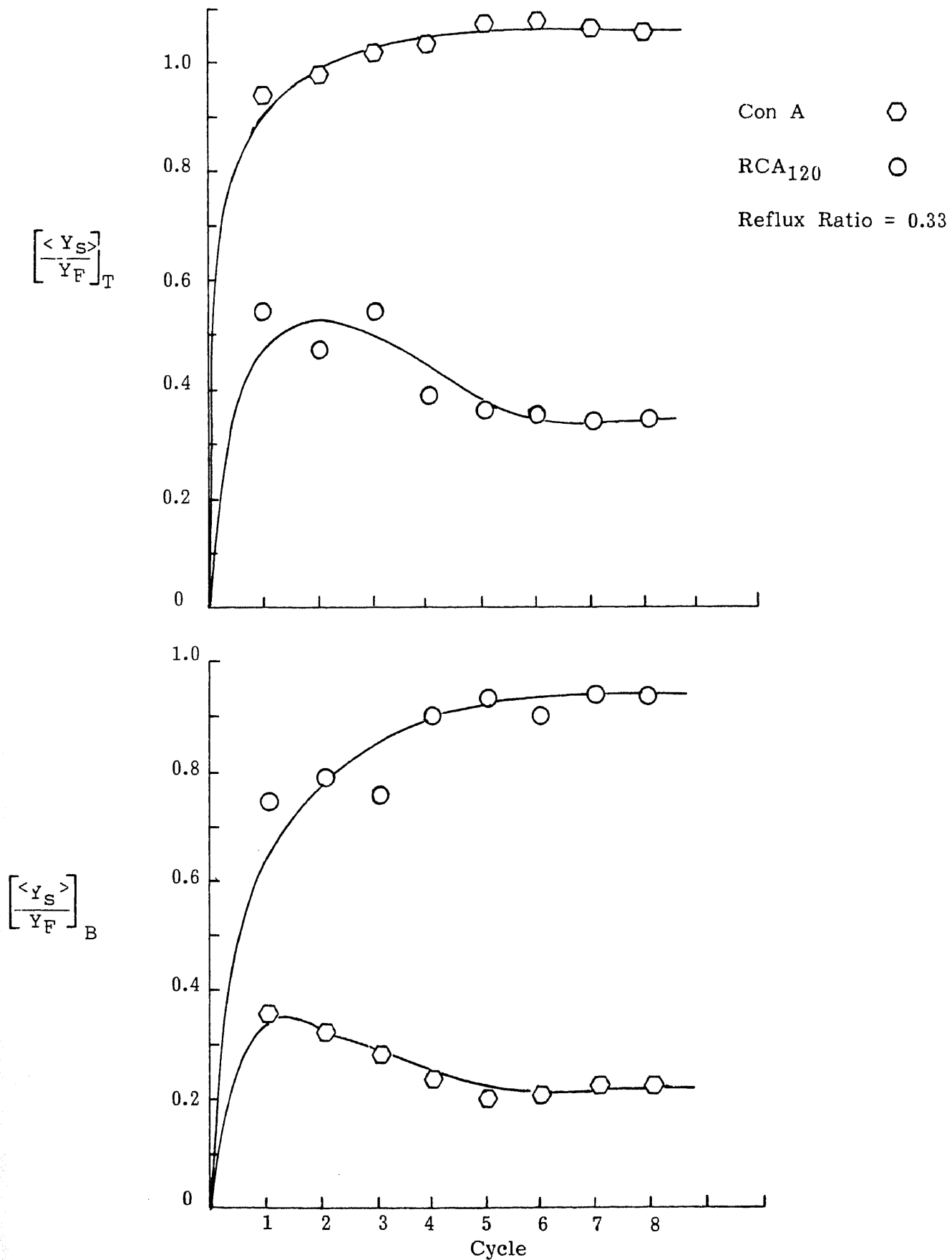Experimental Results for the Parametric Pumping System
(without reflux)

$$\left[\frac{<Y_S>}{Y_F}\right]_T$$

Con A ⬡

RCA_{120} ◯

Reflux Ratio = 0.33

$$\left[\frac{<Y_S>}{Y_F}\right]_B$$

Cycle

FIGURE 4.

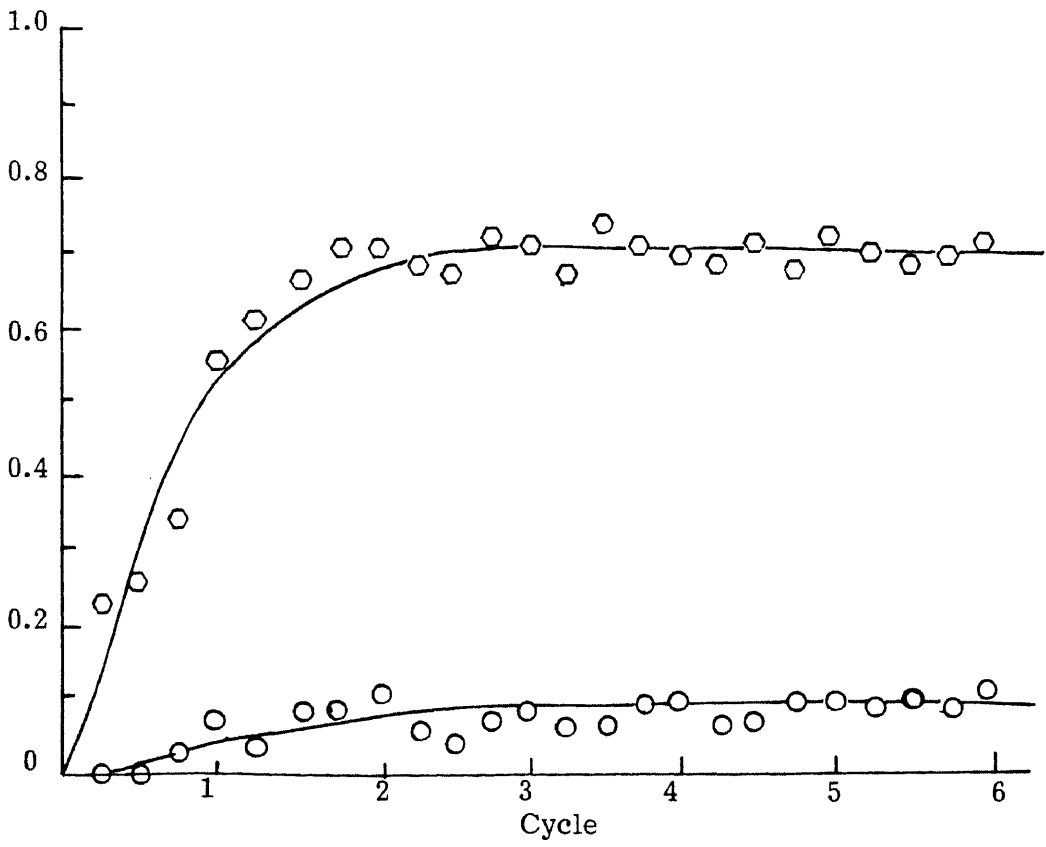Experimental Results for the Practical Reflux Parametric Pumping System

FIGURE 5A.

Experimental Results for the Simulated Moving Bed Operation
(Sepharose 4B Gel)
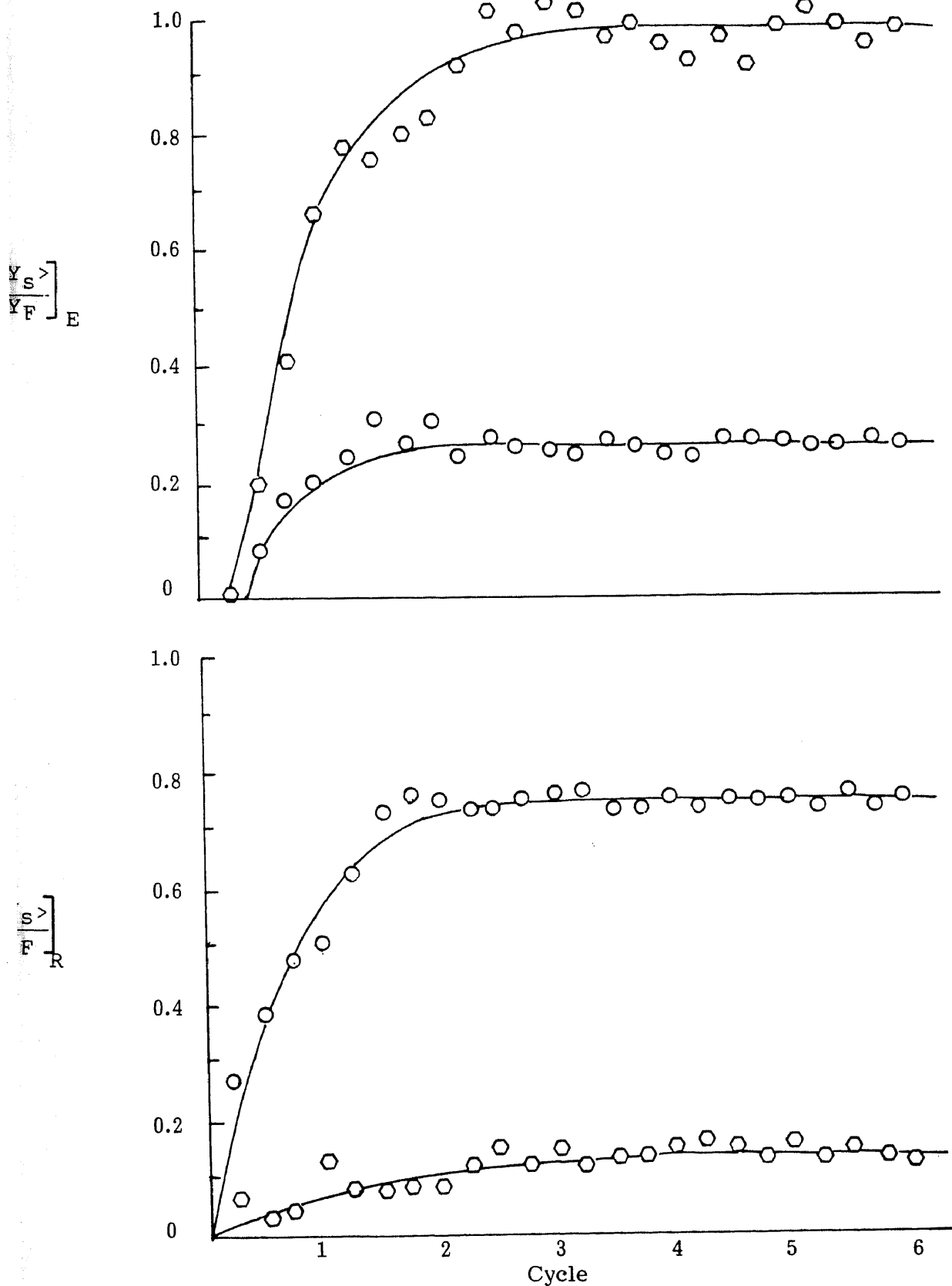
FIGURE 5B.

Experimental Results for the Simulated Moving Bed Operation
(Sephadex G-150 Gel)

LIQUID COMPOSITION, %

Feed: A + B
Desorbent: D
Raffinate: B
Extract: A + D
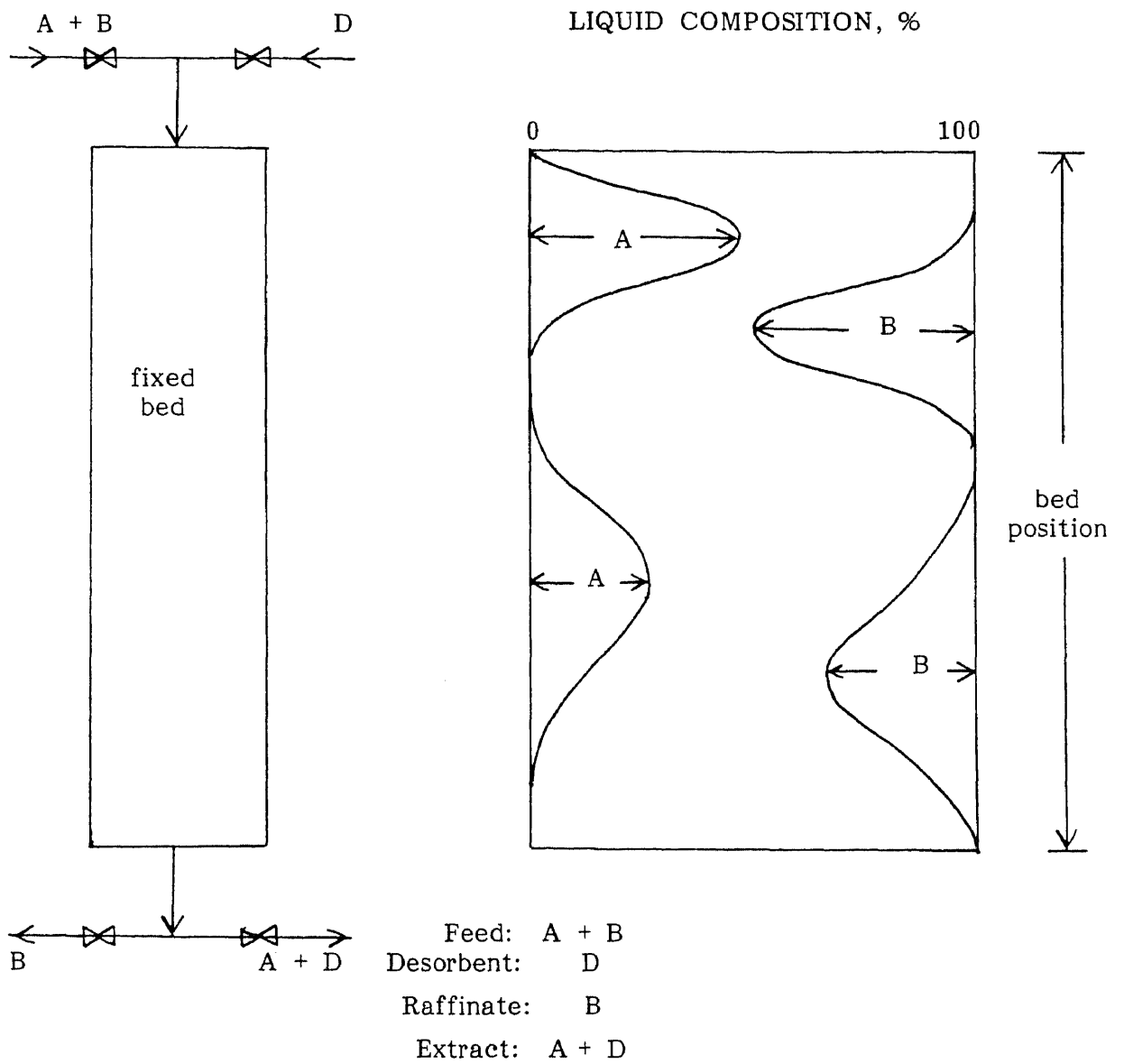
FIGURE 6.

Batch Operation

LITERATURE CITED

1. Broughton, D.B., Chem. Eng. Prog., 64, 60 (1968).

2. Broughton , D.B., R.W. Neuzil, J.M. Pharis and C.S. Brearley, Chem. Eng. Prog., 66, 70 (1970).

3. Chan, Y.N.I., F.B. Hill and Y.W. Wong, Chem. Eng. Sci., 36, 243 (1981).

4. Chen, H.T., Y.W. Wang and S. Wu, AIChE Journal, 25, 320 (1979).

5. Chen, H.T., W.T. Yang, U. Pancharoen and R.J. Parisi, AIChE Journal, 26, 839 (1980).

6. Chen, H.T., Z.M. Ahmed and V. Rollan, Ind. Eng. Chem. Fund., 20, 171 (1981).

7. Oren, Y. and A. Soffer, Journal Electrochem. Soc., 125, 869 (1978).

8. Rice, R.G. and S.C. Foo, Ind. Eng. Chem. Fund., 20, 150 (1981).

9. Shaffer, A.G. and C.E. Hamrin, AIChE Journal, 21, 782 (1975).

10. Sharon, N. and Lis, Science, 177, 949 (1972).

11. Wilhelm, R.H., A.W. Rice, R.W. Rolke and N.H. Sweed, Ind. Eng. Chem. Fund. 7, 337 (1968).

PARAMETRIC PUMPING—A UNIQUE

SEPARATION SCIENCE

by

C.R. Huang,* J.F. Chao and J.J. Huang

Department of Chemical Engineering and Chemistry
New Jersey Institute of Technology
Newark, New Jersey 07102

---

*Author to whom inquiries should be directed.

ABSTRACT

Parametric pumping is a unique separation or purification process for a mixture of components in a fluid phase. The process includes cyclic steps of fluid passing through an immobile phase and change of an intensive thermodynamic variable. The intensive variable which causes the separation can be temperature, pH, ionic strength, electric field or affinity. We have studied the model systems such as toluene-aniline-n-heptane, glucose-fructose-water, haemoglobin-albumin and alkaline phosphatase-other proteins. Results indicate that parametric pumping has the capability to separate or purify biochemicals where other conventional methods might fail. Recently, our efforts have been concentrated on the application of this unique technique to biochemicals such as proteins and enzymes. Our aim is to serve the pharmaceutical industry with this new separation or purification process. We shall be happy to work with any pharmaceutical company to solve a real separation problem in which higher purification is demanded.

INTRODUCTION

Parametric pumping was named by Wilhelm in 1966 (1) to describe a new separation process. It involves the reciprocating flow of a fluid mixture to be separated through a fixed bed in which one or more of the fluid components can be physically or chemically adsorbed (or reacted) to the solid. The principle of parametric pumping is characterized by flow reversal coupled to a change of a thermodynamic intensive variable. The alternation of an applicable intensive variable, such as temperature, pressure, pH, ionic strength, electric field or affinity, results in a differential shift in the adsorption distribution of the components in fluid mixture. This shift in the adsorption constitutes the basic principle in the separation process of parametric pumping. Wilhelm and Sweed (2) first introduced a semicontinuous single column parametric pumping process to separate a toluene-n-heptane solution by using temperature as the intensive variable. Since then, many similar processes were developed. The variation of flow conditions, number of columns, and thermodynamic intensive variables were studied by different investigators (3,4,5,6,7,8,10). In this paper, we utilize pH parametric pumping to separate a haemoglobin and albumin fluid mixture passing through a CM sepharose packed column.

EXPERIMENTAL

Proteins carry both negatively and positively charged groups which can normally bound to anionic or cationic exchangers. The net charge is dependent on the pH level. At low pH, the net charge is positive. At high pH, it is negative. At the isoelectric point, that is no net charge, the proteins are not bound to any type of ion exchangers. The effect of pH on protein structure is schematically shown in Figure 1.

In the present study, a haemoglobin-albumin mixture was selected as the model system for the parametric pumping separation scheme. Some physical properties of these two proteins are listed in Table 1.

As shown in the above table, the molecular weights of haemoglobin and albumin are similar; thus, separation methods based on molecular weight will be difficult. Since the difference in isoelectric point for these two species is about 2, pH was selected as the thermodynamic intensive variable of parametric pumping.

Worthington human haemoglobin and human serum albumin were used. For the solid adsorbent, a CM sepharose cationic resin manufactured by Pharmacia Fine Chemicals was chosen. CM sepharose is a macroporous, bead formed ionic resin derived from the cross linked agarose gel.

Two buffer solutions were prepared with $pH_1=8$ and $pH_2=6$, so that only the isoelectric point of haemoglobin lies between

these two pH values. At pH=6, the negatively charged haemo-globin is adsorbed on the cationic resin and the positively charged albumin remains in the solution. However, at pH=8, both proteins are positively charged and are not adsorbed.

The experimental apparatus is shown schematically in Figure 2. The column (0.016m inner diameter and 0.15m length) was packed with the cationic resin (porosity = 0.72) and maintained at a constant temperature at 288°K. Reciprocating flow within the system was introduced by a peristalic pump. The pump was connected to a dual timer to have the flow direction reversed automatically at the end of each forward flow and backward flow. Four automatic valves, wired to two timers, were used so that the low and high pH feeds were alternately directed to the top and bottom of the column. At the same time, the top and bottom products were withdrawn from the column, respec-tively, during the bottom and top feeds.

The pH levels in the reservoirs were maintained constant by titrating with hydrochloric acid and sodium hydroxide solu-tions. The strength of the acid and base were so chosen that the effects on the product and reservoir concentrations were minimal. To ensure perfect mixing with the titrant in the reservoirs, magnetic stirrers were used.

The mode of operation is depicted in Figure 3. Initially, the top reservoir was filled with the pH=6 feed solution and the bottom reservoir was filled with pH=8 buffer solution. The buffer solutions were made of 0.05M Tris-maleate and 0.05M

NaOH. The feed solutions were a buffer solution with 0.02 weight percent of each protein. Simultaneously, the column is saturated with pH=8 buffer by circulating the buffer with bottom reservoir. The operation of one complete cycle contains four distinct stages as outlined below.

(I) Downward Adsorption:

The feed with volume Q_{t_I} from the top reservoir enters the top of the column, and the buffer solution which initially in the column is displaced out from the bottom of the column into the bottom reservoir for time t_I. As the feed passes through, the pH value in the column is shifting from 8 to 6 and adsorption of haemoglobin is taking place in the column.

(II) Feed from the Bottom & Product Taken from Top:

Feed solution with pH=6 is introduced at the bottom of the column during time t_{II} and with volume $Q_{t_{II}}$. The solution originally in the column enriched with albumin flows out from the top of the column. It is taken as the top product.

(III) Upward Desorption:

The pH=8 solution flows from the bottom reservoir to the column during time t_{III} and with volume $Q_{t_{III}}$. The solution in the column is pushed to the top reservoir. As the liquid passes through, the pH value in the column is shifting from 6 to 8 and the haemoglobin which is originally bound on the solid adsorbent is released to the liquid.

(IV) Feed from Top & Product Taken from Bottom:

.   Feed solution with pH=8 is added to the top of the column during time t_{IV} and with volume Qt_{IV}. The solution originally in the column enriched with haemoglobin is displaced from the column as the bottom product.

At this point, one cycle of the process is completed. By repeating the cycle described above, the process is capable of separating most of the haemoglobin to the bottom product and the albumin to the top product.

Samples taken from the product streams at the end of each cycle were analyzed by using a spectrophotometer (Bausch & Lomb Spectronic System 400-3). The haemoglobin concentration was determined directly from the absorbance at a wavelength of 403μm. The Bio-Rad Protein assay was used to obtain the total protein concentration. Hence, subtraction of the haemoglobin concentration from the total value gave the concentration of albumin.

RESULTS AND DISCUSSION

A typical result of the described parametric pumping process is plotted in Figure 4 with weight fraction of products versus the number of cycles (9). The weight fraction is defined as the ratio of weight of haemoglobin or albumin to the total weight of proteins. In this run, the displacements were: $Q_{t_I} = Q_{t_{III}} = 22.5 cm^3$, $Q_{t_{II}} = 15 cm^3$ and $Q_{t_{IV}} = 10 cm^3$. The flow rate was $8.33 \times 10^{-3} cm^3/sec$. The dead volumes of both reservoirs were equal to $10 cm^3$. As shown in Figure 4, the product concentrations reach limiting values after a few initial transient cycles. At steady state, the weight fraction of haemoglobin in the bottom product can reach up to 0.95. For albumin in the top product, the weight fraction is 0.87. The result demonstrates the capability of pH parametric pumping in the separation of haemoglobin and albumin is good.

PRESENT RESEARCH WORK AT NJIT

The first stage of research work in parametric pumping at the New Jersey Insitute of Technology was to explore and to demonstrate the separation capability of this unique technique. In the last ten years, we have tried almost all the applicable intensive variables: temperature, pressure, pH, electric field and affinity (13). Different model compounds have been used and different design of processes have been employed. In each case, the separation factor as a function of the number of cycles was studied to determine the effects of reservoir displacement, feed flow rate, feed concentration, and cyclic time (9,10,11,12). Encouraging results have lead us to the next stage of the research project. It is the application of parametric pumping to separate chemicals in real systems in which conventional methods might fail to achieve a good separation. More specifically, we are working on the following areas:

(1) Mathematical modeling of parametric pumping process: Coupling simultaneous partial differential equations to describe the concentration variation of each component in the liquid and solid phases of a column. The solution can therefore be used to predict the performance of a parametric pumping system which involves a sequence of flow in one or more columns.

(2) Scale up of parametric pumping processes: Instead of

separating proteins in the quantity of milligrams, we aim to separate them in large quantities. Certain chemical and physical parameters which govern the performance of a parametric pumping system can be measured. Incorporation of this information with the modeling equations, we can scale up a system to meet the needs of industrial production.

(3) Optimization of a parametric pumping system: There are constraints in almost all the separation processes. For parametric pumping, a most important constraint is the differential shift in the adsorption distribution of proteins due to the alternation of the intensive variable. With the aid of design equations for the system, we can optimize the separation factors or the yield of production by selecting the best operating conditions in order to achieve the desired separation at a minimum cost.

(4) Separation of proteins or other biochemicals: We intend to concentrate our efforts on the separation of proteins or other biochemicals via parametric pumping. The intensive variables, pH, ionic strength and affinity, will be emphasized in further investigations. Our aim is to serve the pharmaceutical industries and medical institutions, where techniques of purification and separation are demanded.

REFERENCES

1. Wilhelm, R.H., A.W. Rice and A.R. Bendelius, "Parametric Pumping: A Dynamic Principle for Separating Fluid Mixtures," Ind. Eng. Chem. Fund., 5, 141 (1966).

2. Wilhelm, R.H. and N.H. Sweed, "Parametric Pumping: Separation of Mixture of Toluene and n-Heptane," Science, 159, 522 (1968).

3. Sweed, N.H., in E.S. Perry and C.J. Von Oss (Eds.), "Progress in Separation and Purification," 4, Wiley (Interscience), New York, 1971, p. 171.

4. Sweed, N.H., in N. Li. (Ed.), "Recent Developments in Separation Science," 1, Chemical Rubber Co., Cleveland, 1972, p. 59.

5. Wankat, P.C., "Cyclic Separation Processes, " Separation Science, 9, 85 (1974).

6. Wankat, P.C., "Cyclic Separation Techniques," NATO, (1978).

7. Rice, R.G., "Progress in Parametric Pumping," Sep. Purif. Methods, 5, 139 (1976).

8. Chen, H.T., T.K. Hsieh, H.C. Lee and F.B. Hill, "Separation of Proteins Via Semicontinuous pH Parametric Pumping," AIChE Journal, 23, 695 (1977).

9. Chen, H.T., Y.W. Wong and S. Wu, "Continuous Fractionation of Protein Mixtures by pH Parametric Pumping," AIChE Journal, 25, 320 (1979).

10. Chen, H.T., W.T. Yang, C.M. Wu, C.O. Kerobo and V. Jajalla, "Semicontinuous pH Parametric Pumping: Process Characteristics and Protein Separations," Sep. Sci. and Tech., 16, 43 (1981).

11. Chen, H.T., W.T. Yang, U. Pancharoen and R.J. Parisi, "Separation of Proteins via Multicolumn pH Parametric Pumping," AIChE Journal, 26, 839 (1980).

12. Chen, H.T., U. Pancharoen, W.T. Yang, C.O. Kerobo and R.J. Parisi, "Separation of Proteins via pH Parametric Pumping," Sep. Sci. and Tech., 15, 1377 (1980).

13. Chen, H.T., C.O. Kerobo, H.C. Hollein and C.R. Huang, "Research on Parametric Pumping," Chem. Eng. Educ., 166 (Fall, 1981).

Table 1

Species	Molecular Weight	Isoelectric Point	uv-403* (μm)	uv-595* (μm)
Haemoglobin	63,000-68,000	6.7	1.00	0.35
Albumin	69,000-72,000	4.7	0.00	0.35

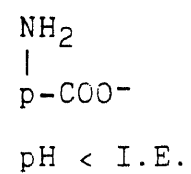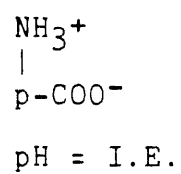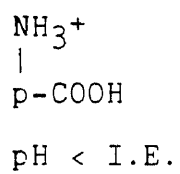*Adsorbance reading reference taken as zero for distilled water.

NH_3^+
|
$p-COOH$

$pH < I.E.$

NH_3^+
|
$p-COO^-$

$pH = I.E.$

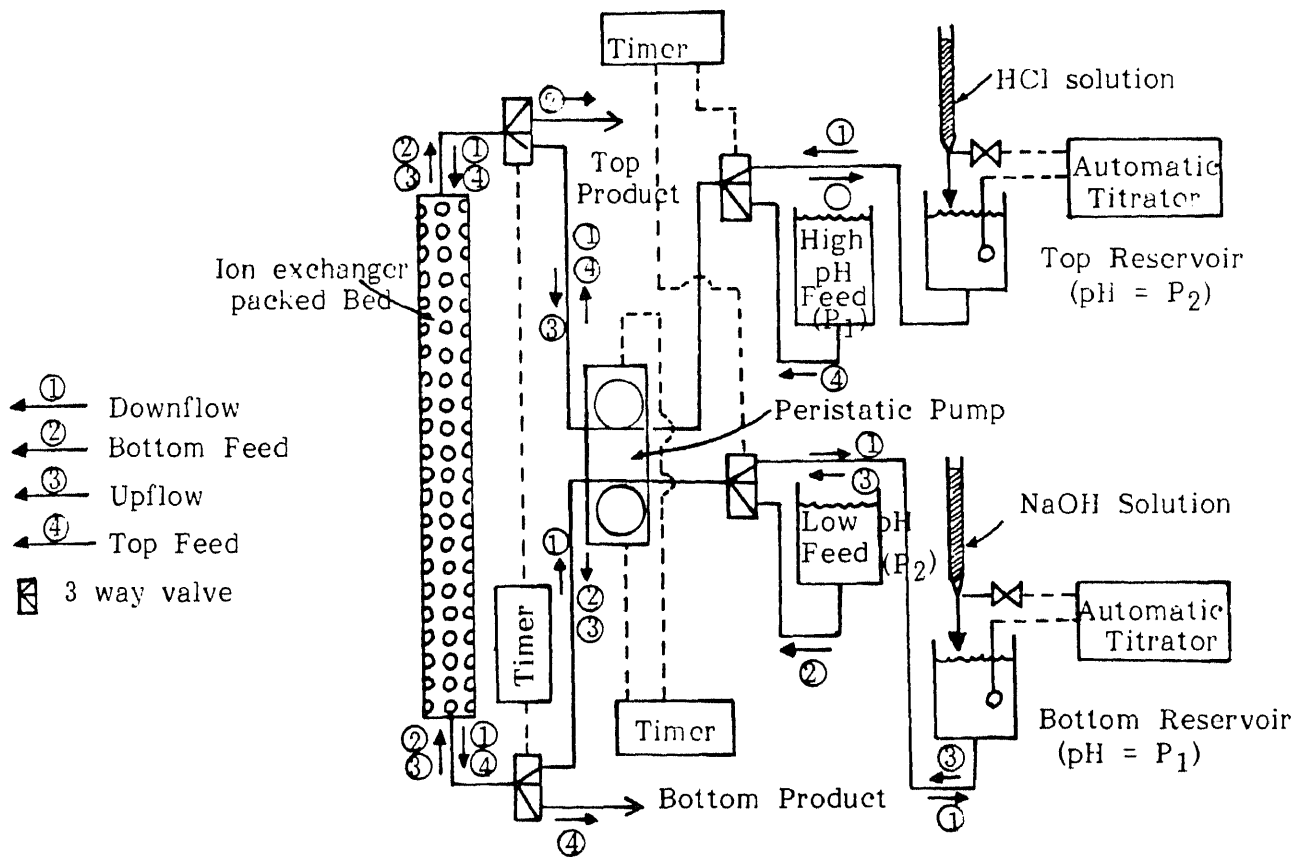NH_2
|
$p-COO^-$

$pH < I.E.$

Figure 1

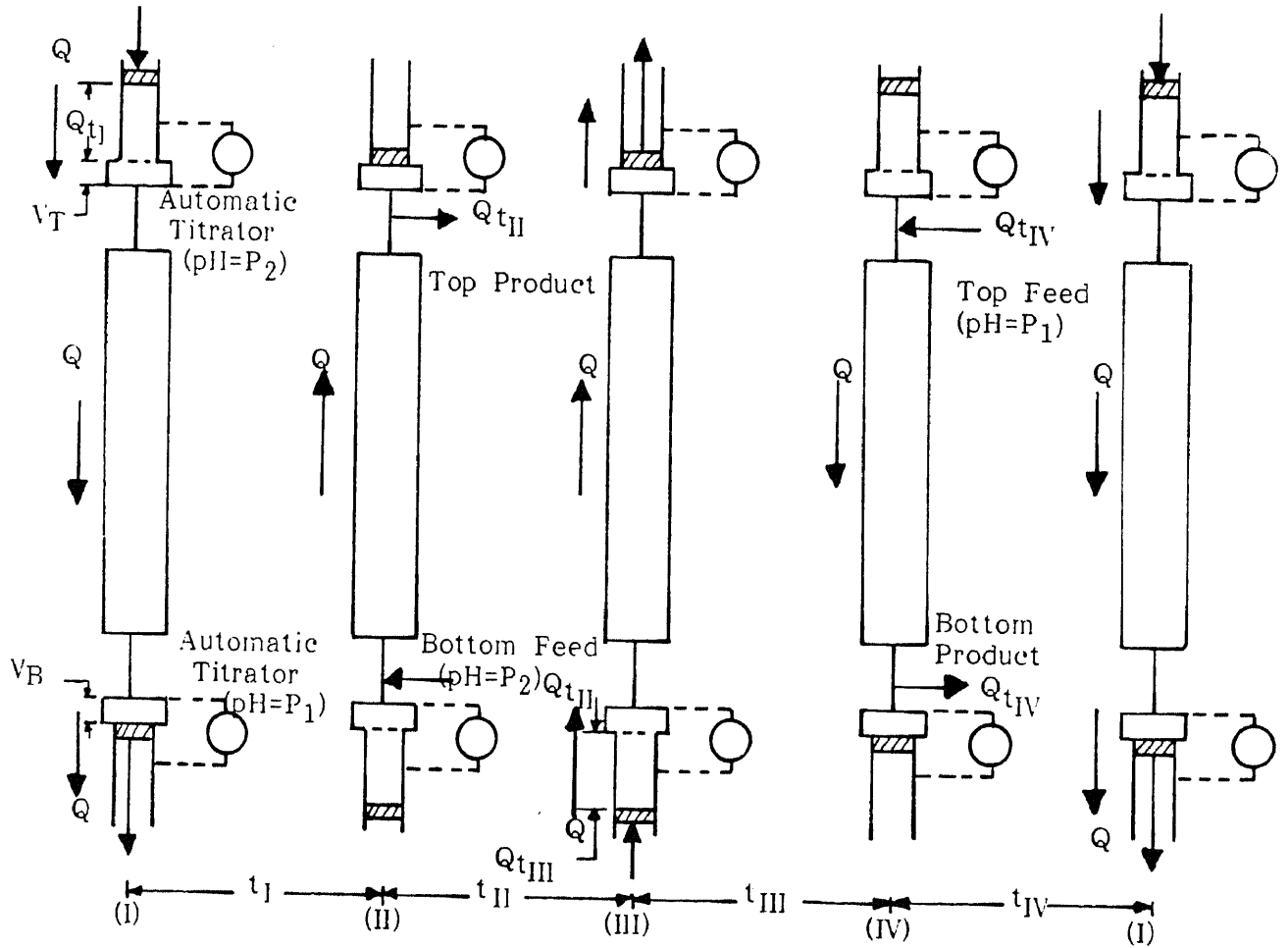FIG. 2. Experimental apparatus for pH parametric pumping
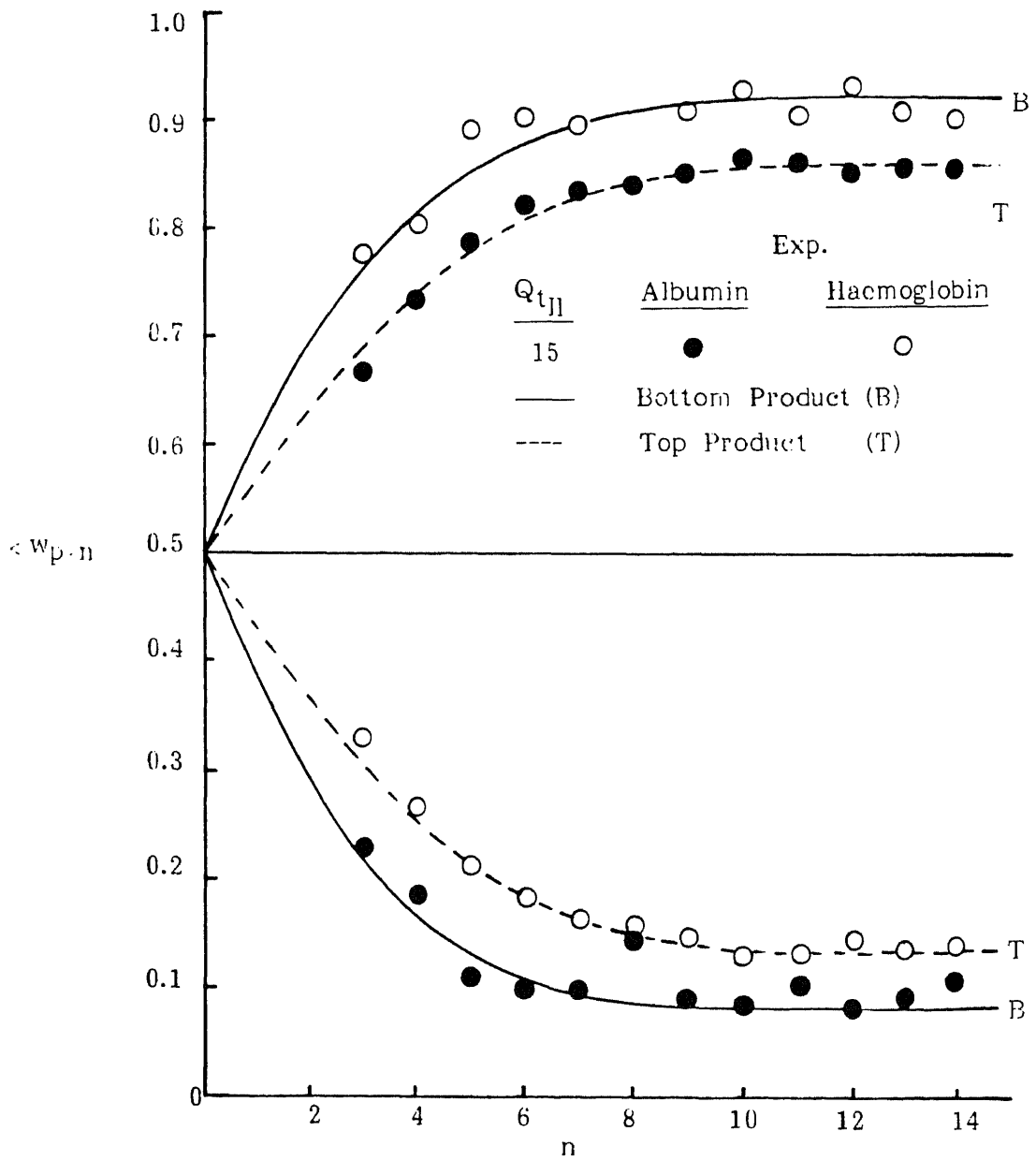
FIG. 3. Column diagram for pH parametric pumping

FIG. 4. Concentration transients for the top and bottom products

SELECTED BIBLIOGRAPHY

1. Langmuir, I., "The Constitution and Fundamental Properties of Solids and Liquids," J. Amer. Chem. Soc., 38, 2221 (1916).

2. Bird, R.B., W.E. Stewart and E.N. Lightfoot, Transport Phenomena, Wiley, example 22.6-2, 702.

3. Lapidus, L. and N.R. Amundson, "Mathematics of Adsorption in Beds. VI. The Effect of Longitudinal Diffusion in Ion Exchange and Chromatographic Column," J. Phys. Chem. 56, 984 (1952).

4. Rasmuson, A. and I. Neretnieks, "Exact Solution of a Model for Diffusion in Particles and Longitudinal Dispersion in Packed Beds," AIChE J., 26, 686 (1980).

5. Anzelius, A., "Über Erwärmung Vermittels Durchströmender Medien," Z. angew. Math. U. Mech., 6 291 (1926).

6. Katch, S., T. Kambayashi, R. Deguchi, and F. Yoshida," Performance of Affinity Chromatography Columns," Biotechnol. Bioeng., 20, 267 (1978).